AD-A049 538 SOUTHWEST RESEARCH INST SAN ANTONIO TEX F/G 11/4
STUDY OF ENVIRONMENTAL EFFECTS ON THERMOMECHANICAL BEHAVIOR OF --ETC(U)
NOV 77 T S COOK, D E WALRATH F44620-76-C-0093
UNCLASSIFIED AFOSR-TR-77-1312 NL

1 OF 2
AD
A049538

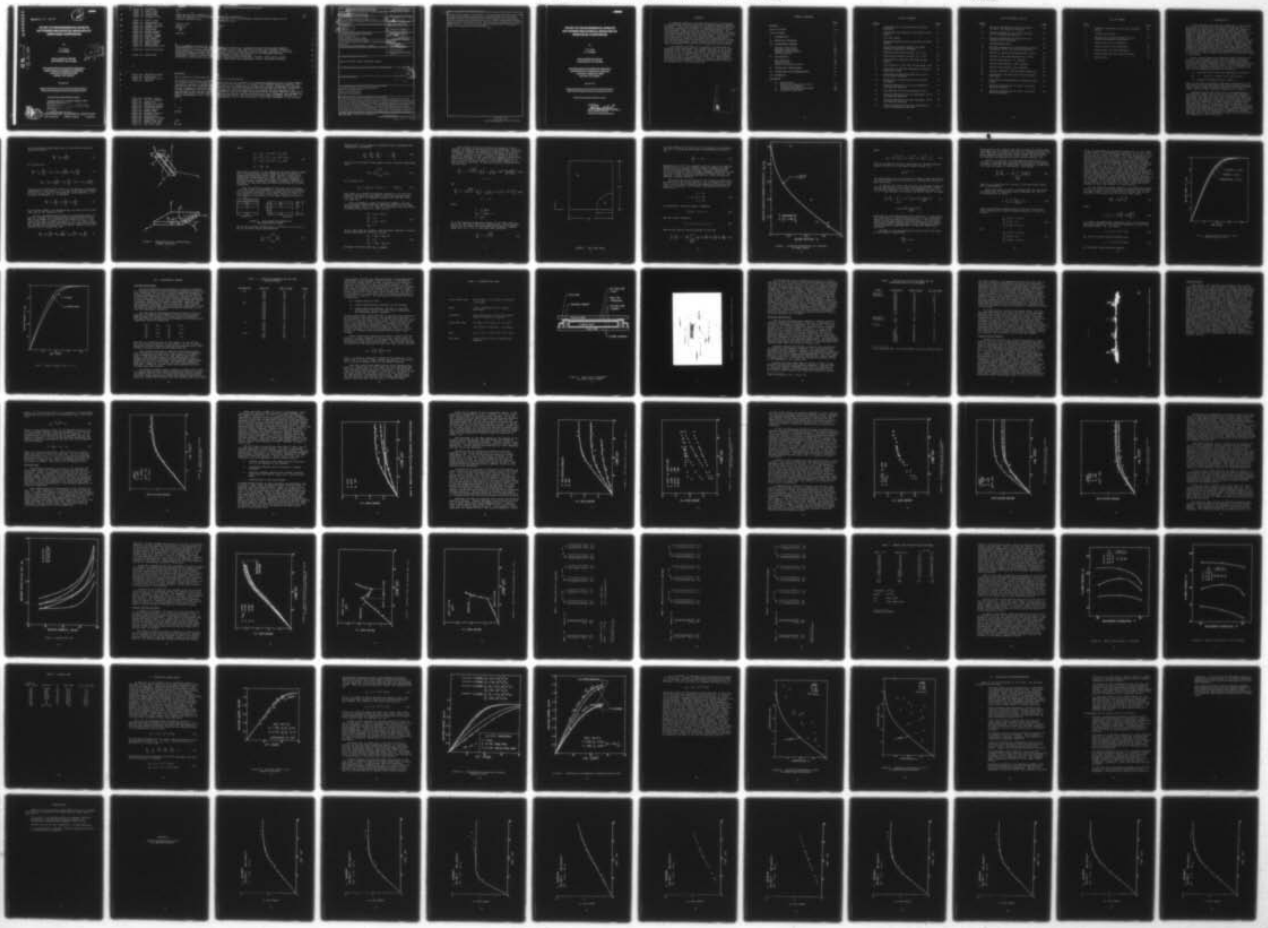


OF
9538

AFOSR-TR- 77 - 1312

B.S.

STUDY OF ENVIRONMENTAL EFFECTS ON THERMO-MECHANICAL BEHAVIOR OF RESIN BASE COMPOSITES

by

T. S. Cook
D. E. Walrath

FINAL SCIENTIFIC REPORT
SwRI PROJECT NO. 02-4559

AIR FORCE OFFICE OF SCIENTIFIC RESEARCH
DIRECTORATE OF AEROSPACE SCIENCES
CONTRACT F44620-76-C-0093
PROJECT NO. 9782-04

November 1977

Research Sponsored by Air Force Office of Scientific Research
Directorate of Aerospace Sciences, United States Air Force

"Approved for public release; distribution unlimited"

SOUTHWEST RESEARCH INSTITUTE
SAN ANTONIO CORPUS CHRISTI HOUSTON

AD NUMBER		E000099
FIELD 2:	FLD/GRP(S)	20110
FIELD 3:	ENTRY CLASS	U
FIELD 4:	NTIS PRICES	HC MF
FIELD 5:	SOURCE NAME	NAVAL RESEARCH LAB WASHINGTON D C
FIELD 6:	UNCLASS. TITLE	TRANSIENT RESPONSE OF TWO FLUID-CO INCIDENT PRESSURE PULSE.
FIELD 7:	CLASS. TITLE	
FIELD 8:	TITLE CLASS.	U
FIELD 9:	DESCRIPTIVE NOTE	INTERIM REPT.,
FIELD 10:	PERSONAL AUTHORS	HUANG,H. ;
FIELD 11:	REPORT DATE	23 DEC 77
FIELD 12:	PAGINATION	28P
FIELD 13:	SOURCE ACRONYM	
FIELD 14:	REPORT NUMBER	NRL-8185
FIELD 15:	CONTRACT NUMBER	
FIELD 16:	PROJECT NUMBER	
FIELD 17:	TASK NUMBER	
FIELD 18:	MONITOR SOURCE	
FIELD 19:	MONITOR SERIES	
FIELD 20:	REPORT CLASS	U
FIELD 21:	SUPPLEMENTARY NOTE	THIS RESEARCH WAS SPONSORED BY THE 99QAXSF502, WORK UNIT 10, WORK UNI
FIELD 22:	ALPHA LIMITATIONS	DISTRIBUTION OF DOCUMENT CONTROLLE 2628, WASHINGTON, DC 20375. THIS D CATALOGING INFORMATION SUPPLIED BY
FIELD 23:	DESCRIPTORS	•TRANSIENTS, •ELASTIC SHELLS, •PRE STRUCTURES, INTERACTIONS, WAVE EQU
FIELD 24:	DESCRIPTOR CLASS.	RESPONSES U
FIELD 25:	IDENTIFIERS	FLUID COUPLING, LPN-NRL-F02-128
FIELD 26:	IDENTIFIER CLASS.	U
FIELD 27:	ABSTRACT	THE TRANSIENT RESPONSE OF A SYSTEM BY AN IDEAL FLUID AND IMPINGED BY CLASSICAL TECHNIQUES OF SEPARATION FOR SOLVING THE WAVE EQUATIONS GOV MOTION. A SCHEME OF ITERATIVE CONV LAPLACE TRANSFORMS THAT FACILITATE THE RESPONSE OF THE SHELLS. A SAMP RESULTS ARE COMPARED TO THE CASE I RESULTS DEMONSTRATES THAT A THIN O PULSE.
FIELD 28:	ABSTRACT CLASS.	U
FIELD 29:	INITIAL INVENTORY	0
FIELD 30:	ANNOTATION	
FIELD 31:	SPECIAL INDICATOR	@
FIELD 32:	REGRADING CATEGORY	
FIELD 33:	LIMITATION CODES	1 21
FIELD 34:	SOURCE SERIAL	
FIELD 35:	SOURCE CODE	251950
FIELD 36:	DOCUMENT LOCATION	7
FIELD 37:	CLASSIFIED BY	
FIELD 38:	DECLASSIFIED ON	
FIELD 39:	DOWNGRADED TO CONF.	
FIELD 40:	GEOPOLITICAL CODE	1100
FIELD 41:	SOURCE TYPE CODE	N
FIELD 42:	TAB ISSUE NUMBER	@@--@@

29 ••••••••••••••••••••••••••SCN-2 AJN18D

MF

2

ESEARCH LAB WASHINGTON D C
NT RESPONSE OF TWO FLUID-COUPLED SPHERICAL ELASTIC SHELLS TO AN
T PRESSURE PULSE.

REPT.,
;
77

5

EARCH WAS SPONSORED BY THE DEFENSE NUCLEAR AGENCY UNDER SUBTASK
502, WORK UNIT 10, WORK UNIT TITLE DOUBLE HULL RESPONSE EVALUATION.
UTION OF DOCUMENT CONTROLLED BY NAVAL RESEARCH LABORATORY, ATTN: CODE
ASHINGTON, DC 20375. THIS DOCUMENT IS NOT AVAILABLE FROM DDC.
ING INFORMATION SUPPLIED BY NRL.
ENTS, *ELASTIC SHELLS, *PRESSURE, *PULSES, SHOCK WAVES, FLUIDS,
RES, INTERACTIONS, WAVE EQUATIONS, MOTION, EQUATIONS OF MOTION,

ES

OUPLING, LPN-NRL-F02-12B

NSIENT RESPONSE OF A SYSTEM OF TWO CONCENTRIC SPHERICAL ELASTIC SHELLS COUPLED
DEAL FLUID AND IMPINGED BY AN INCIDENT PLAN PRESSURE PULSE IS ANALYZED. THE
AL TECHNIQUES OF SEPARATION OF VARIABLES AND LAPLACE TRANSFORMS ARE EMPLOYED
VING THE WAVE EQUATIONS GOVERNING THE FLUID MOTIONS AND THE SHELL EQUATIONS OF
A SCHEME OF ITERATIVE CONVOLUTION WAS DEVISED FOR THE INVERSION OF THE
TRANSFORMS THAT FACILITATES THE CALCULATION OF ACCURATE TRANSIENT SOLUTIONS OF
PONSE OF THE SHELLS. A SAMPLE CALCULATION OF SHELL RESPONSES WAS PERFORMED AND
ARE COMPARED TO THE CASE IN WHICH THE OUTER SHELL IS ABSENT. THIS SET OF
DEMONSTRATES THAT A THIN OUTER SHELL TENDS TO BE TRANSPARENT TO THE INCIDENT

SECURITY CLASSIFICATION OF THIS PAGE (When Data Entered)

REPORT DOCUMENTATION PAGE

READ INSTRUCTIONS BEFORE COMPLETING FORM

1. REPORT NUMBER: AFOSR-TR-77-1312	2. GOVT ACCESSION NO.
3. RECIPIENT'S CATALOG NUMBER	
4. TITLE (and Subtitle): STUDY OF ENVIRONMENTAL EFFECTS ON THERMOMECHANICAL BEHAVIOR OF RESIN-BASE COMPOSITES.	5. TYPE OF REPORT & PERIOD COVERED: FINAL Scientific rept. May 1976 - Sep 77
	6. PERFORMING ORG. REPORT NUMBER: SwRI Project 02-4559
7. AUTHOR(s): T. S. COOK, D. E. WALRATH	8. CONTRACT OR GRANT NUMBER(s): F44620-76-C-0093
9. PERFORMING ORGANIZATION NAME AND ADDRESS: SOUTHWEST RESEARCH INSTITUTE, 6220 CULEBRA RD., SAN ANTONIO, TEXAS 78284	10. PROGRAM ELEMENT, PROJECT, TASK AREA & WORK UNIT NUMBERS: 2307 B1 9782, 61102F, B1,04
11. CONTROLLING OFFICE NAME AND ADDRESS: AIR FORCE OFFICE OF SCIENTIFIC RESEARCH/NA, BLDG 410, BOLLING AIR FORCE BASE, D C 20332	12. REPORT DATE: Nov 77
	13. NUMBER OF PAGES: 129 (130 P.)
14. MONITORING AGENCY NAME & ADDRESS (if different from Controlling Office)	15. SECURITY CLASS. (of this report): UNCLASSIFIED
	15a. DECLASSIFICATION/DOWNGRADING SCHEDULE

16. DISTRIBUTION STATEMENT (of this Report)

Approved for public release; distribution unlimited.

17. DISTRIBUTION STATEMENT (of the abstract entered in Block 20, if different from Report)

18. SUPPLEMENTARY NOTES

19. KEY WORDS (Continue on reverse side if necessary and identify by block number)

GRAPHITE-EPOXY COMPOSITE MATERIALS
MOISTURE ABSORPTION
MOISTURE DIFFUSION
COMPOSITE LAMINATES

20. ABSTRACT (Continue on reverse side if necessary and identify by block number)

A combined analytical and experimental study was designed to characterize moisture absorption in graphite/epoxy composite materials. Tests were designed to investigate the influence on moisture absorption of a number of composite parameters including thickness, fiber volume, and lay-up configuration. The environmental parameters investigated were the effects of temperature and humidity; the effect of small applied strains was also evaluated by use of four point bend specimens. The results were analyzed by comparing the weight gain characteristics of the various panels, and by evaluating the coefficients of diffusion for the specimens. Based on these diffusivities, one and three dimensional

DD FORM 1 JAN 73 1473 EDITION OF 1 NOV 65 IS OBSOLETE

UNCLASSIFIED
SECURITY CLASSIFICATION OF THIS PAGE (When Data Entered)

328 200 SOB

solutions to Fick's equation were evaluated. A micromechanical model for laminates were developed and analyzed; the experimental data showed the model to be a lower bound solution. Moreover, the results indicate the classical solution to the one dimensional Fick's law based on effective diffusivity can be used to predict weight gain of a graphite/epoxy panel due to the presence of water. This model cannot currently predict secondary diffusion effects. The results of the bending tests showed no effect of small applied strains on the weight gain of the bend specimens.

STUDY OF ENVIRONMENTAL EFFECTS ON THERMO-MECHANICAL BEHAVIOR OF RESIN BASE COMPOSITES

by

T. S. Cook
D. E. Walrath

FINAL SCIENTIFIC REPORT
SwRI PROJECT NO. 02-4559

AIR FORCE OFFICE OF SCIENTIFIC RESEARCH
DIRECTORATE OF AEROSPACE SCIENCES
CONTRACT F44620-76-C-0093
PROJECT NO. 9782-04

November 1977

Research Sponsored by Air Force Office of Scientific Research
Directorate of Aerospace Sciences, United States Air Force

"Approved for public release; distribution unlimited"

APPROVED:

Ulric S. Lindholm, Director
Department of Materials Sciences

ABSTRACT

A combined analytical and experimental study was designed to characterize moisture absorption in graphite/expoxy composite materials. Tests were designed to investigate the influence on moisture absorption of a number of composite parameters including thickness, fiber volume, and lay-up configuration. The environmental parameters investigated were the effects of temperature and humidity; the effect of small applied strains was also evaluated by use of four point bend specimens. The results were analyzed by comparing the weight gain characteristics of the various panels, and by evaluating the coefficients of diffusion for the specimens. Based on these diffusivities, one and three dimensional solutions to Fick's equation were evaluated.

A micromechanical model for laminates was developed and analyzed; the experimental data showed the model to be a lower bound solution. Moreover, the results indicate the classical solution to the one dimensional Fick's law based on effective diffusivity can be used to predict weight gain of a graphite/epoxy panel due to the presence of water. This model cannot currently predict secondary diffusion effects. The results of the bending tests showed no effect of small applied strains on the weight gain of the bend specimens.

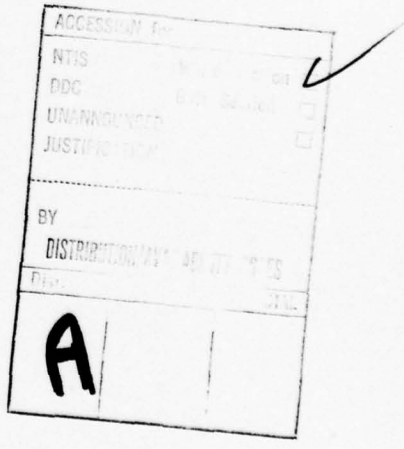

TABLE OF CONTENTS

	Page
ABSTRACT	i
LIST OF FIGURES	iii
LIST OF TABLES	v
I. INTRODUCTION	1
II. ANALYTICAL MODELLING	3
III. EXPERIMENTAL PROGRAM	19
Specimen Fabrication	19
Moisture Conditioning	25
Constant Strain Testing	27
Tensile Testing	29
IV. TEST RESULTS	30
Data Reduction	30
Moisture Data	32
Tensile and Spiking Tests	47
V . DIFFUSIVITY COEFFICIENTS	61
VI. CONCLUSIONS AND RECOMMENDATIONS	69
VII. REFERENCES	72
APPENDICES	
A. Publications	73
B. Weight Gain Results for 125°F, 95% Relative Humidity	75
C. Constant Deformation Specimens	88
D. Sequencing Specimens	113

LIST OF FIGURES

Figure		Page
1	Coordinates for a Unidirectional Fibrous Composite.	5
2	Flow Normal and Parallel to the Plane of the Fibers.	6
3	Unit Cell Model	9
4	Effective Diffusivity as a Function of Fiber Volume.	11
5	Theoretical Moisture Content for Three Composite Laminates (3D Model).	15
6	Theoretical Moisture Content, $V_F = 0.65$.	17
7	Theoretical Moisture Content, $V_F = 0.52$.	18
8	Setup Used to Fabricate Low Fiber Volume Panels.	23
9	Cross-Section of 30% Fiber Volume Panel, 50X.	24
10	Fixturing for Constant Deformation Moisture Absorption Tests.	28
11	Predicted and Measured Weight Gain for an 8 Ply [$\pm$45°] Laminate.	31
12	Weight Gain for Edge Sealed and Unsealed Specimens.	33
13	Moisture Absorption for $[0°]_8$ Composites, 70% Relative Humidity.	35
14	Test Results for $[0°]_8$ Laminates, 125°F.	37
15	Moisture Absorption for 4 Thicknesses, 125°F, 95% Relative Humidity.	38
16	Moisture Absorption for Two Laminates, 125°F, 95% Relative Humidity.	40
17	Moisture Absorption for Three Laminates at 125°F, 95% Relative Humidity.	41

LIST OF FIGURES (Cont'd)

Figure		Page
18	Moisture Absorption for Three Laminates at 125°F, 70% Relative Humidity.	42
19	Moisture Absorption for 4 Fiber Volumes, 125°F, 95% Relative Humidity.	44
20	Moisture Absorption for Neat Resin and Composite Test Specimens.	45
21	Maximum Weight Gain.	46
22	Moisture Absorption for Strained Neat Resins Specimens, 125°F, 95% Relative Humidity.	48
23	Results of Three Step Sequence Test, 125°F.	49
24	Results of Two Step Sequence Test, 125°F.	50
25	Tensile Test Results, 0° Laminate.	56
26	Tensile Test Results, 0/90° Laminate.	57
27	Tensile Test Results, $\pm$45° Laminate.	58
28	Moisture Content in Two Unsealed Composites.	62
29	Experimental and Analytical Moisture Absorption Data.	64
30	Predicted and Experimentally Measured Weight Gains.	65
31	Effective Diffusivity at 125°F, 95 Percent Relative Humidity.	67
32	Effective Diffusivity at 175°F, 70 Percent Relative Humidity.	68

LIST OF TABLES

Table		Page
1	Composite Parameters for the Test Specimen Panels.	20
2	Standard Cure Cycle	22
3	Typical Set of Test Specimens for One Temperature-Humidity Environment.	26
4	Tensile Data for 0° Specimens.	51
5	Tensile Data for ±45° Specimens.	52
6	Tensile Data for 0/90° Specimens.	53
7	Tensile Data for Neat Resin Specimens.	54
8	Spiking Data.	60

I. INTRODUCTION

As new materials move from the laboratory to field usage, one of the key concerns is the material's behavior as it encounters an uncontrolled environment. Since the absorption of moisture by epoxy matrix or bonding materials has been shown to cause some change in the mechanical properties of the composite, considerable interest has been expressed in the effect of moisture on composite materials. This interaction between a composite material and the environment is a very complex event involving a number of physical processes. As such, it may be viewed in several different ways, ranging from the physics of the interface to the behavior of a large panel subjected to an outdoor environment. Ultimately, each of these viewpoints will become part of the total understanding of the effects of temperature and moisture on the material. However, at the present time it seems more appropriate to view the overall picture as this will point the way for more detailed studies in the future.

While organic fibers can themselves absorb considerable moisture, the inorganic fibers, such as graphite and boron, are not known to absorb moisture to any significant degree. In terms of present structural usage, the high modulus inorganic fibers are of primary interest, and so, for this program, we can rule out moisture absorption by the fiber. Moisture, however, can be transported through the matrix by

(1) capillary action along the fiber/matrix interface,

(2) voids, pores, or cracks in the resin system,

(3) diffusion through the resin itself.

Thus, in the case of inorganic fiber/epoxy composites, it is anticipated that problems associated with moisture absorption would be more severe in "matrix dominated" laminates, such as (±45), than in "fiber dominated" layups such as (0/90).

Absorbed moisture has been found to be predominately, if not entirely, water; work by the Air Force Flight Dynamics Laboratory has shown that over 90% of desorption products are pure water. The time scale for water absorption by other than artificial environmental conditions is on the order of weeks. Some moisture apparently is always present; estimates have been made that 0.2 - 0.3% water by weight is present in a thermosetting composite immediately upon removal from the oven. Since this moisture level, as a minimum, is apparently always present in the thermosetting epoxy, it should be considered as the reference level for measuring environmentally induced moisture levels, unless measures are taken to dry and preserve the composite in such a dry state.

A number of experimental observations have been made on moisture levels in epoxy resin composites as a function of temperature, humidity, and exposure time. "Saturation" levels appear to be in the range of 1 - 2% moisture by weight, with the actual equilibrium levels of water being a function of the void content and fiber volume of the composite, as well as the humidity conditions surrounding the composite. The rate of water absorption depends on the temperature as well as the thickness, but it is not clear whether the equilibrium moisture content is independent of temperature.

II. ANALYTICAL MODELLING

As already mentioned, the approach taken to describing moisture absorption in this program has been to consider the absorption in a structural sense. That is, we wish to describe the overall response of the composite, i.e., weight gain, to the particular temperature-humidity environment. However, since a composite structure is composed of many different composite parameters, such results may not be very general since they are necessarily structure dependent. To avoid the necessity of testing all composite structures, we have used a micromechanical model to describe the overall response in terms of combinations of simpler elements. Based on information gained by testing unidirectional panels, it is then possible to predict the weight gain of multilayer composites.

While the basic formulation of the diffusion problem is well established, it bears some repetition here both for completeness and to emphasize some key points. The basic postulate of the diffusion problem is that the rate of transfer of the diffusing substance is proportional to the gradient of the concentration. For an isotropic body this only involves the normal gradient but for an anisotropic material the concentration gradients in other directions can be involved as well. In general then the flow in the i^{th} direction is given by

$$-F_i = D_{ij} \frac{\partial C}{\partial \xi_j} \qquad i,j = 1, 2, 3, \text{ sum on } j \tag{1}$$

where D_{ij} reflects the flow in the i^{th} direction due to a concentration gradient in the j^{th} direction. This means that for flow at an angle to a unidirectional ply, gradients perpendicular to the flow direction can exist and influence the flow. Fortunately, these effects usually average out, as we shall show, but one must be aware that such terms are not zero but are only neglected through an averaging process.

If we then consider conservation of matter,

$$\frac{\partial C}{\partial t} = - \frac{\partial F_i}{\partial \xi_i} \tag{2}$$

where C is the concentration of diffusing material, then substituting (2) into (1), we obtain

$$\frac{\partial C}{\partial t} = \frac{\partial}{\partial \xi_i} \left(D_{ij} \frac{\partial C}{\partial \xi_j} \right) \tag{3}$$

If the diffusion coefficients are not functions of position, then we can write

$$\frac{\partial C}{\partial t} = D_{ij} \frac{\partial^2 C}{\partial \xi_i \partial \xi_j} \tag{4}$$

or, written out

$$\frac{\partial C}{\partial t} = D_{11} \frac{\partial^2 C}{\partial \xi_1^2} + (D_{12} + D_{21}) \frac{\partial^2 C}{\partial \xi_1 \partial \xi_2} + D_{22} \frac{\partial^2 C}{\partial \xi_2^2} \tag{5}$$

$$+ (D_{23} + D_{32}) \frac{\partial^2 C}{\partial \xi_2 \partial \xi_3} + D_{33} \frac{\partial^2 C}{\partial \xi_3^2} + (D_{31} + D_{13}) \frac{\partial^2 C}{\partial \xi_3 \partial \xi_1}$$

Since D_{ij} is a second order tensor, we can perform a coordinate transformation and obtain (5) in terms of the principal diffusivities, D_1, D_2, and D_3. Performing the transformation to the principal coordinates x_i, (5) becomes

$$\frac{\partial C}{\partial t} = D_1 \frac{\partial^2 C}{\partial x_1^2} + D_2 \frac{\partial^2 C}{\partial x_2^2} + D_3 \frac{\partial^2 C}{\partial x_3^2} \tag{6}$$

For isotropic bodies, the diffusivities are equal and the right hand side of (6) reduces to $D\nabla^2 C$.

So far, the discussion has been for anisotropic bodies in general. Consider now a unidirectional fibrous composite with the y axis normal to the plane of the fibers and x, z in the fiber plane; this is shown in Figure 1. If $\theta = 0$, then x and z are the principal inplane directions and (6) describes the flow. For inplane flow at an angle to the fibers, however, the cross product term is retained so that

$$\frac{\partial C}{\partial t} = D_{11} \frac{\partial^2 C}{\partial x^2} + 2D_{13} \frac{\partial^2 C}{\partial x \partial z} + D_{33} \frac{\partial^2 C}{\partial z^2} + D_{22} \frac{\partial^2 C}{\partial y^2} \tag{7}$$

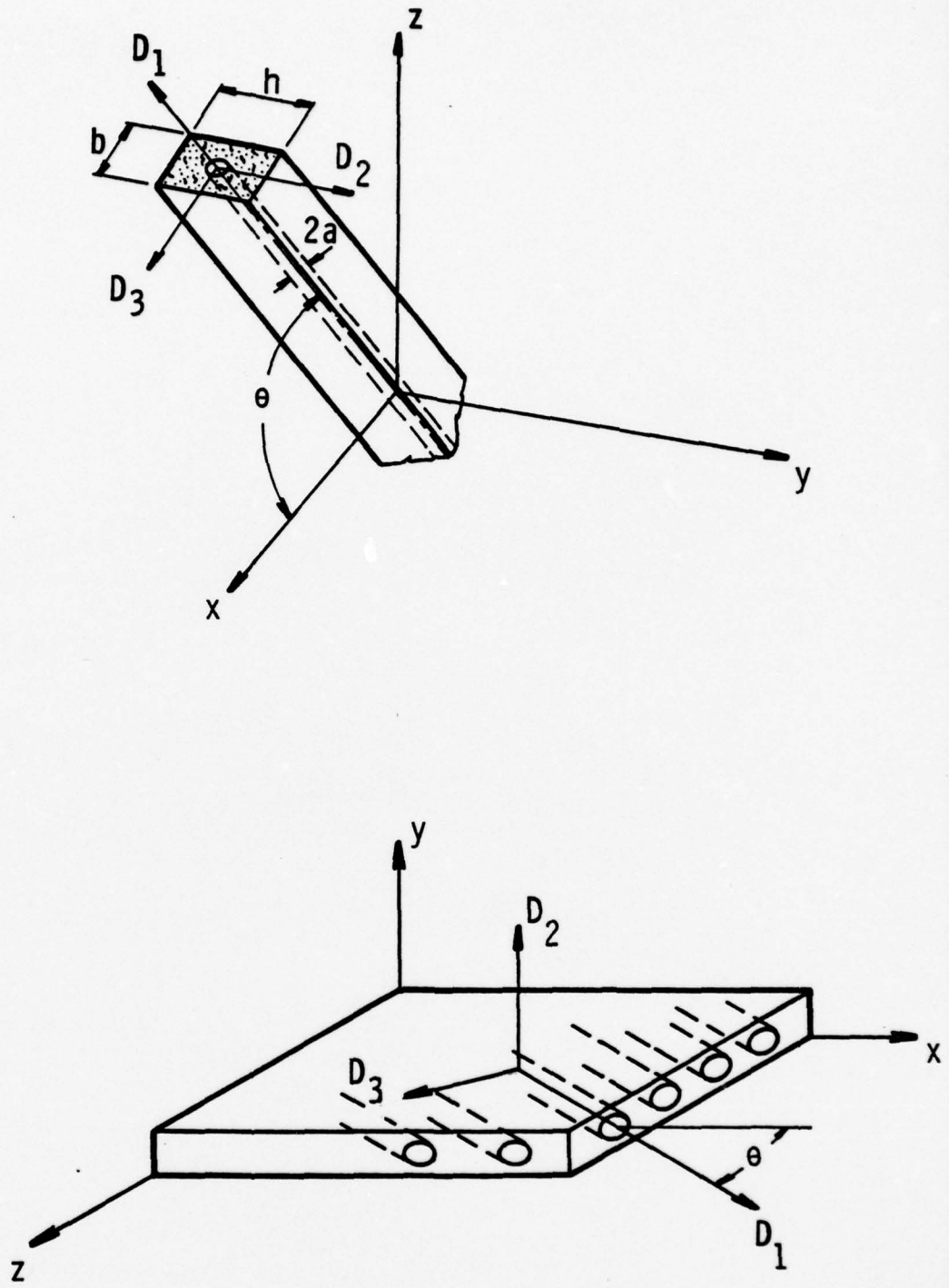

FIGURE 1. COORDINATES FOR A UNIDIRECTIONAL FIBROUS COMPOSITE.

where

$$
\begin{aligned}
D_x &= D_{11} = D_1 \cos^2\theta + D_3 \sin^2\theta \\
D_{xz} &= D_{13} = (D_3 - D_1) \sin\theta \cos\theta \\
D_z &= D_{33} = D_1 \sin^2\theta + D_3 \cos^2\theta \\
\\
D_y &= D_{22} = D_2
\end{aligned}
\tag{8}
$$

Note that in writing (7) the assumption has been implicity made that a unidirectional fibrous composite can be treated as a homogeneous anisotropic body. Since inorganic fibers do not absorb significant amounts of water, this is a reasonable assumption. In the event that either the fibers themselves or the fiber-matrix interfaces transport significant amounts of moisture, it does mean that an effective diffusivity is being considered.

Once the diffusion parameters are known for a unidirectional ply, then it is possible to describe moisture transport in a multilayer structure. If we consider the two cases of (i) flow normal to the plane of the fibers (Figure 2a) and (ii) flow parallel to the plane of the fibers (Figure 2b) then we

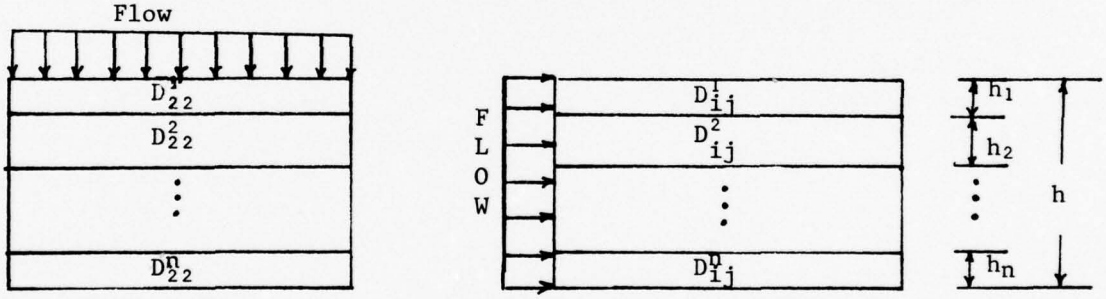

Figure 2a Figure 2b

FIGURE 2. FLOW NORMAL AND PARALLEL TO THE PLANE OF THE FIBERS.

obtain the effective diffusivities as follows. For the flow in 2a, we can use a series approximation,

$$
\frac{1}{\bar{D}_{22}} = \frac{1}{h} \int_{-h/2}^{h/2} \frac{d_y}{D_{22}} \tag{9}
$$

where the $\bar{D}_{ij}$ is an average or effective value. Performing the integration, one obtains

$$\frac{h}{\bar{D}_{22}} = \frac{h_1}{D_{22}^1} + \frac{h_2}{D_{22}^2} + \ldots + \frac{h_n}{D_{22}^n} \tag{10}$$

For flow in the plane of the fibers, we use a parallel approximation,

$$\bar{D}_{ij} = \frac{1}{h} \int_{-h/2}^{h/2} D_{ij}\, d_y \tag{11}$$

or in series form

$$\bar{D}_{ij}\, h = D_{ij}^1\, h_1 + D_{ij}^2\, h_2 + \ldots + D_{ij}^n\, h_n \tag{12}$$

Note there is no effect of stacking sequence in (10) for flow normal to the plane of the fibers. It can also be seen from (11) and (8) that, for symmetric layups, the cross ply terms will drop out.

Let us consider a couple of specific examples. For the unidirectional laminate the two directions normal to the fiber are equivalent, so $D_2 = D_3$. Then for a crossply layup with equal thickness plies, each at $\theta = \pm 45°$, we get

$$\begin{aligned} \bar{D}_x &= (D_1 + D_2)/2 \\ \bar{D}_y &= D_2 \\ \bar{D}_z &= (D_1 + D_2)/2 \\ \bar{D}_{xz} &= 0 \end{aligned} \tag{13}$$

On the other hand if we have a core and shell laminate, 10 plies thick, with layup $[0, (\pm 45)_2]_s$, we get

$$\begin{aligned} \bar{D}_x &= (6D_1 + 4D_2)/10 \\ \bar{D}_y &= D_2 \\ \bar{D}_z &= (4D_1 + 6D_2)/10 \end{aligned} \tag{14}$$

and again the cross term, $\bar{D}_{xz}$, vanishes.

This analysis allows us to obtain the behavior of the laminate in terms of unidirectional layer properties. By representing the composite as composed of a series of unit cells, it is possible to obtain the diffusion coefficients in terms of the volume fraction of fiber. A number of different unit cell models are possible but for simplicity we assume a square array. Referring to Figure 3, the unit cell has dimensions b by h, with a circular fiber of radius a, and a fiber volume V_f. For flow normal to the fiber, we have the effective diffusivity of the unit cell,

$$\frac{D_2}{D_m} = 1 - 2\sqrt{\frac{V_f\, f}{\pi}} + \frac{f}{B_D}\left[\pi - \frac{4}{\sqrt{1 - C}} * \text{TAN}^{-1}\frac{\sqrt{1 - \sqrt{C}}}{\sqrt{1 + \sqrt{C}}}\right], \quad (15a)$$

$$1 - C > 0$$

and

$$\frac{D_2}{D_m} = 1 - 2\sqrt{\frac{V_f\, f}{\pi}} + \frac{f}{B_D}\left[\pi - \frac{2}{\sqrt{C - 1}} * \ln\left\{\sqrt{C} + \sqrt{C - 1}\right\}\right] \quad (15b)$$

$$C - 1 > 0,$$

where

$$C = V_f\, B_D^2/\pi f$$

$$B_D = 2\,(D_m/D_f - 1)$$

$$f = h/b.$$

D_2 is the effective diffusivity normal to the fiber while D_m and D_f are the matrix and fiber diffusivities. If the moisture content of the fibers can be ignored and we assume a square unite cell, i.e., f = 1, (15a) and (15b) reduce to

$$\frac{D_2}{D_m} = 1 - 2\sqrt{\frac{V_f}{\pi}} \quad (16)$$

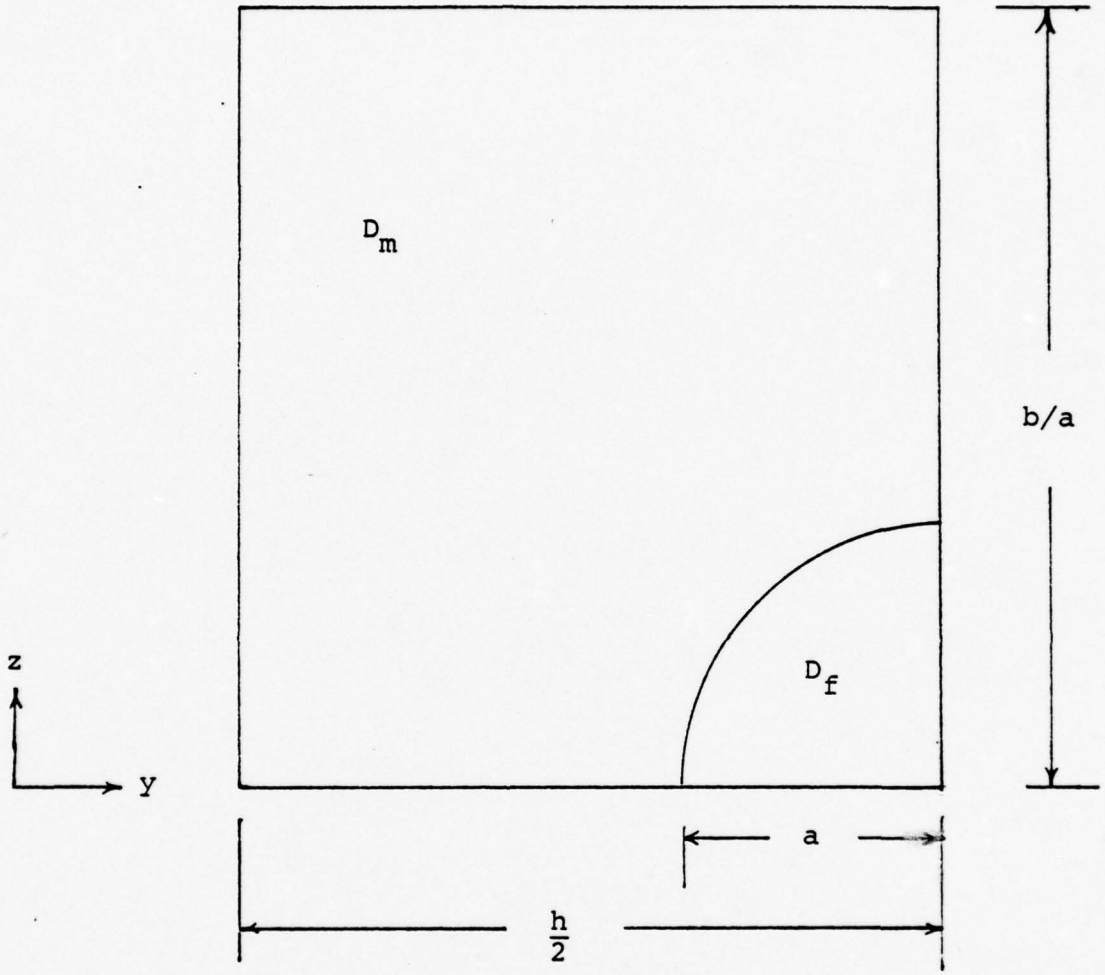

FIGURE 3. UNIT CELL MODEL

for flow normal to the fibers. For flow parallel to the fibers, the flow is reduced by the volume of nontransporting fibers, i.e.

$$\frac{D_1}{D_m} = 1 - V_f \tag{17}$$

Expression (16) and (17), together with (8), give the effective diffusivities of a unidirectional fibrous composite in terms of the fiber orientation. Moreover, when the unidirectional plies are layered to form a multiply laminate, equations (9) and (11) can be used to arrive at effective diffusivities for the laminate. Figure 4 shows the diffusivity, D_2/D_m, plotted as a function of volume fraction.

With some idea of the nature of the diffusion coefficients, we can turn to the actual solution [1,2] to equation (7); however, we shall only be dealing with symmetric laminates so D_{xz} term in (7) vanishes. If we specify the boundary and initial conditions as

$$C = C_o \begin{cases} x = \pm \ell \\ y = \pm h \\ z = \pm b \end{cases} \tag{18}$$

or alternately, since the body is symmetric

$$\partial C/\partial x_i = 0, \; x_i = 0 \tag{19}$$

and the initial condition,

$$C\,(t, x, y, z) = C_i, \; t \leq 0 \tag{20}$$

then we can obtain a series solution in the form

$$\frac{C - C_i}{C_o - C_i} = 1 - \frac{64}{\pi^3} \sum_{\substack{i,j,k \\ \text{odd}}} \frac{1}{ijk} \cos \frac{i\pi x}{2\ell} \cos \frac{j\pi y}{2h} \cos \frac{knz}{2b} \tag{21}$$

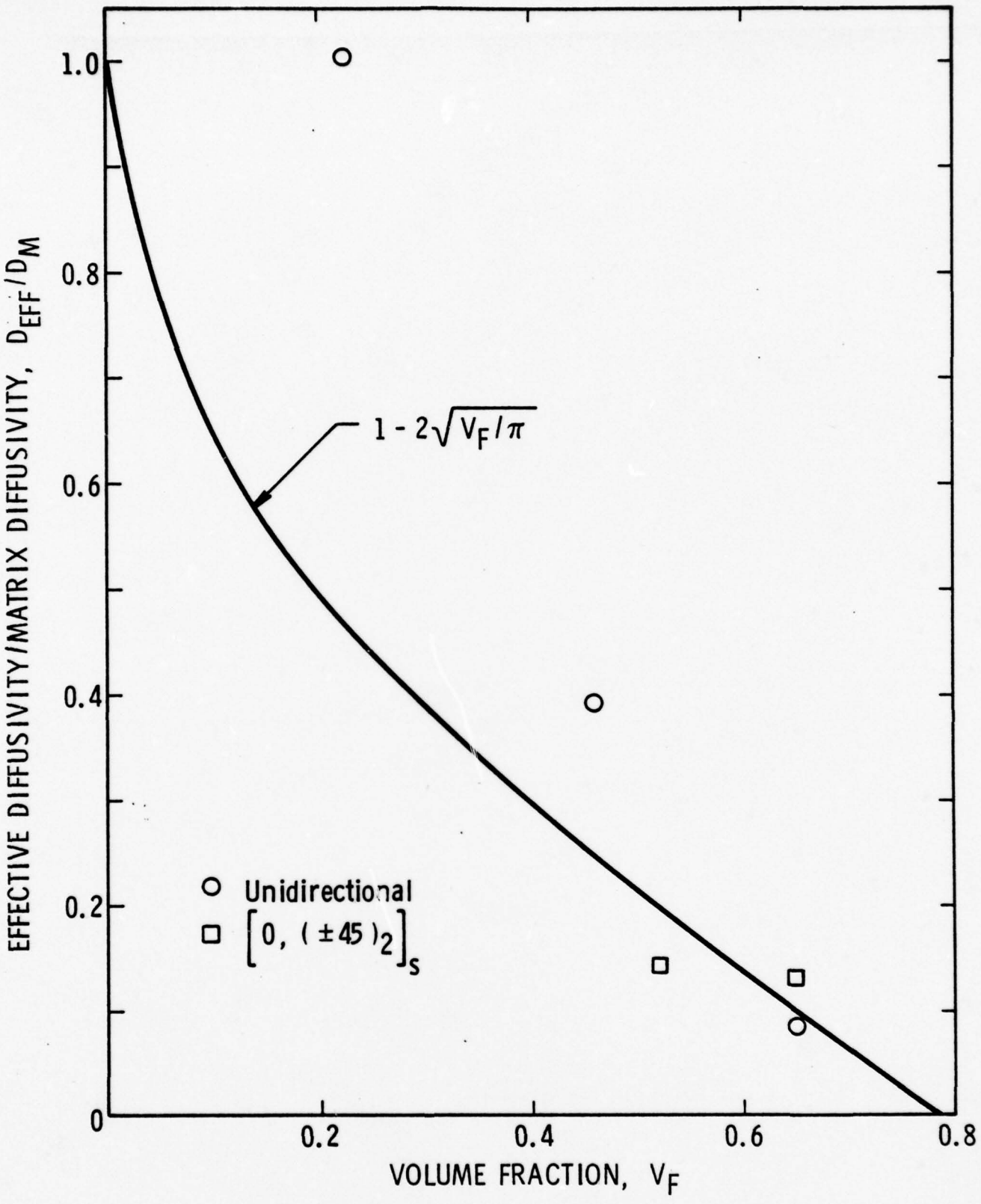

FIGURE 4. EFFECTIVE DIFFUSIVITY AS A FUNCTION OF FIBER VOLUME.

where

$$\lambda_{ijk} = \frac{\pi^2}{4}\left(\left(\frac{i}{\ell}\right)^2 D_x + \left(\frac{j}{h}\right)^2 D_y + \left(\frac{k}{b}\right)^2 D_z\right) \qquad (22)$$

This is the general solution, applicable for suitably defined systems. However, for very small values of time, i.e.

$$4D_y t/h^2 << 1$$

(or equivalently, one of the other two terms if they are larger), the series converges very slowly and an alternative solution is more convenient.

To develop this short time solution, we consider an infinite slab so that we have a one-dimensional diffusion flow. Taking the Laplace transform of (4) for a one-dimensional flow, i.e., i = j = 1 and applying the boundary conditions (18-20) we obtain

$$\frac{C - C_i}{C_o - C_i} = \sum_{n=o} (-1)^n \left[\operatorname{erfc} \frac{(2n+1)\,h - y}{2\sqrt{Dt}} + \operatorname{erfc} \frac{(2n+1)\,h + y}{2\sqrt{Dt}}\right] \qquad (23)$$

where erfc is the complimentary error function, D is the effective diffusivity in the y direction and 2h is the thickness of the slab. (For more details, see Reference 1.) For very short times, the moisture entering from one surface will not interact with any other surface; hence a three dimensional solution can be obtained by superimposing the three one dimensional solutions.

Weitsman [3] has estimated that only the first two terms of (23) need be retained for

$$\frac{4D_y t}{h^2} < 0.01.$$

Since $D_y \approx 2 * 10^{-6}$ in^2/hr, and $h \approx 0.06$ inches for these panels, this means that for times on the order of 14 hours and less, the error function is appropriate. Since the experimental program being reported deals with much longer times, the majority of the modeling has employed the cosine series solution, (21).

Since it is difficult to determine the concentration of moisture in the material, the total weight gain by the specimen is usually obtained. The weight gain is computed by integrating (21) over the volume of the material. This yields

$$\frac{M - M_i}{M_m - M_i} = 1 - \frac{8^3}{\pi^6} \sum_{\substack{i,j,k \\ \text{odd}}} \frac{e^{-\lambda_{ijk} t}}{i^2 j^2 k^2} \tag{24}$$

where λ_{ijk} is given by (22), and M_m is the equilibrium weight gain of the material.

With this result, we have a complete model for predicting the weight gain of multilayer panel. Combining (16) and (17) to eliminate D_m, we obtain

$$D_1 = \left[\frac{1 - V_f}{1 - 2\sqrt{V_f/\pi}} \right] D_2 \tag{25}$$

Using the effective diffusivities for the ten ply core and shell laminate,(14), and two volume fractions, 0.52 and 0.65, we have

$$\begin{aligned} \bar{D}_x\ (0.65) &= 2.73\ D_2 \\ \bar{D}_y\ (0.65) &= D_2 \\ \bar{D}_z\ (0.65) &= 2.15\ D_2 \end{aligned} \tag{26}$$

and

$$\begin{aligned} \bar{D}_x\ (0.52) &= 1.95\ D_2 \\ \bar{D}_y\ (0.52) &= D_2 \\ \bar{D}_z\ (0.52) &= 1.63\ D_2 \end{aligned} \tag{27}$$

Using the experimentally determined diffusivity for flow normal to the fibers in a unidirectional composite, $D_2 = 1.68 * 10^{-6}$ in^2/hr, we use (26-27) and compute the total weight gain of the two specimens as shown in Figure 5. (For later comparison, we used 4.0 x 0.060 x 2.0 and 1.0 x 0.067 x 1.0 inches for the 65 and 52 percent volume specimens, respectively.) Moreover, the figure also shows the predicted weight gain for a unidirectional composite. In all cases the initial moisture content of the composite is zero, $M_i = 0$. The plot shows that for thin flat panels, the model predicts that the stacking sequence plays a small role since the lateral edge area is so small. The unidirectional panel shows a slightly more rapid gain because of the higher diffusivity in the x direction; however the difference is extremely small. The difference between the two core and shell laminates is somewhat larger; the larger diffusivities of the higher volume fraction panel make the difference. Overall, however, it is clear that the effect of stacking sequence in thin panels is not expected to be large. These curves are compared to some test results in a later section.

In [4], Shen and Springer suggest a one dimensional approximation for weight gain. This method is based on the fact that for short times, it can be shown that the weight gain is proportional to the square root of the time. This yields

$$\frac{M(t)}{M_o} = \frac{4}{h}\sqrt{\frac{t}{\pi}}\sqrt{d} \tag{28}$$

where

$$d = D_y \left(1 + \frac{h}{\ell}\sqrt{\frac{D_x}{D_y}} + \frac{h}{b}\sqrt{\frac{D_z}{D_y}}\right)^2 . \tag{29}$$

d is thus a one dimensional diffusivity that is corrected for the lateral surfaces. Using the same parameters as the micromechanical model, (26), we obtain

$$d = 1.92 * 10^{-6} \text{ in}^2/\text{hr} \tag{30}$$

for the 0.65 volume fraction material and

$$d = 2.34 * 10^{-6} \text{ in}^2/\text{hr} \tag{31}$$

for the small volume fraction material.

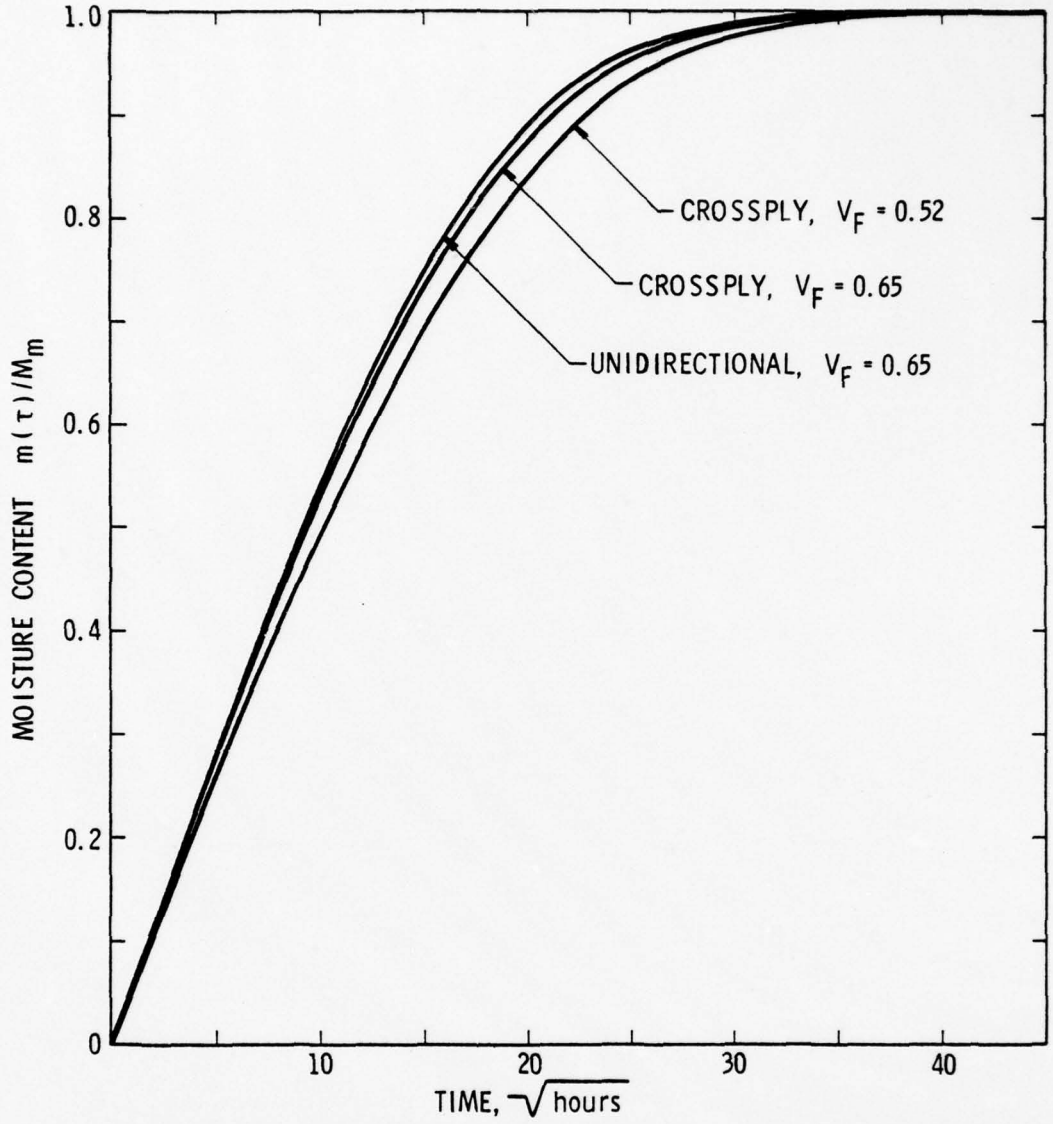

FIGURE 5. THEORETICAL MOISTURE CONTENT FOR THREE COMPOSITE LAMINATES (3D MODEL).

These two values, when substituted into (28) result in curves slightly higher than their respective three dimensional models; this is shown in Figures 6 and 7.

In deriving (5), the assumption was made that the flow depended only on the concentration gradient. Since it is known that an applied stress can influence the flow of water in a porous medium, there is a question of whether or not the level of stress in a composite will influence diffusion in the composite. In other words, can the elastostatic problem be solved separately from the diffusion relation, (5)? In [5], Gurtin presented work which showed that, for isotropic bodies, the problem does uncouple and the level of strain does not affect the concentration of moisture in the body. At the same meeting, however, Broutman [6] presented data which showed that loaded specimens gained considerably more weight during a humidity test than did unstrained specimens. The data presented by Broutman was for specimens at fairly high levels of applied strain; the level was sufficiently high that there could have been considerable cracking and void formation within the specimen. If this is indeed the case, then the properties of the composite would have been significantly altered and this would account for the high weight gain values.

Since there is not presently available a theory of thermo-hydroelasticity for anisotropic materials, it is not possible to theoretically predict the effect of applied stress on moisture gain. Moreover, the results of [6] are unclear as to whether the gain is due to an influence on the material or an alteration in the material microstructure. The tests in this program have,therefore, been conducted at a relatively low level of applied strain to determine the need for such a theory.

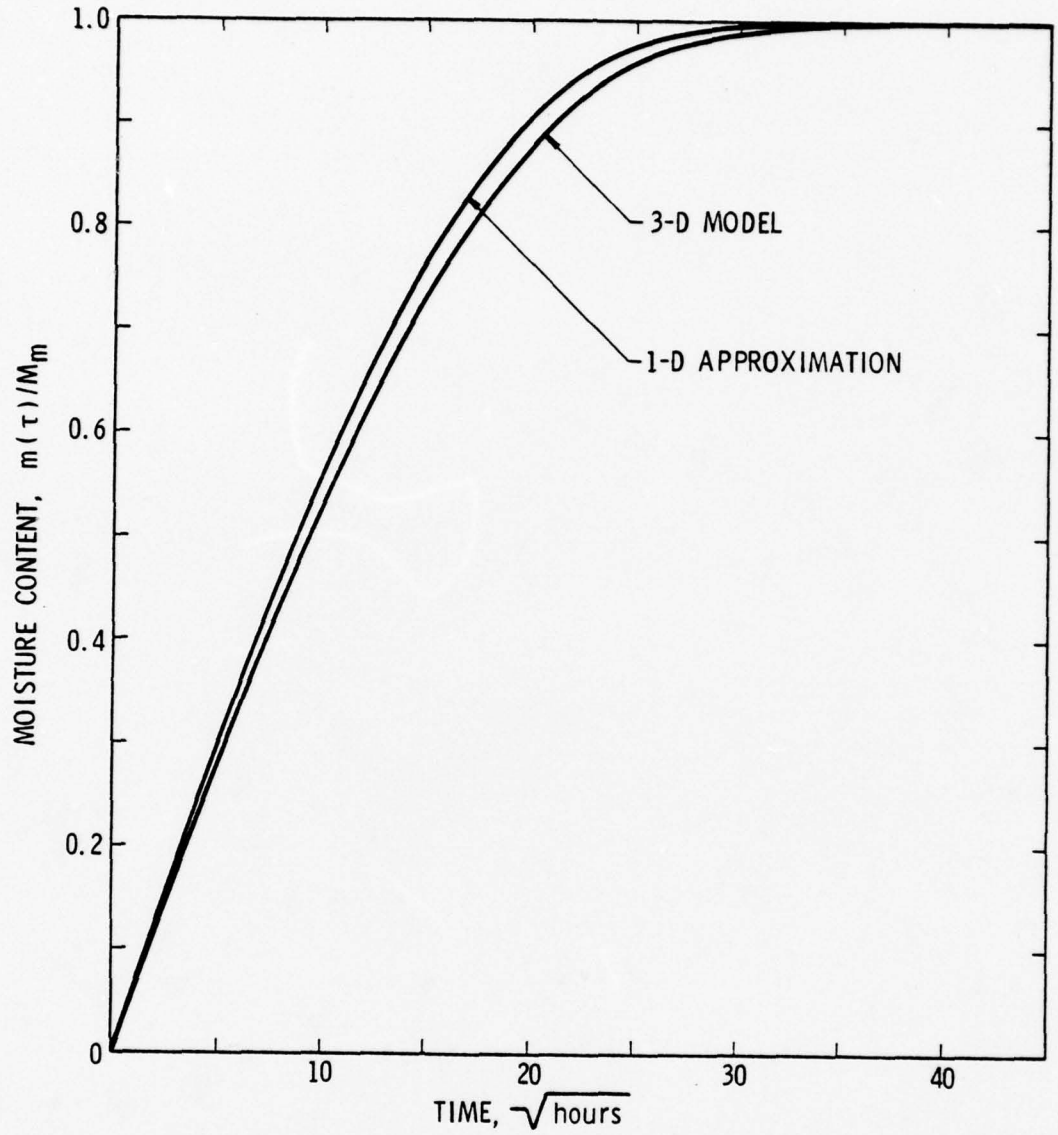

FIGURE 6. THEORETICAL MOISTURE CONTENT, V_F = 0.65.

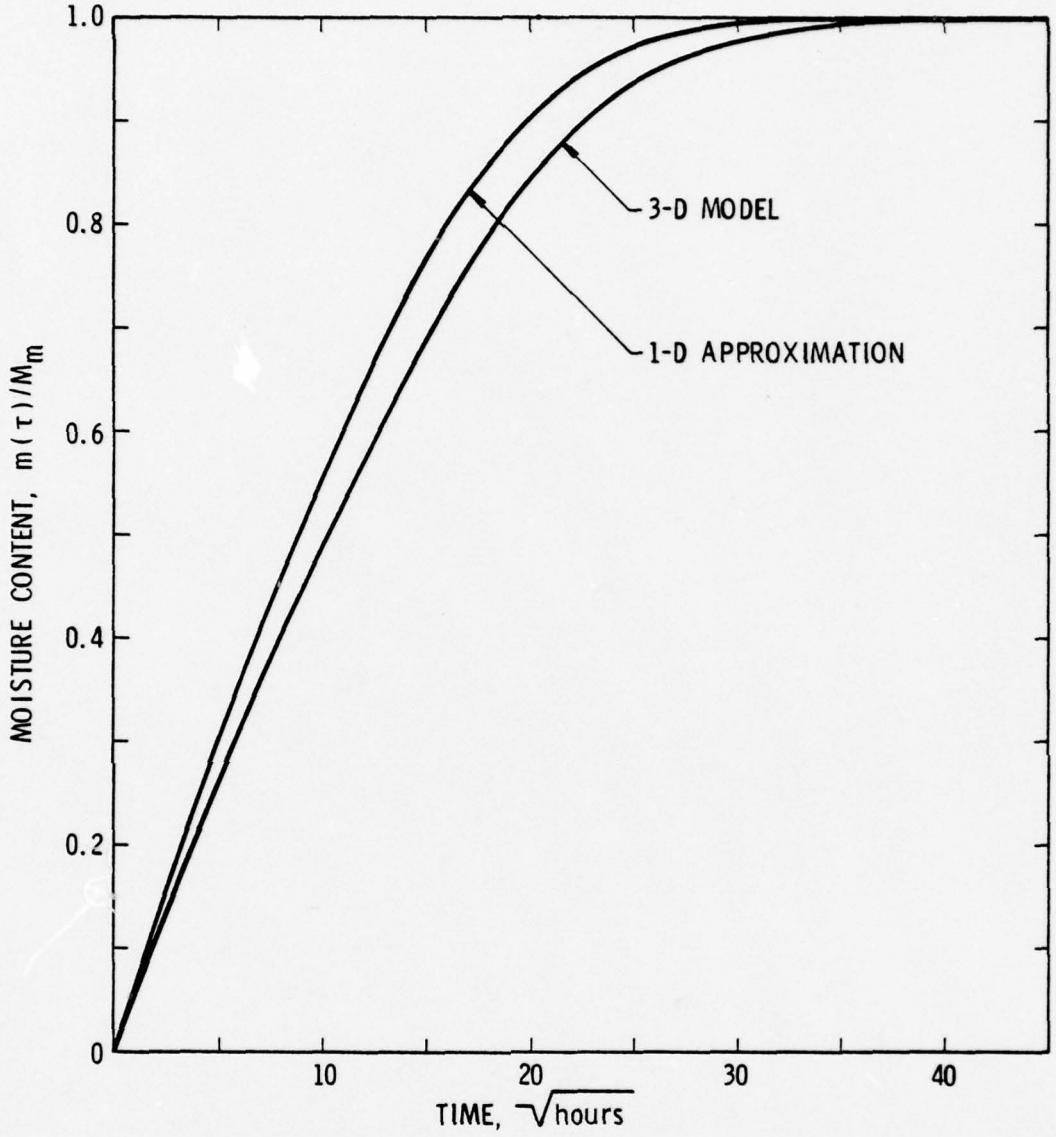

FIGURE 7. THEORETICAL MOISTURE CONTENT, V_F = 0.52.

III. EXPERIMENTAL PROGRAM

Specimen Fabrication

To better understand the mechanism of moisture absorption in composite materials, precision moisture absorption tests have been conducted. The effects of various composite parameters on moisture absorption have been examined as well as the effects of different temperatures and humidities. Specimens were of two general types; the first was used to measure moisture absorption in various composite layups, while the second tested the effects of moisture absorption on tensile properties. Laminates were fabricated with different fiber orientations, fiber volumes, and different thicknesses. An effort was also undertaken to seal the edges of many of the moisture absorption specimens to provide one-dimensional diffusion.

All test panels fabricated during the course of this program were constructed with NARMCO T-300/5208 graphite/epoxy prepreg tape. This material is widely used and according to data published by the manufacturer possesses the following room temperature material properties:

S_x^{tu}	215	E_x^t	20.5
S_y^{tu}	6.75	E_y^t	1.47
S_x^{fu}	295	E_x^f	22.0
S_y^{fu}	11.5	E_x^f	1.6

Strength (S) properties are 10^3 psi, moduli (E) are 10^6 psi. The x direction is parallel to the fibers, y is the transverse direction. Ultimate tensile properties are denoted as tu, while ultimate flexural properties are superscript fu.

This material was used to fabricate 23 laminated panels with various fiber orientations, fiber volumes, and numbers of plies. Parameters for each of the test panels are listed in Table 1. Test specimens were cut from these panels with a diamond cutting wheel. Crossply tensile specimens measured 9 inches long and 0.75 inches wide; unidirectional tensile specimens were 9 inches by 0.5 inches. All other test specimens measured 4 inches by 2 inches. Neat resin specimens were saw cut from neat resin plates.

To provide a uniform surface finish, all panels were cured in a heated platten press. Normal fabrication utilizes a cavity or blanket press but this type press cannot be used to produce low fiber volume specimens; to avoid two different surface finishes, all panels were produced with the platten press. High fiber

TABLE 1. COMPOSITE PARAMETERS FOR THE TEST SPECIMEN PANELS.

Orientation	Panel No.	Fiber Volume	Plies
±45	103	61	4
	102	57	8
	104	60	16
	105	54	20
	106	58	24
±45	108	63	8
	114	62	8
	107	43	8
	127	41	8
	118	39	8
	109	30	8
	110	30	8
	111	26	8
	126	21	8
	125	16	8
0°	101	51	8
	112	67	6
	115	55	6
	121	37	6
	128	12	6
0/90	124	28	8
	119	43	8
	129	62	8

volume panels (60-65%) were fabricated using the manufacturer's recommended curing schedule, given in Table 2. The required lower fiber volume panels (20-60%) were much more difficult to fabricate and required a small development program. It was possible, by altering the manufacturers cure cycle and by adding neat resin film between the prepreg plies, to achieve a panel with a fiber volume fraction as low as 46 percent. In order to produce panels with still lower fiber volumes, the cure cycle was carried out in a setup more akin to a molding technique, as illustrated in Figure 8. The curing cycle for these low fiber volumes were:

(1) Preheat press to 355°F.

(2) Insert layup and apply pressure for six minutes.

(3) Slowly apply full pressure, 200 psi, to push the pressure plate down to the shim stops, compressing the coroprene boundary supports.

The particular fiber volume achieved in the panel was controlled by the height of the shim stop. The height of the stop was calculated from the desired fiber volume and the cured ply thickness of a 60 percent fiber volume panel. Fiber volumes as low as 13% were achieved in this manner. Sectioning of some low fiber volume specimens revealed pockets of resin, but fiber distribution was fairly uniform as shown in Figure 9. Void content increased as fiber volume decreased, with void content as high as 5 percent being calculated for the lowest fiber volumes.

Fiber volumes were determined by taking a sample from the center of a panel, weighing it first in air, then in water to determine the panel density as per ASTM D792, "Specific Gravity and Density of Plastics by Displacement." Fiber volume was then calculated from the densities of resin and fiber by the equation:

$$V_F = \left(\frac{\rho_C - \rho_R}{\rho_F \quad \rho_R} \right) \times 100\%$$

where ρ is density, subscript C refers to the composite, R is resin, and F is fiber. Fiber volumes determined in this manner are of course an average value for the sample measured.

Neat resin panels were fabricated by first degassing the resin in a vacuum oven at 250°F until the resin had stabilized. Resin was then poured into a mold consisting of release agent coated aluminum plates shimmed 0.1 inch apart. The edges of the mold were sealed and the resin cured in an oven according to the manufacturer's recommended curing cycle. Specimens were cut from the neat resin plates with a diamond cutting wheel. Tensile specimens were then machined to a dogbone shape.

TABLE 2. STANDARD CURE CYCLE

Initial heat rise	RT-275 $\pm^{5}_{10}$°F. (135 $\pm$ $^{3}_{6}$°C) @ 4-6°F/min. (2-3°C/min.)
Dwell	60 min. beginning @ 265°F (129°C) part temp.
Pressurize	Apply 85-100 psig (5.98-7.03 kgf/cm^2) vent at 20 psig (1.4 kgf/cm^2)
Final heat rise	275 $\pm^{5}_{10}$°F (135 $\pm$ $^{3}_{6}$°C) to 355 $\pm$ $^{10}_{5}$°F (179 $\pm$ $^{6}_{3}$°C) @ 4-6°F/min. (2-3°C/min.)
Cure	120 $\pm$ 5 min. @ 355 $\pm$ 10°F (179 + $^{6}_{3}$°C)
Cool down	Cool to 140°F (60°C) or below under pressure

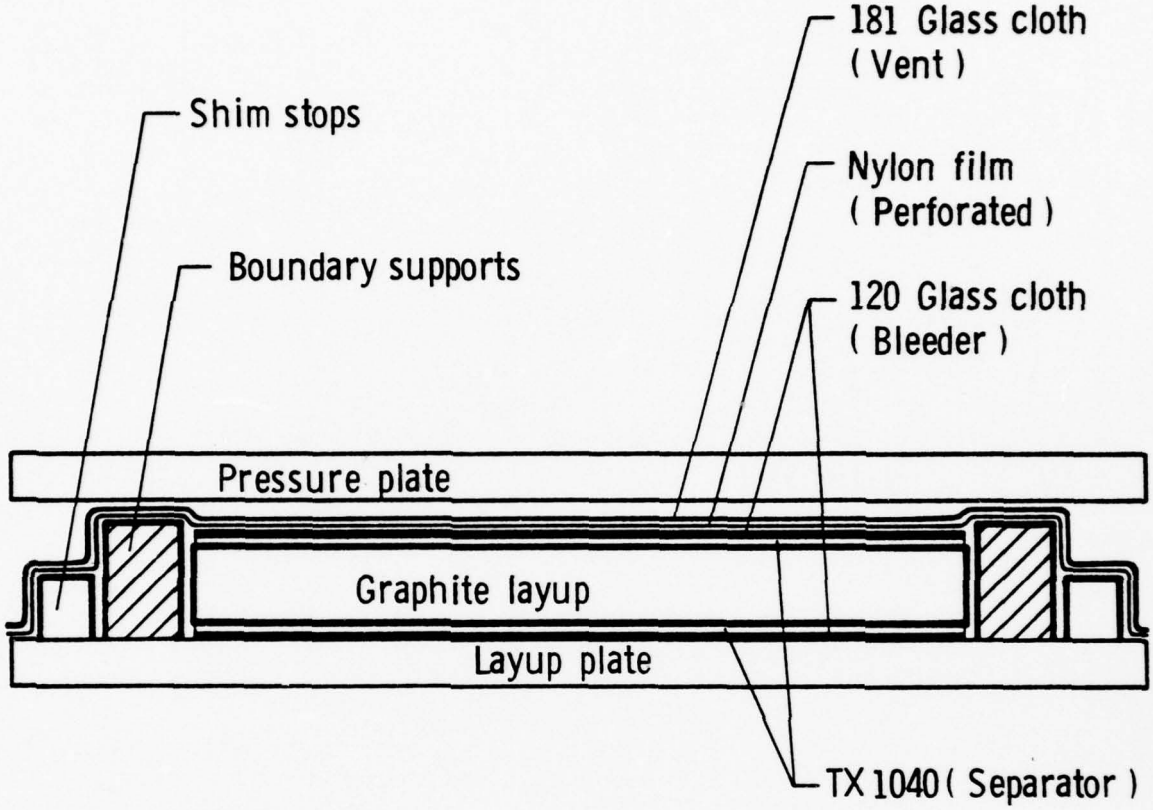

FIGURE 8. SETUP USED TO FABRICATE LOW FIBER VOLUME PANELS.

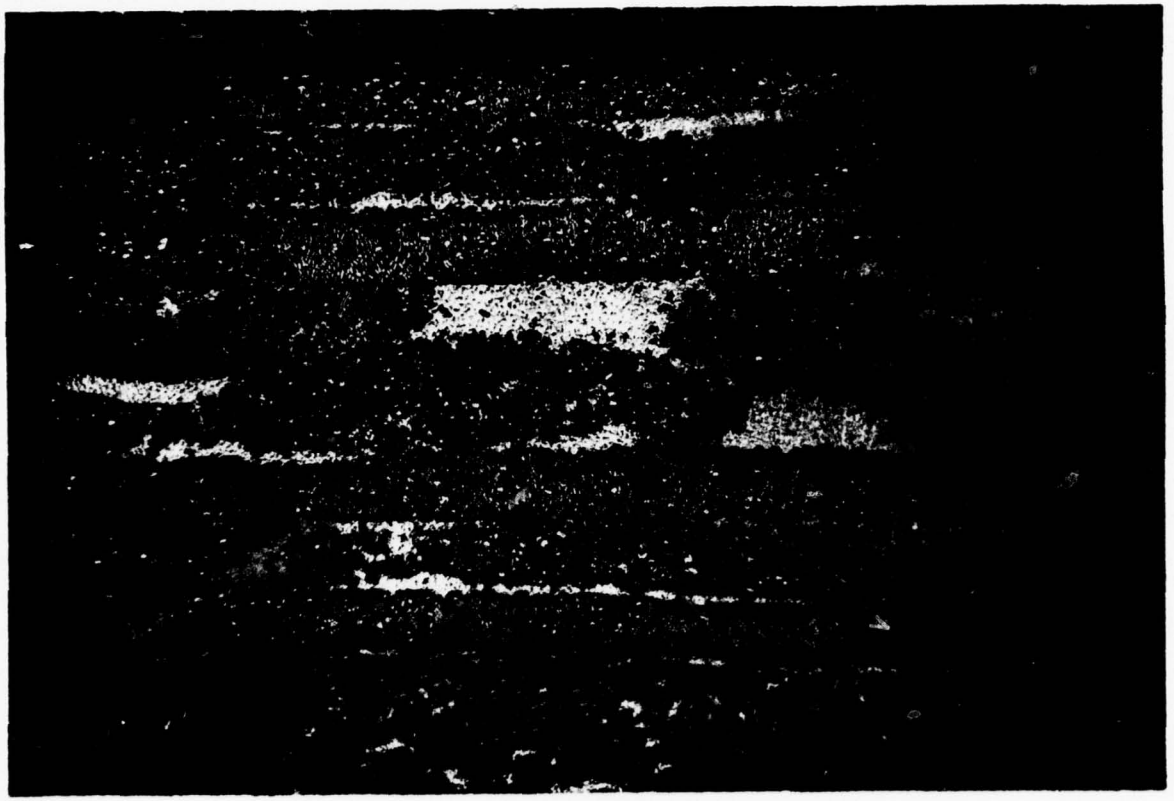

FIGURE 9. CROSS-SECTION OF 30% FIBER VOLUME PANEL, 50X.

To provide data on one dimensional diffusion, an effort was made to seal the edges of the moisture absorption specimens. This proved to be more difficult than at first realized because the seal coating itself could not be allowed to absorb moisture, thereby disturbing measurements of moisture absorption in the composites. As a first attempt, aluminum was vacuum deposited on the edges of several specimens. However, the sealed specimens gained weight more quickly than did comparable specimens with bare edges. It was then decided to use an aluminum foil seal attached with a nonmoisture absorbing adhesive. The foil seal consists of an aluminum foil sanwiched between layers of mylar film and polyethylene film. The polyethylene surface was bonded to the specimen edge with an anerobic adhesive, as anerobic adhesives are moisture resistant. Polyethylene is easier to bond to than the aluminum surface would be, thereby avoiding the usual extensive cleaning procedures required when bonding to aluminum. Indications are that this sealing arrangement, while not perfect, is a reasonably effective means of limiting moisture absorption by the edges.

Moisture Conditioning

Sets of test specimens were exposed to constant humidity, constant temperature environments. Each set of specimens at a particular environment consisted of 34 test pieces. Of these, 12 were 2" x 4" moisture absorption specimens used to measure percent weight of water gained, 12 were 2" x 4" test pieces subjected to a constant bending deformation to measure the effect of small strains on moisture absorption, and 10 test specimens were tensile test pieces to determine the effect of moisture absorption on tensile properties. Tensile test specimens were untabbed during moisture conditioning. Specifications for a typical set of test specimens subjected to one temperature-humidity environment are shown in Table 3. Three specimens with unsealed edges were also included in some tests.

Constant temperature-humidity conditions were established in controlled environmental chambers. Heat was supplied by resistance heating elements; moisture was supplied by injecting steam into the cabinet. Humidity was measured and controlled from wet and dry bulb temperature measurements. The first chamber put in use was a commercially* manufactured cabinet capable of temperatures of -30 to 350°F and humidities ranging from 20 to 95% depending on the temperature.

Because each test might take as long as 30 days, it was decided to build other environmental chambers. This was done by using the freezer compartment from an old refrigerator as an insulated cabinet. Platten heaters were attached to the inner wall of this cabinet, and steam was injected to provide

*Tenny Engineering, Inc., Union, NJ.

TABLE 3. TYPICAL SET OF TEST SPECIMENS FOR ONE TEMPERATURE-HUMIDITY ENVIRONMENT.

Type	Orientation	Fiber Volume	No. of Plies
Moisture Absorbtion	±45	61	4
	±45	57	8
	±45	60	16
	±45	54	20
	±45	58	24
	±45	43	8
	±45	41	8
	±45	30	8
	±45	26	8
	±45	21	8
	0	51	8
	N.R.	0	-
Constant Deformation*	0	55	6
	±45	62	8
	N.R.	0	-
Tensile	0	12	6
	0	37	6
	0	67	6
	+45	16	8
	±45	39	8
	±45	63	8
	0/90	28	8
	0/90	43	8
	0/90	62	8
	N.R.	0	-

*Four specimens each, at four different levels of applied strain.

the proper humidity. Two temperature controllers were used to set the particular environmental condition. One controller operated the platten heaters and was dependent on the dry bulb temperature within the cabinet, measured with a thermocouple. The other controller operated immersion heaters in a small boiler to initiate steam injection, and was dependent on the wet bulb temperature in the cabinet, measured with a thermocouple covered by a wet cotton cloth. The difference between temperature set points determined relative humidity within the cabinet. A small fan was used to continuously circulate and mix the atmosphere within the chamber. Both wet and dry bulb temperatures were monitored continuously for a period of several days and found not to vary more than 1°F, therefore providing the necessary constant environmental conditions required for the tests.

As stated earlier, moisture absorption within the specimens was determined by the change in weight of the specimens. Specimens were dried two or more days in a 150°F oven, then weighed prior to edge sealing. Edges were sealed, specimens reweighed then stored in a desicated bottle until a particular moisture test was run. During testing, the specimens were periodically removed from the moisture cabinets and weighed. A typical weighing resulted in at most a 10 minute period during which the specimen was exposed to room temperature conditions. Specimens were weighed on a Mettler balance capable of 0.0001 gram resolution then returned to the cabinet. Constant deformation specimens were of course removed from the loading fixture for weighing, then returned to the fixture and chamber.

Constant Strain Testing

Composites in service will normally be subject to some loading. One goal of this program was to determine what effect small strains will have on the moisture absorption process. Ideally, specimens would be placed in fixtures designed to subject the test specimens to a state of constant stress. Practically, 12 such fixtures would be somewhat difficult to fit in a conventional moisture chamber. Gripping would also be a problem, as the specimens are removed periodically and weighed. During this program, 2 inch by 4 inch specimens were subjected to a constant 4 point bending deformation, in fixtures of the type shown in Figure 10. Each fixture holds 4 specimens, taken from the same panel, subjected to 4 levels of applied constant deformation. Four point bending was selected because it provides a constant maximum strain between the inner loading points. Deformation (strain) is measured through small holes in the bottoms of the fixtures. Again, the object was to detect any major effect on moisture absorption caused by application of small strains, with small strains being used to avoid cracking of the specimens. Bending strains used during these tests ranged from 7.5×10^{-4} to 3.0×10^{-3}.

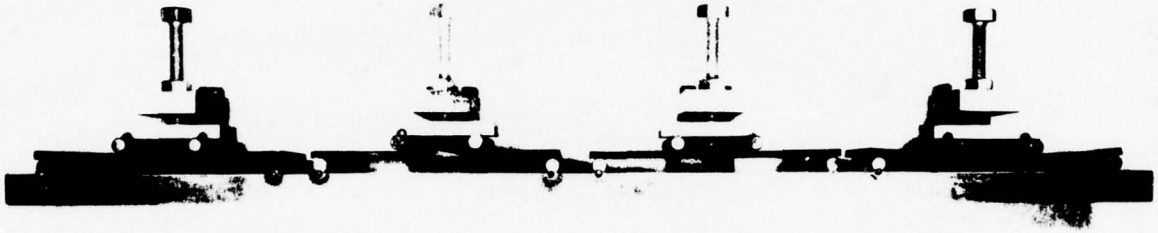

FIGURE 10. FIXTURING FOR CONSTANT DEFORMATION MOISTURE ABSORPTION TESTS.

Tensile Testing

When tensile test specimens had reached a state of moisture equilibrium, i.e. when weight gain ceased, they were removed from the environmental chamber and tabbed with glass/epoxy tabs. These tabs were attached with a room temperature setting adhesive in a process taking about 2 hours. The specimens were then returned to the moisture chamber for 48 hours to restore them to moisture equilibrium. An alternative method would have been to tab these specimens prior to exposing them to the temperature/humidity environment. This would have avoided the 2 hour time period out of a moisture chamber in order to apply tabs. However, moisture absorption in composites is very much a function of thickness, therefore the tabbed specimens would have required much more time to come to moisture equilibrium with the atmosphere as a result of the thicker end sections. More importantly, the percent weight gain method of measurement could not differentiate between moisture absorbed by the tabs, and moisture absorbed by the test specimen. For these reasons it was decided to allow the test specimens to reach moisture equilibrium before application of the tabs, then return the specimens to the moisture chamber to reabsorb lost moisture. Application of tabs to single specimens does make proper alignment more difficult to achieve, however. The tensile tests were conducted at room temperature and humidity in a standard tensile testing machine. Strains were measured with an extensometer to provide stress-strain data for elastic modulus calculation. Tests were conducted at a constant crosshead displacement rate of 0.02 inches/minute, each test lasting approximately 3 minutes.

IV. TEST RESULTS

Data Reduction

Because of the large amount of test data generated during the weight gain experiments, an automated process for storing and plotting moisture absorption data was developed for this program. The weight of the wet specimen as well as the date and time of weighing were entered into a Tektronix 4051 microcomputer for permanent storage on magnetic tape cartridges. Specimen dimensions and composite characteristics such as fiber volume were also stored. The tensile test results were also part of the data bank and were available for recall and analysis. The principal means of data presentation has been to plot the percentage weight gain versus time$^{1/2}$. The percent weight gain is calculated by

$$\Delta W = \frac{(W - W_s)}{W_i} \times 100 \tag{32}$$

where ΔW is percentage weight gain, W is weight during test, W_s is the weight of the specimen and edge seal, and W_i is the weight of the bare specimen. A typical plot is shown in Figure 11. As part of the software package, routines were written to enable superposition of several different sets of data. This means that weight gain results could be compared for any of the composite or environmental parameters.

Two parameters are needed to describe the weight gain curves typified by Figure 11; these are the diffusivity and the equilibrium moisture content, M_m. Since the majority of the specimens employed in this program had sealed edges, the diffusion was one dimensional, with flow normal to fibers, and so the diffusion coefficient is simply $D_y = D_2$. Again, because of the amount of data involved, software was written to automate calculation of effective diffusivity coefficients, using the trial and error approach described by Springer [4]. In this procedure, two points are selected on a percentage weight gain plot, one point on the initial linear slope of the curve and one point past the linear region and in the regime in which the slope of the curve is decreasing. A diffusivity D_y is assumed and the value of G is calculated for the first point from the equation

$$G = 1 - \frac{8}{\pi^2} \sum_{j=0}^{\infty} \frac{\exp\left[-(2j+1)^2 \left(\frac{D_y t}{h^2}\right)\right]}{(2j+1)^2} \tag{33}$$

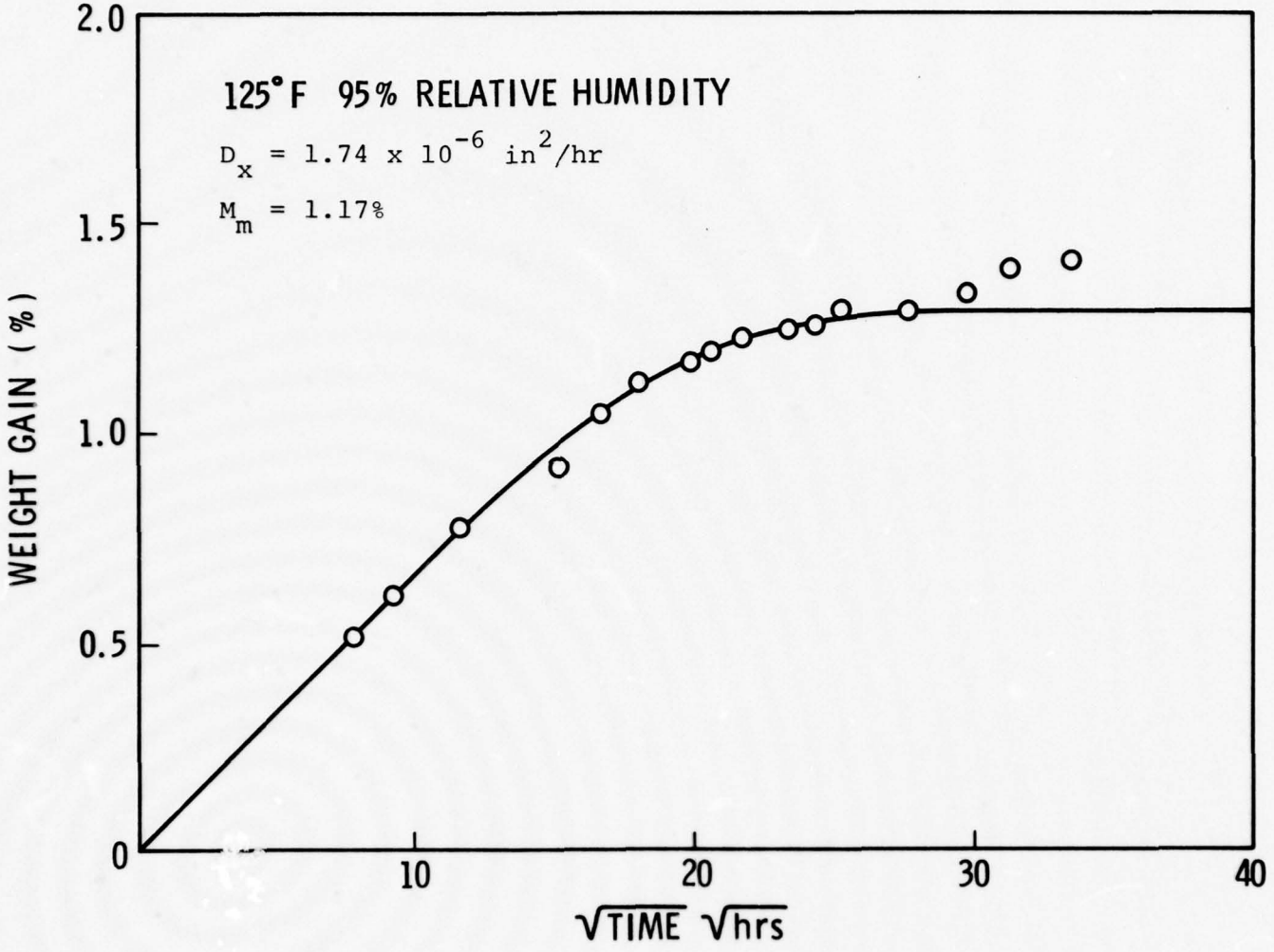

FIGURE 11. PREDICTED AND MEASURED WEIGHT GAIN FOR AN 8 PLY [±45°] LAMINATE.

where t is time in hours and h is the thickness of the specimen. The maximum moisture content of the specimen, M_m is then found from

$$M_m = \frac{M - M_i}{G} + M_i \qquad (34)$$

where M is the moisture content of the specimen and M_i is the initial moisture content. The same procedure is followed for the second point and the two M_m values are compared. If the values differ, a new diffusivity D_y is selected, and the procedure is repeated. Once D_y and M_m have been determined, the moisture content of the specimen for any time can be computed from the equation

$$M = G(M_m - M_i) + M_i \qquad (35)$$

where G is as given previously. The solid line in Figure 11 shows the results of such a calculation. For this specimen, the diffusivity is $D_y = 1.74 \times 10^{-6}$ in^2/hr while the maximum moisture content is 1.17%. Note this assumes the weight gain continues to level off and ignores the subsequent upturn in data after 30 $\sqrt{\text{hours}}$. This point will be discussed later.

Moisture Data

As previously discussed, the bulk of the specimens had their edges sealed in an attempt to obtain one dimensional diffusion. Figure 12 compares the weight gain for two unidirectional eight ply laminates, one with sealed and one with unsealed edges. The data is virtually identical, although the sealed specimen shows slightly higher gain than the unsealed specimens. Since other experiments on larger surfaces showed the seals to be fairly effective, this indicates that edges did not contribute significantly to the moisture absorption by these thin laminates.

Four temperatures were investigated in this program; 75°, 125°, 175°, and, because of its relevance to the B-1 program, 260°F. A number of different moisture conditions were investigated at these temperatures. A water bath and 75 and 95 percent relative humidities were used at all temperatures, while 40 percent relative humidity was completed at 125° and 175°F. Lower humidity tests were planned but because of the very long times necessary to complete the test, these tests were not completed. Because of the large volume of data collected, only selected comparisons will be presented.

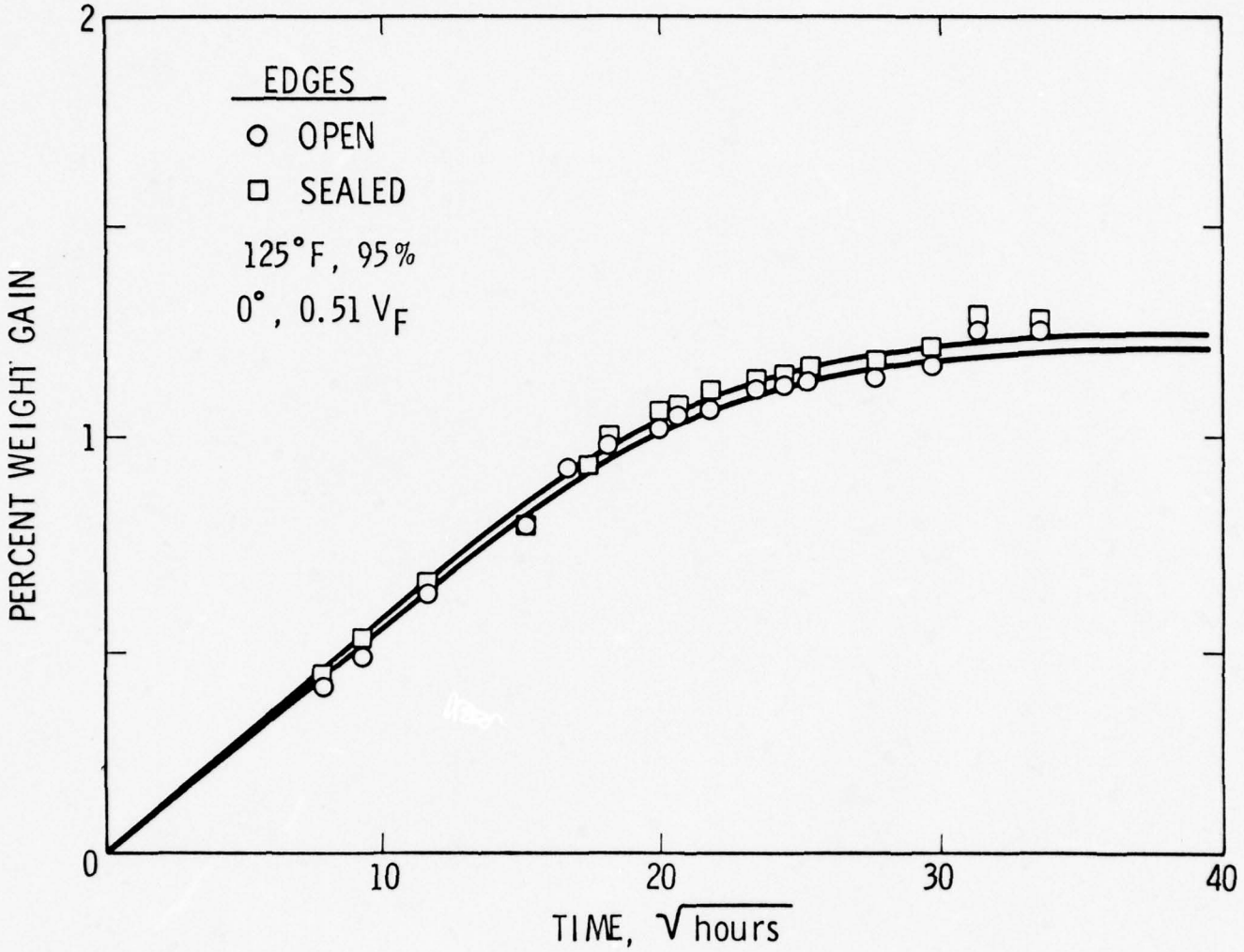

FIGURE 12. WEIGHT GAIN FOR EDGE SEALED AND UNSEALED SPECIMENS.

There have been a number of areas of disagreement among investigations regarding the effect of certain parameters. For example, McKague et. al. [7], tested identical composite specimens at the same relative humidity but different temperatures and found that the specimens reached the same equilibrium moisture content, M_m. Other work by Springer [8] showed specimens tested at the same relative humidity but different temperatures reached different equilibrium moisture contents, equilibrium moisture content increasing with temperature. Shirrell [10] reported similar findings. Because moisture concentration in the air increases with temperature for a constant relative humidity, different equilibrium moisture contents within the composites would be expected. Figure 13 compares the weight gain for $[0°]_8$ laminates tested at three temperatures at 70% relative humidity. This curve shows the expected behavior for the 75° and 125°F conditions, but a lower weight gain at 175°F. Similar results were obtained for other laminates included in these tests.

The 175°F data is puzzling as after about 4 days, many of the specimens began to lose weight. In fact, at 95 percent relative humidity, a few of the specimens even showed a negative weight gain. The severity of the weight loss problem decreased with decreasing humidity, but there still appeared to be some effect at 40 percent humidity. Weight loss in this type of experiment can be attributed to one of several causes:

1. Flaking, chipping or some other physical deterioration of the specimen in the chamber.

2. A postcure condition which drives off a gaseous component.

3. Swelling, perhaps combined with residual stresses, which close the cracks, voids, etc., and drive off water.

4. Deterioration of the sealed edges.

Of these possibilities, we saw no evidence for mechanical loss of weight. Also, since the specimens were cured at 350°F, a postcure condition seems unlikely. Hence, it is more likely that the loss is the result of the latter two conditions. At 175°F, as the test continued, we noted a pronounced deterioration in the edge seals. While not observed, there could have been some physical loss of edge sealant material which would have more effect than the increased absorption through the edges. In fact, we became convinced of the lack of effectiveness of the seals at this temperature and the 40 percent humidity specimens were not sealed. Since this condition did not show as severe effects, and these effects did not appear until late in the test, the swelling of the material forcing out the moisutre could explain this.

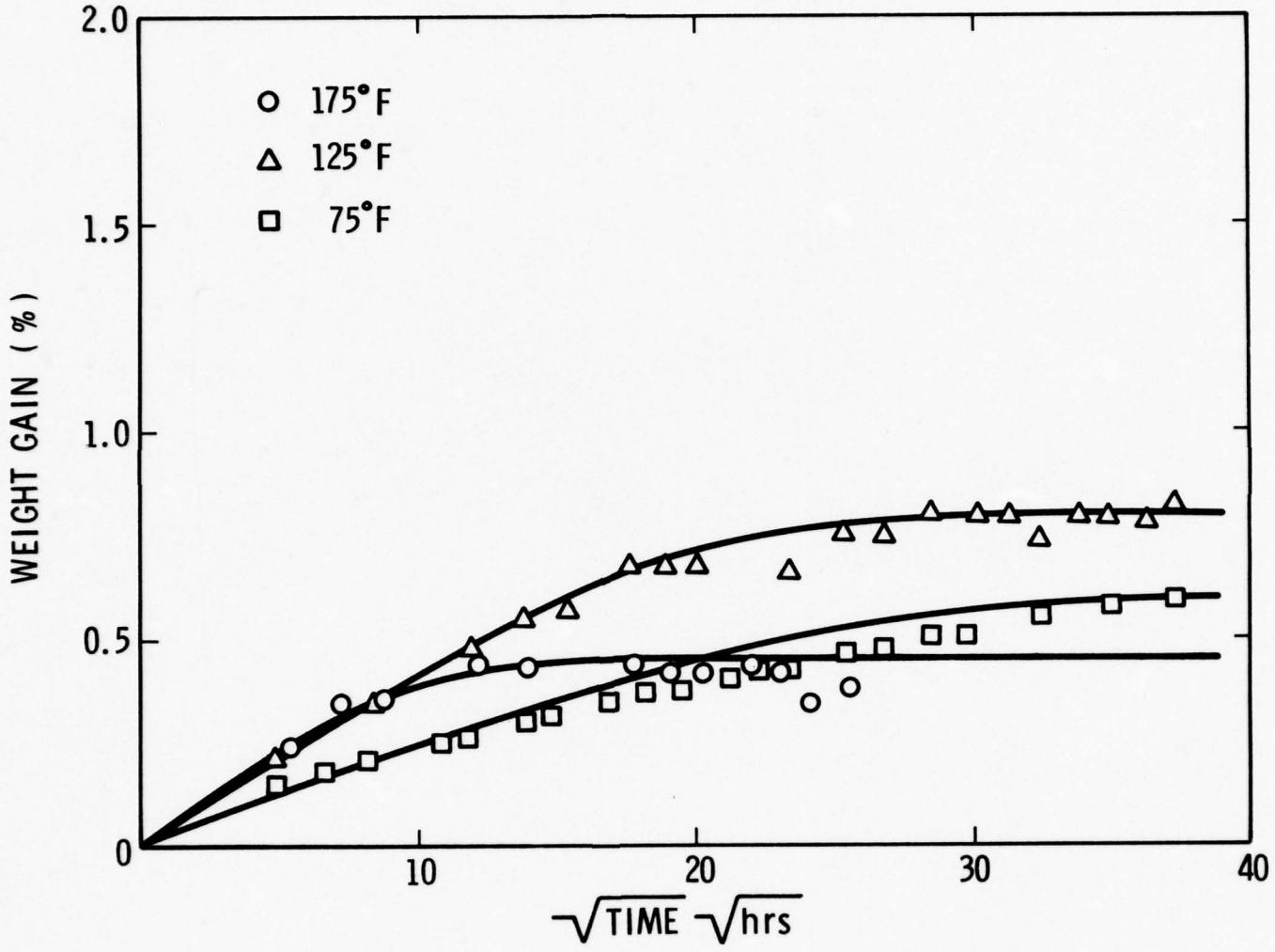

Figure 13. Moisture Absorption for $[0°]_8$ Composites, 70% Relative Humidity

There did not appear to be any consistent pattern in the weight gain experiments at 175°F. However, the thicker specimens did not appear to be particularly affected. At 70 percent humidity, we ran identical sealed and unsealed specimens. The unsealed specimen did not show a weight loss like the sealed specimen, but its equilibrium moisture content was significantly below the equilibrium content at 125°F. It should be noted that not all the sealed specimens showed a weight loss. If, as seems likely, we are seeing two sources of weight loss, i.e., the edge seals and the swelling, we are unable to explain why our experiments were especially affected by swelling when other work on nonpostcured 5208/T300 does not show such an effect [10].

When specimens at the same temperature are exposed at different relative humidities, then the weight gain should be proportional to the relative humidity. Figure 14 shows a typical result for a unidirectional panel tested at 125°F at three humidities. Similar results were observed for other composites and neat resin test specimens.

Figures 11 and 14 illustrate a pattern of behavior observed in many of the present tests as well as in other experiments [9]. After the specimen has seemingly reached equilibrium, on the order of four weeks, an upturn in the weight gain is noted. It has been suggested that this increase is due to void and crack formation in the specimen, these openings filling with water to produce the gain. Some limited sectioning experiments have, however, failed to substantiate this hypothesis.

It should also be pointed out that while this behavior is often referred to as non-Fickian diffusion, this is not really true. It is true that the weight gain relationship (24) cannot be used to predict this secondary behavior; however, it should not be expected to as the two materials are different. That is, there is no reason, at the present, to believe that we could not predict such behavior if we knew the proper diffusion coefficients for material with voids and/or cracks as well as the more homogeneous material at the beginning of a test. Models of hydrogen entrapment in metals have been developed [11,12] and show that virtually any concentration vs time behavior can be obtained depending on the particular entrapment-release parameters. Similar models for moisture entrapment in voids are being developed by Gurtin [13] and show that this is a feasible model for explaining anomolous diffusion behavior.

Thickness, as would be expected, also affects the moisture absorption process. Thicker specimens take a longer period of time to reach their equilibrium moisture content. Figure 15 shows percent weight gain versus $\sqrt{\text{time}}$ for four [$\pm$45°] laminates with different numbers of plies. These particular specimens were all tested at 125°F, 95% relative humidity. As can

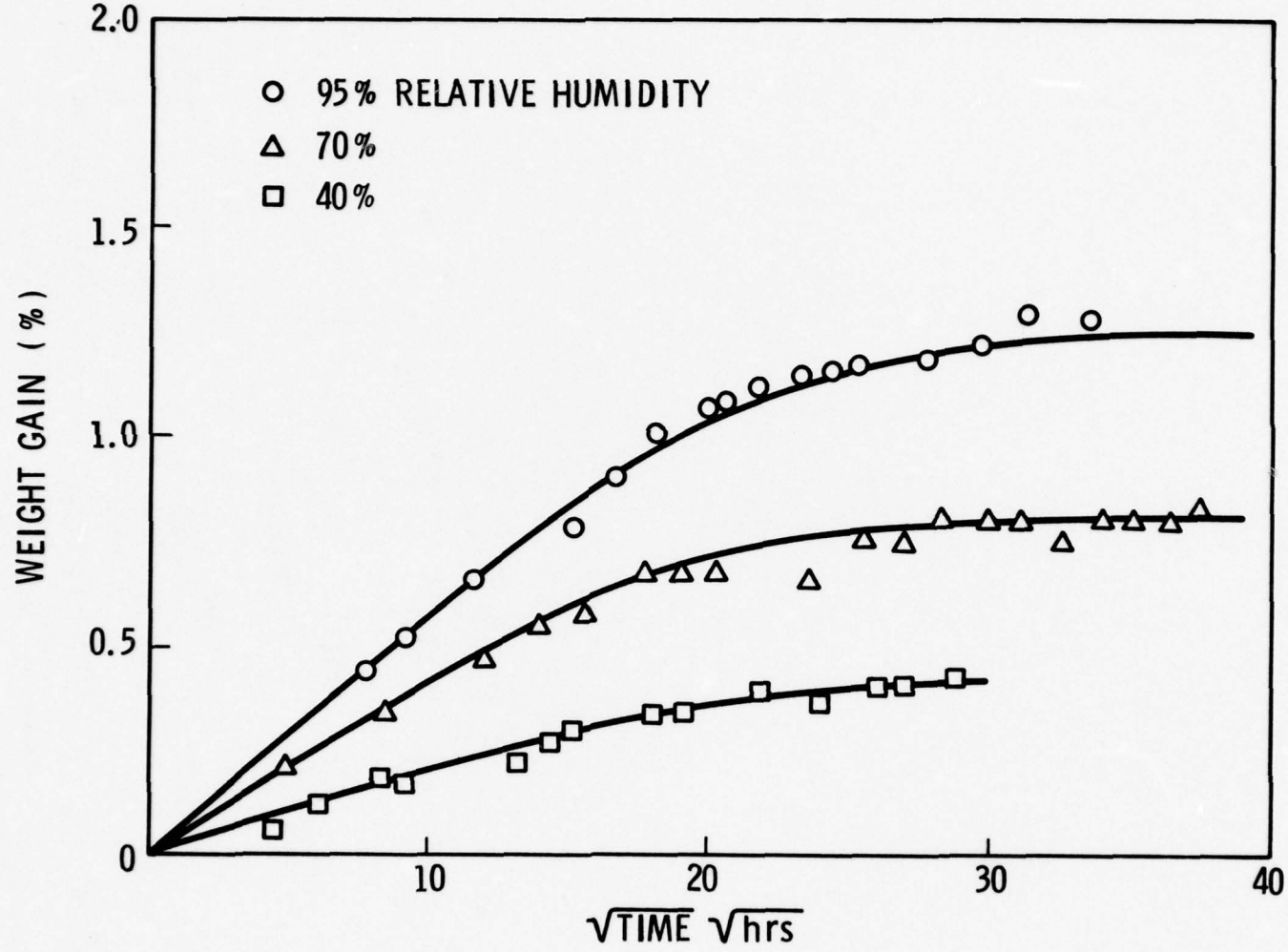

FIGURE 14. TEST RESULTS FOR $[0°]_8$ LAMINATES, 125°F.

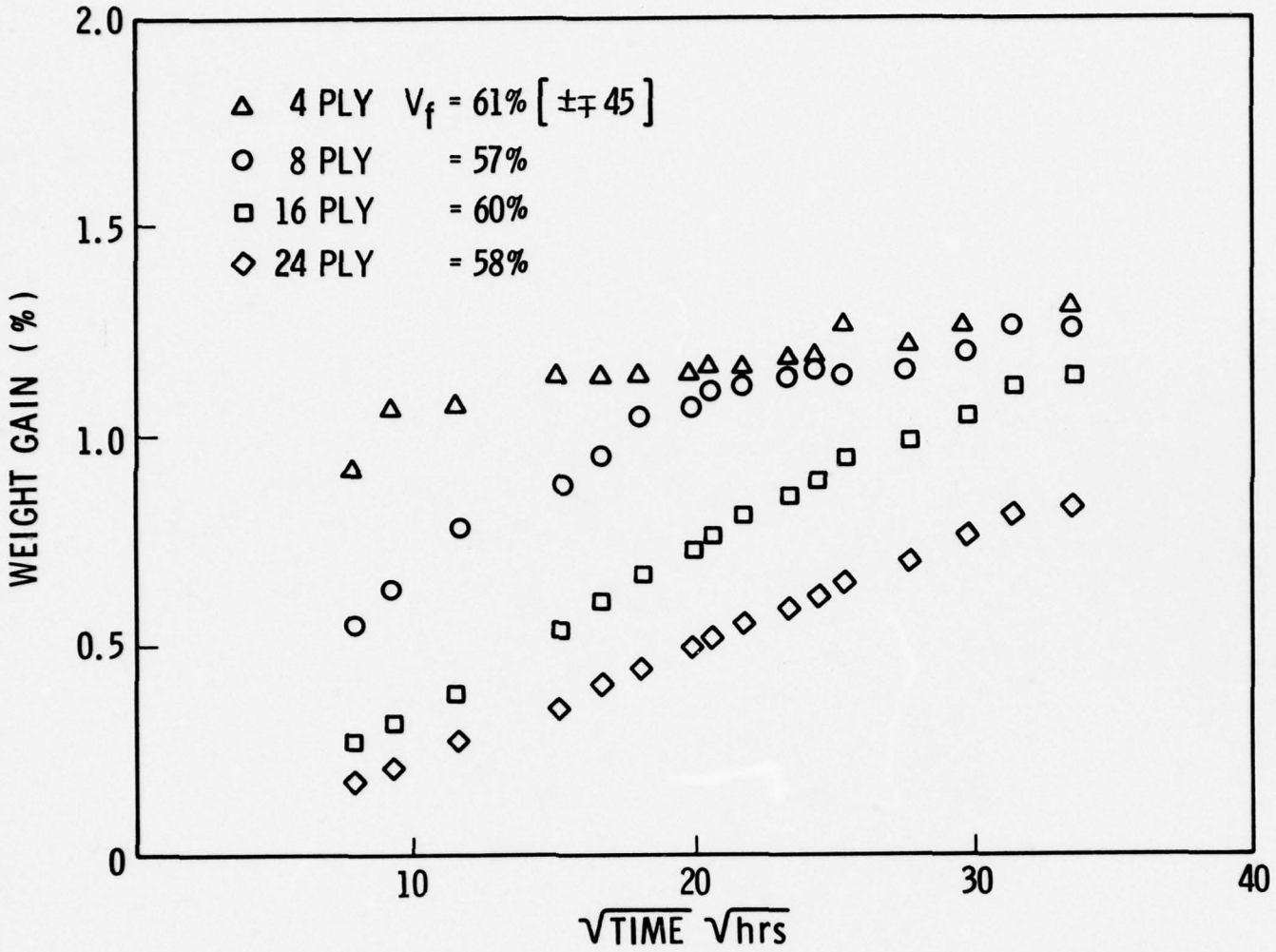

FIGURE 15. MOISTURE ABSORPTION FOR 4 THICKNESSES, 125°F, 95% RELATIVE HUMIDITY.

be seen in the figure, the thinnest specimen, 4 plies, reached its equilibrium moisture content relatively quickly. Specimens with greater thicknesses took longer periods of time; the 24 ply specimen did not reach equilibrium, even after 50 days. These tests of varying thicknesses again illustrate the necessity of developing a useful analytical model, as moisture absorption tests on structural composites will be quite time consuming.

In the one dimensional analytical model no difference in moisture absorption characteristics would be expected attributable to a variation in stacking sequence. The three dimensional model does predict a difference in moisture absorption characteristics, but this is a result of edge effects. Figure 16 compares the moisture absorption results for a cross-ply laminate and a unidirectional specimen, both exposed to 125°F, 95% relative humidity environments. Both pieces contained 8 plies and are close in fiber volume. As can be seen from the plot, the [±45] laminate initially gained weight slightly faster than did the [0°] test specimen. Both reached the same equilibrium moisture content by the conclusion of the test. Since edge seals were placed on these specimens, the moisture absorption was one dimensional. Therefore, the difference in weight gain characteristics indicates that there is a possible stacking order effect.

Figures 17 and 18 compare the three laminates used in this program at two humidity conditions; the fiber volume for these specimens range from 62-67 percent. At the lower humidity, the weight gain curves are very close, but at the 95 percent value, the 0°/90° lay-up gained much more weight. Based on all the data obtained in the program, the 0°/90° specimens generally gained more weight than the ±45° specimens, which in turn gained slightly more than the unidirectional specimens. The large variation in M_m shown in Figure 17 was unusual; most of the differences between the three ply orientations were small, as in Figure 18. Since the three specimens in these two tests were cut from the same panel, the extent of the variation in weight gain is surprising.

In comparing the results of Figures 16-18 and the other tests in this program, it does not appear that a strong case can be made for an effect of stacking sequence on the absorption of moisture. If the edge seals were perfect, then there is no difference between the two cross ply laminates during the environmental exposure and the weight gain should have been identical. If the edge seals were not perfect, then one would still expect to see little variation between the 0°/90° and the ±45° behavior. In the latter case, however, the difference is an edge effect and is not due to the stacking sequence per se. Moreover, as shown in Figure 16, the differences between layups are small. This suggests that the variation in weight gain behavior is due more to individual specimen variation than any stacking sequence effects.

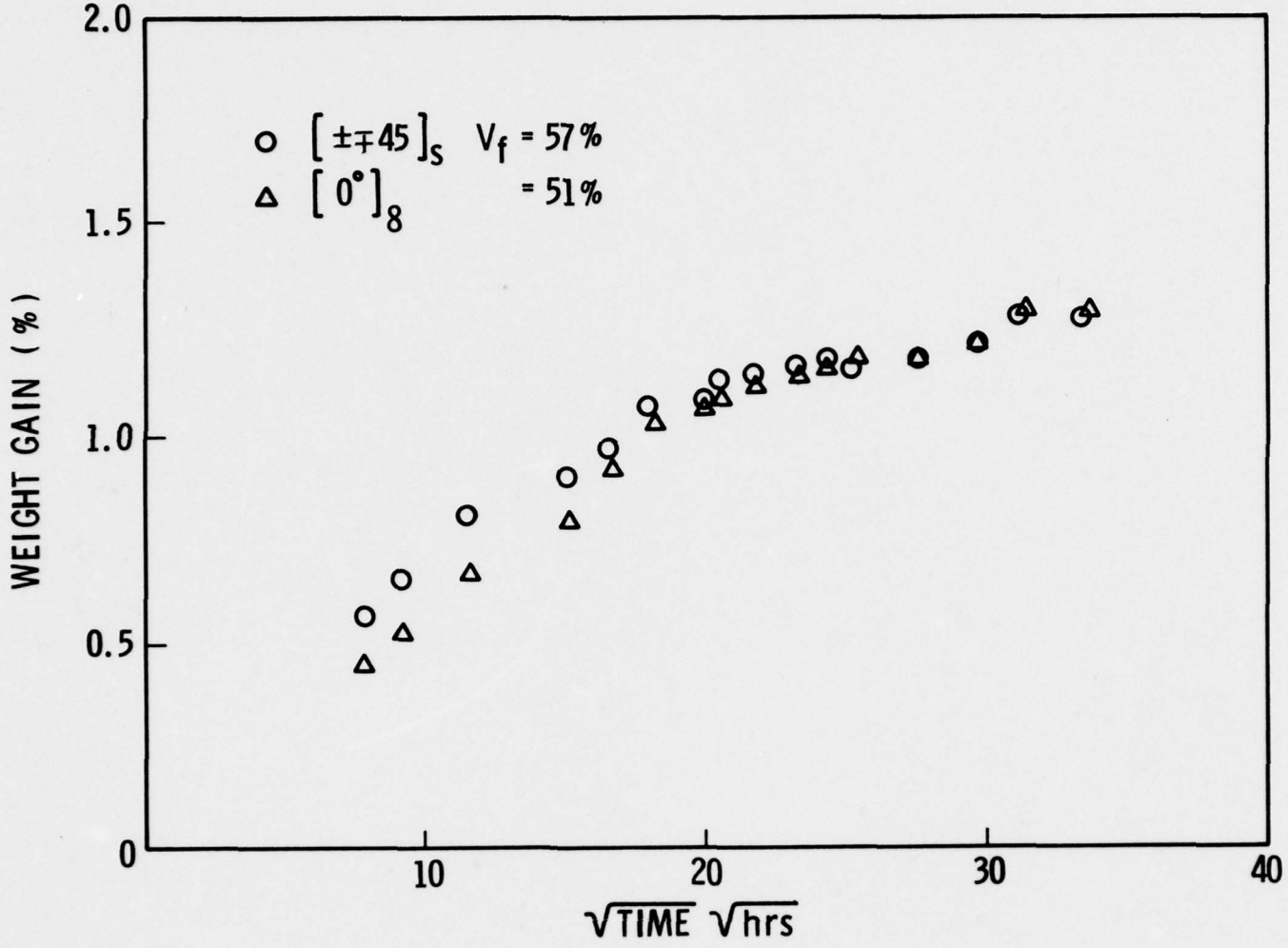

FIGURE 16. MOISTURE ABSORPTION FOR TWO LAMINATES, 125°F, 95% RELATIVE HUMIDITY.

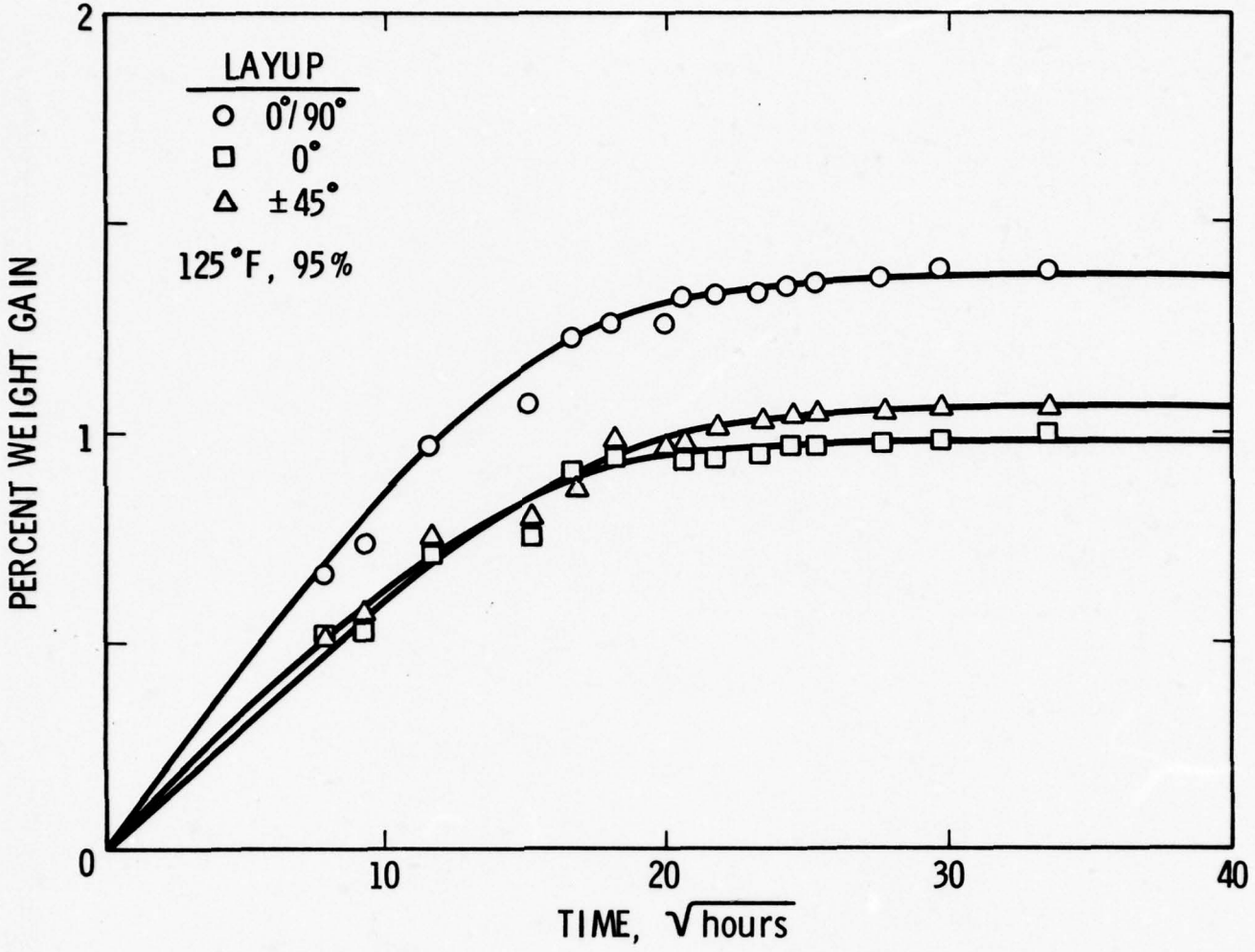

FIGURE 17. MOISTURE ABSORPTION FOR THREE LAMINATES AT 125°F, 95% RELATIVE HUMIDITY

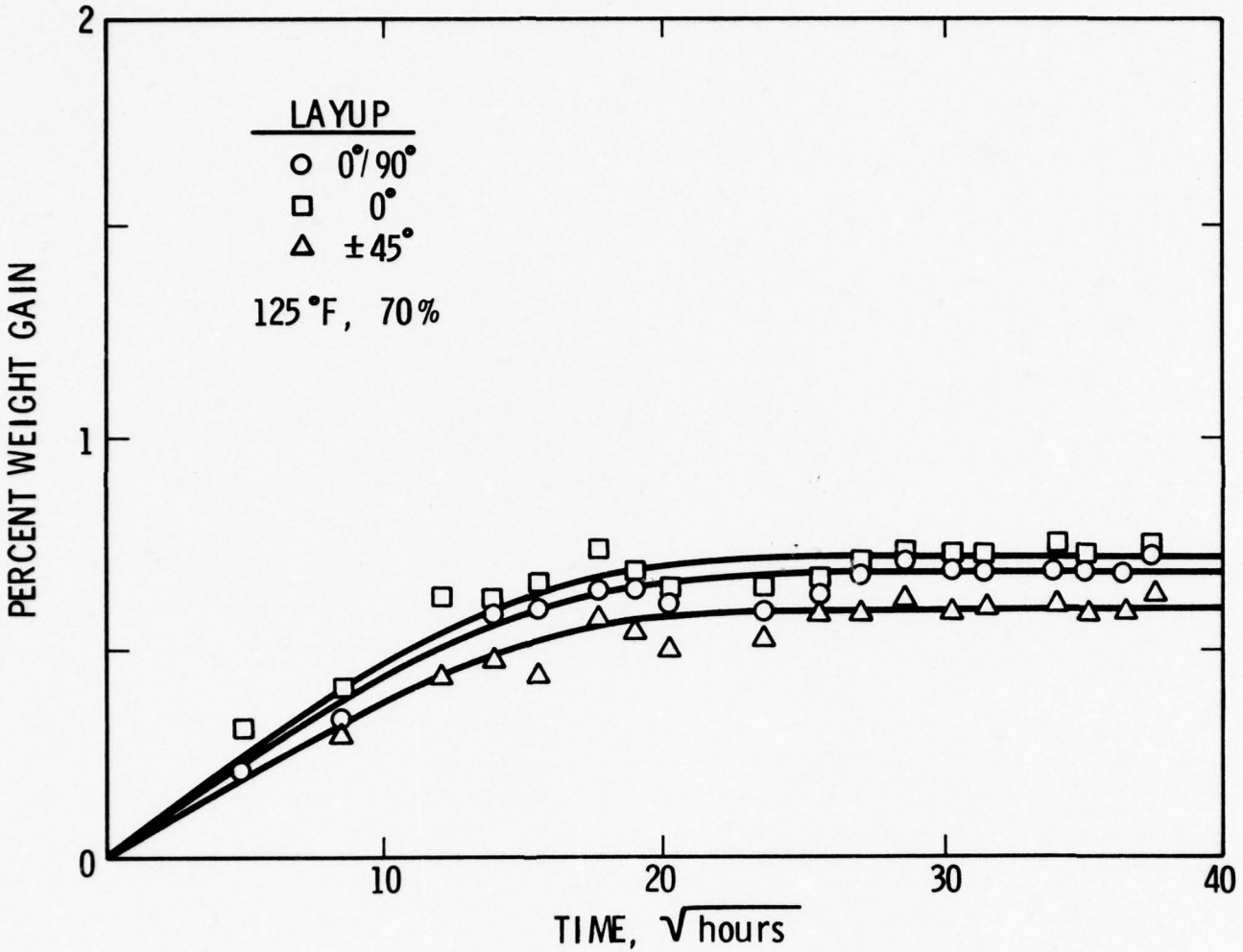

FIGURE 18. MOISTURE ABSORPTION FOR THREE LAMINATES AT 125°F, 70% RELATIVE HUMIDITY

Because moisture absorption takes place in the matrix portion of composites reinforced with inorganic fibers, the fiber volume of the composite should have a strong effect on the moisture absorption process. Total moisture absorbed should increase as the fiber volume decreases, as more matrix material is present to absorb moisture. The test results show this to be true, as can be seen in Figure 19. Here test results for four [±45] eight ply specimens of various fiber volumes tested in a 125°F, 95% relative humidity environment are shown. As can be seen in Figure 19, the amount and rate of moisture absorbed increased as fiber volume decreased. Figure 20 shows results for two neat resin and two composites specimens for two different humidities, all at 125°F. Neat resin specimens gained more weight than the composite specimens for any given set of environmental conditions.

The maximum moisture content attained by the composite is one of the key parameters used to describe the environmental behavior of composites. This weight, M_m, is shown as a function of relative humidity in Figure 21 for the 8 ply ±45° specimens. It should be noted that the M_m plotted is the equilibrium content observed during the primary diffusion stage and does not include any secondary diffusion, if such was observed. The reason for ignoring the secondary gain is that the gain is probably controlled by damage mechanisms which may be different in any given structure. Hence, these secondary effects cannot really be predicted by laboratory tests until the mechanisms of these effects are understood. Thus, while the curves in Figure 21 present minimum values of M_m, they should be representative of the maximum weight gain in undamaged materials.

The high fiber volume laminate, as shown in Figure 21, shows small increase in maximum moisture below 70 percent relative humidity, but the increase accelerates at higher humidity. According to [14], this is indicative of the diffusion becoming concentration dependent as the amount of moisture absorbed is increasing more rapidly than the amount of water available through the increased humidity.

Except for the 41 percent fiber volume data, the curves for the various fiber volumes are generally parallel. The curves show that a high fiber volume composite, operating year round at 70 percent humidity, would only absorb about 0.5 percent moisture. On the other hand, a low fiber volume material might absorb twice as much water. If such a low fiber material were used as a filler, the resulting swelling could cause damage to the structure.

The effect of small strains on moisture absorption were studied by loading some of the specimens in the environmental chamber. This loading was accomplished by using four point bending. Three specimens were used, one neat resin and two laminates. The resulting weight gain curves are given in the

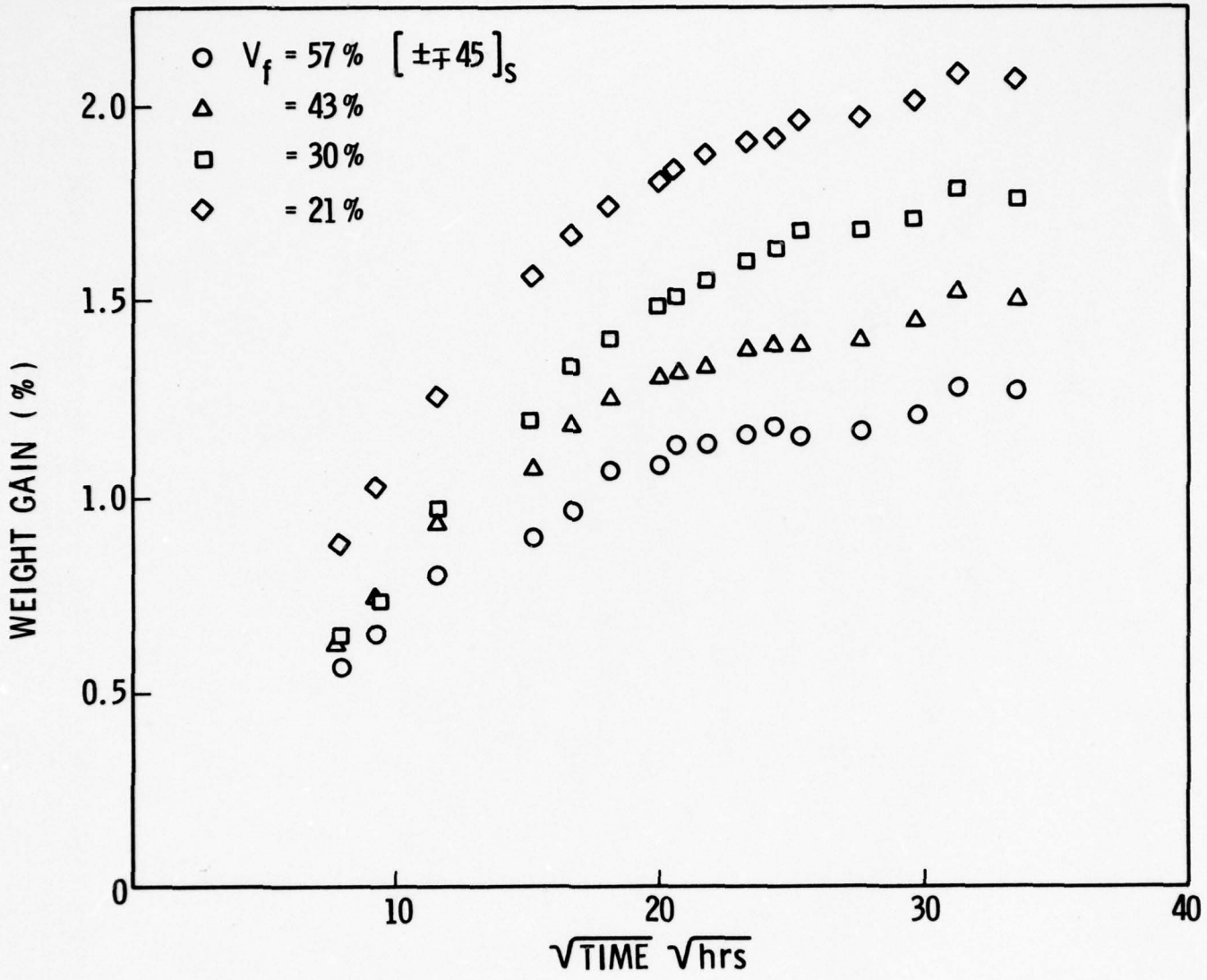

FIGURE 19 . MOISTURE ABSORPTION FOR 4 FIBER VOLUMES, 125°F, 95% RELATIVE HUMIDITY.

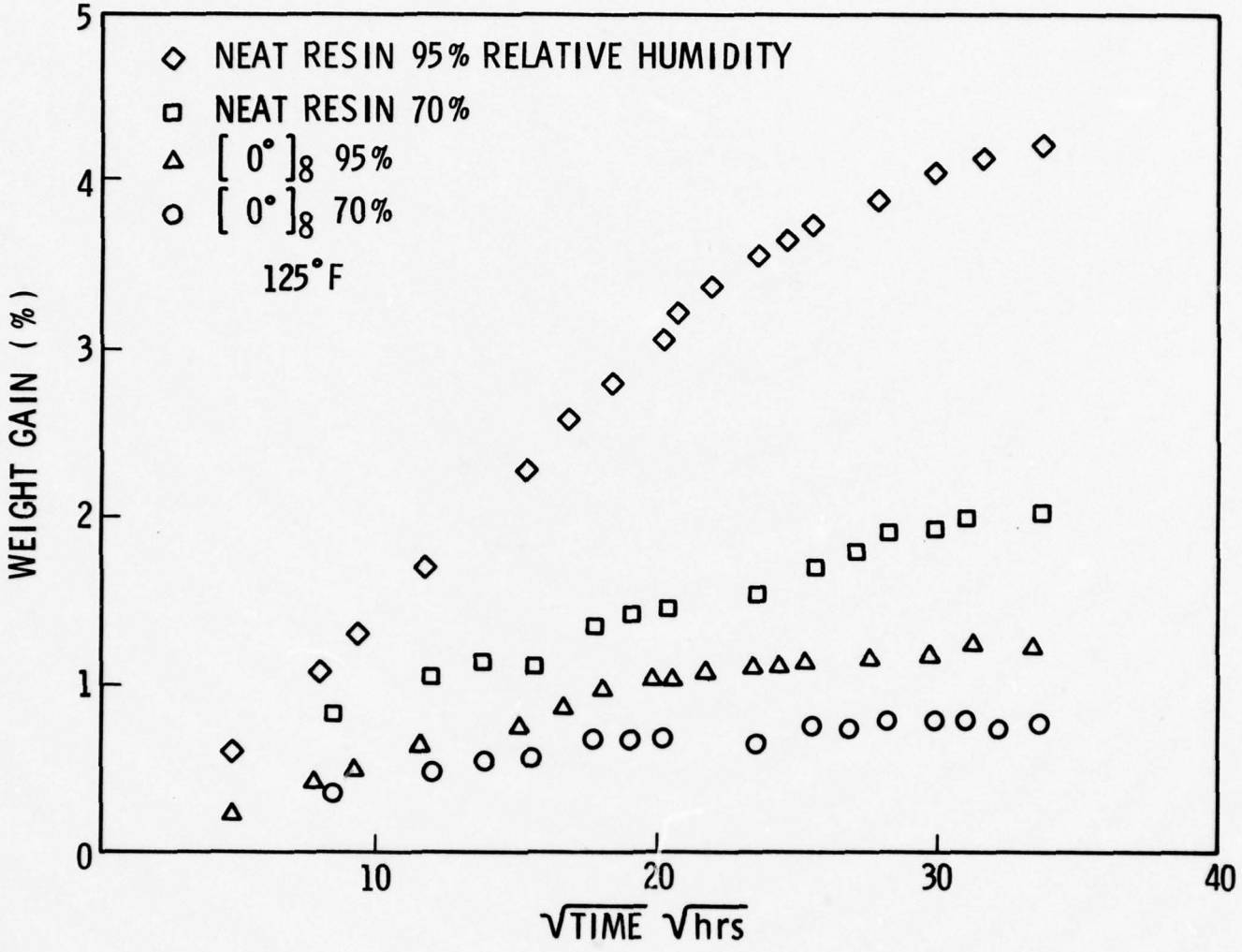

FIGURE 20. MOISTURE ABSORPTION FOR NEAT RESIN AND COMPOSITE TEST SPECIMENS.

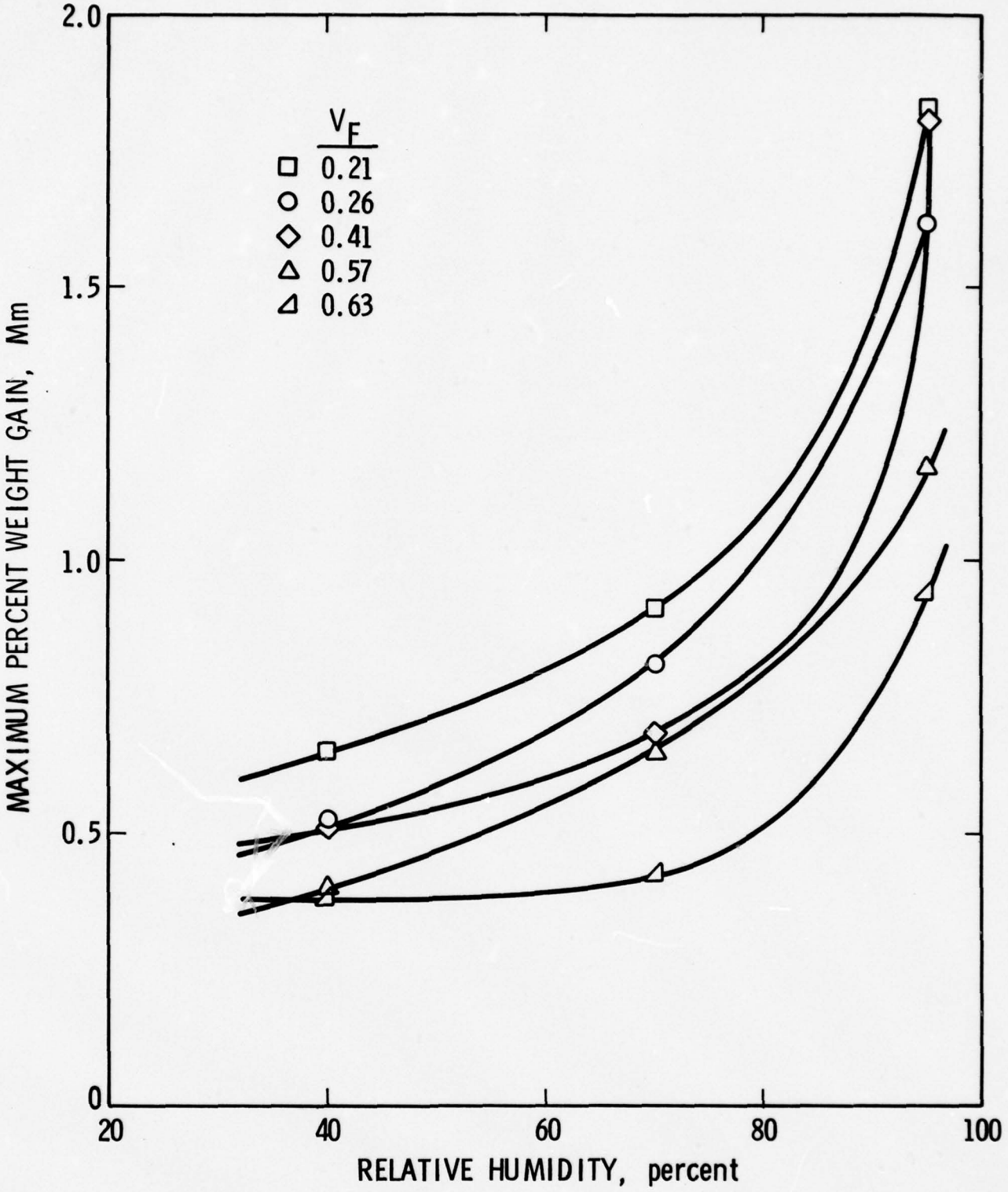

FIGURE 21. MAXIMUM WEIGHT GAIN

Appendix. Figure 22 shows the results of the 125°F, 95 percent humidity test and compares these results to the performance of an unstrained specimen. The figure shows no difference in the weight gain for the strained and unstrained specimens. No consistent pattern could be observed in the relationship of the applied load to the weight gain. This suggests that at low strains where there has been little or no damage introduced into the specimen, there is no effect of applied load. However, at higher loads which can cause cracking or otherwise induce damage into the material, these damage zones will trap moisture and cause a considerable secondary weight gain.

A series of sequence tests were performed at 125°F to check the effects of changing the environment from one humidity level to another. The two humidities used were 95 and 40 percent, with the change taking place after a week at a given level so that the specimens had not achieved equilibrium moisture levels. The weight gain results are given in the Appendix. The main feature of these curves is the extremely rapid weight loss when the humidity level is lowered from 95 percent to 40 percent. Conversely, when the humidity is raised, the initial weight gain is less rapid than in a virgin specimen. These effects are, of course, due to the moisture gradient and the high concentration of moisture at the surface.

Figures 23 and 24 show the two sequence tests for the neat resin as well as the predicted weight gain based on the diffusivities obtained in this program. The agreement is quite good except immediately after the change in humidity. This disagreement is due to the assumption of uniform initial moisture in the specimen. The rapid weight loss at the surface indicates that the surface is undergoing severe changes; if these changes result in swelling or other deformation, the surface could readily develop fatigue cracks under environmental cycling.

Tensile and Spiking Tests

A number of specimens were taken from each condition completed and tensile tested. As previously discussed, these specimens were tested at ambient laboratory conditions and not at the absorption environment. While there is some weight loss during the tensile test, it is restricted to the surface and should not greatly affect the tensile and modulus properties of the bulk material. These effects would be much more important in a long term test since the local swelling can produce surface cracks or defects which would alter the results of a fatigue test, for example.

The tensile results are given in Tables 4-7; some results are also given for the 95 percent relative humidity in Figures 25-27. Because of the unique character of each of the panels and the wide range of the test program, there was not enough material for multiple specimen testing and hence the results,

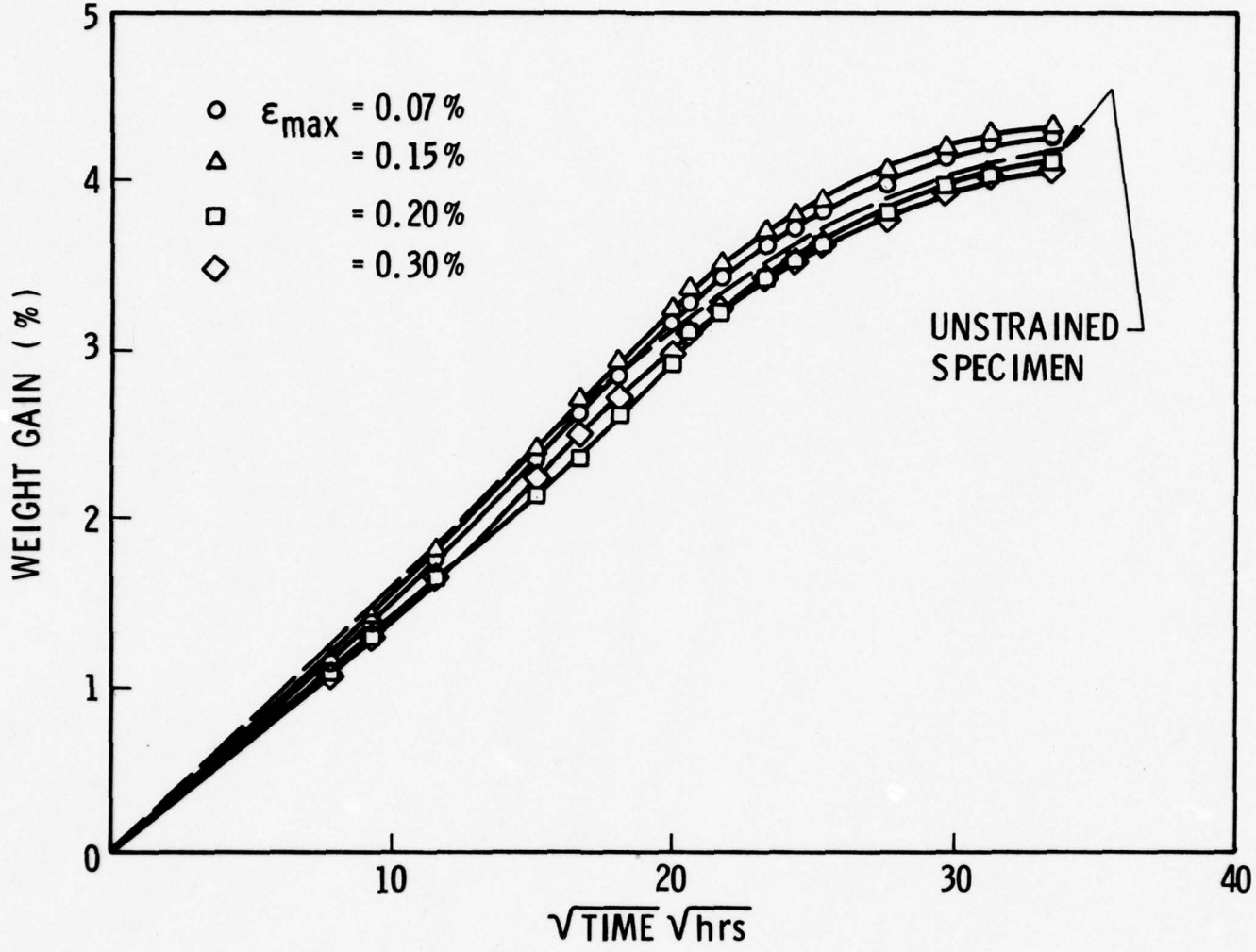

FIGURE 22. MOISTURE ABSORPTION FOR STRAINED NEAT RESINS SPECIMENS, 125°F, 95% RELATIVE HUMIDITY.

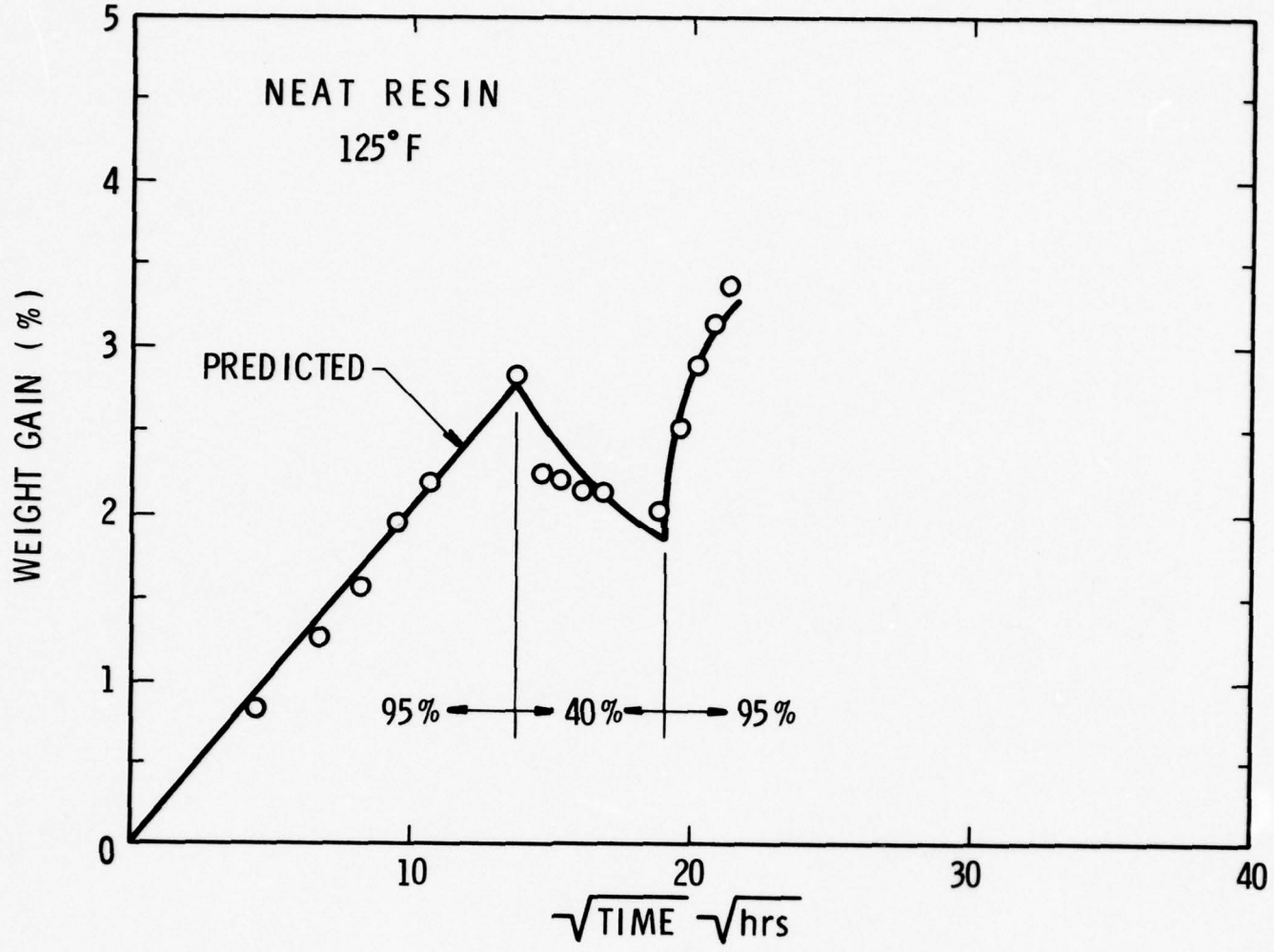

FIGURE 23. RESULTS OF THREE STEP SEQUENCE TEST, 125°F.

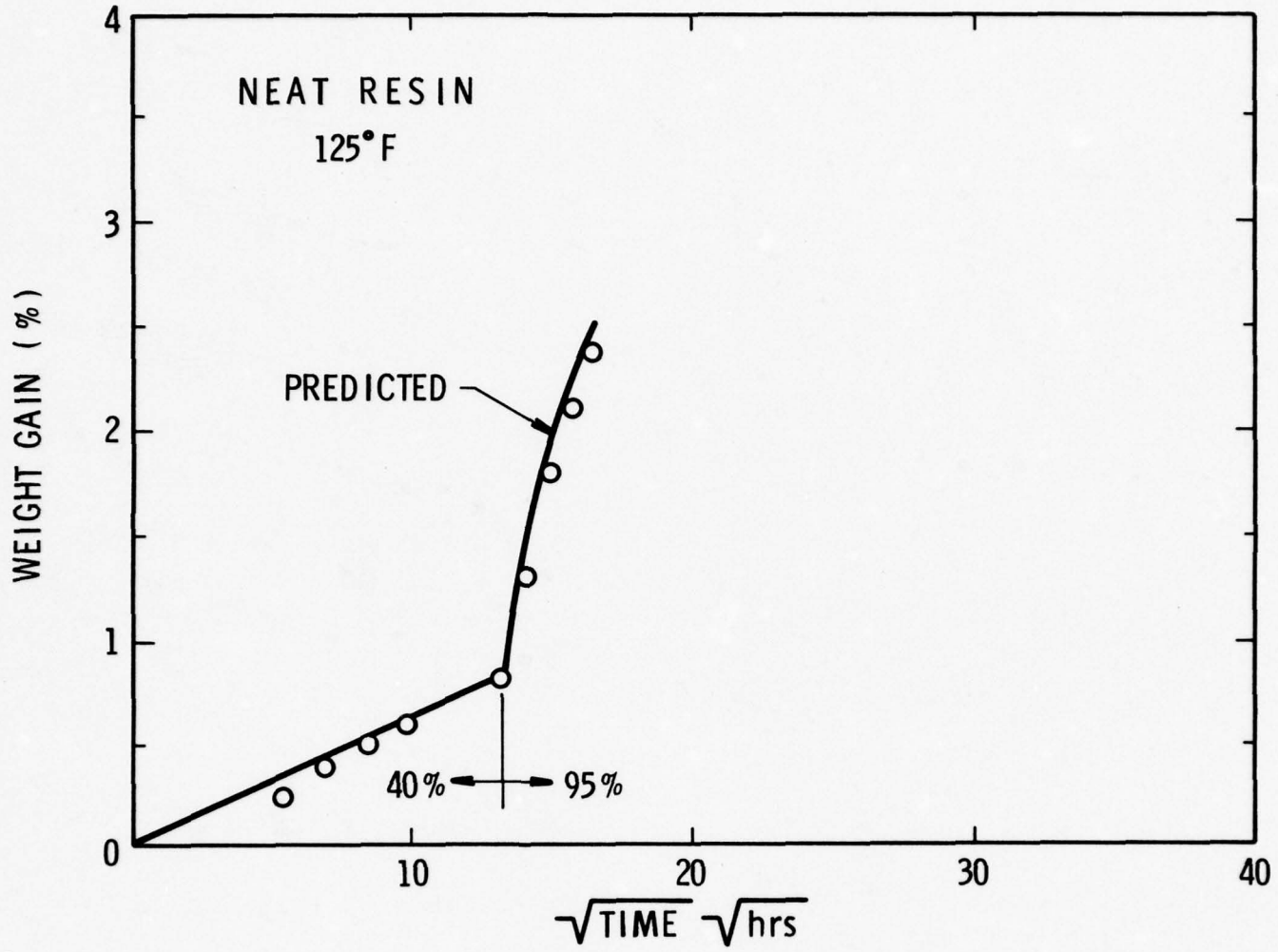

FIGURE 24. RESULTS OF TWO STEP SEQUENCE TEST, 125°F.

TABLE 4. TENSILE DATA FOR 0° SPECIMENS

Temp. (°F)	Humidity (%)	V_f = 12% S_x^{ut}	V_f = 12% E_x	V_f = 37% S_x^{ut}	V_f = 37% E_x	V_f = 67 S_x^{ut}	V_f = 67 E_x
175	95	68.5	11.4	88.2	11.3	80.0	20.0
175	70	75.6	10.0	67.5	13.2	119.3	23.4
175	40	76.4	10.9	51.4	7.0	143.0	21.0
125	95	74.2	12.8	105.0	13.5	93.6	26.2
125	70	73.8	10.1	114.2	11.7	172.5	23.4
125	40	45.3	8.7	49.8	10.2	184.7	18.8
75	95	72.7	9.7	57.4	7.4	86.2	18.0
75	70	60.6	9.5	42.1	9.1	117.6	*
260	W.B.	62.2	17.8	40.5	15.6	49.1	38.6
175	W.B.	68.3	8.1	59.0	13.6	99.3	14.3
125	W.B.	63.0	11.0	55.3	9.8	98.6	21.9
R.T.	Dry	55.1	8.9	64.3	11.4	101.7	20.7
R.T.	Dry	65.8	9.2	56.5	9.3	119.0	23.8

Strengths = 10^3 psi

Moduli = 10^6 psi

W.B. = Water Bath

R.T. = Room Temperature

*Extensometer Slipped

TABLE 5. TENSILE DATA FOR +/-45° SPECIMENS

Temp. (°F)	Humidity (%)	V_f = 16		V_f = 39		V_f = 63	
		S_x^{ut}	E_x	S_x^{ut}	E_x	S_x^{ut}	E_x
175	95	14.5	1.3	16.1	2.4	17.6	2.2
175	70	14.8	1.4	12.2	1.2	20.1	2.4
175	40	13.8	1.4	12.7	1.3	19.3	2.5
125	95	18.6	1.6	13.0	1.2	14.2	2.4
125	70	15.9	1.4	15.3	2.2	12.5	2.4
125	40	15.3	1.5	16.1	1.4	19.4	2.6
75	95	20.8	1.5	19.3	1.5	20.3	2.4
75	70	16.4	1.4	16.3	1.7	23.8	3.1
260	W.B.	11.6	2.3	9.1	2.3	10.4	3.0
175	W.B.	14.4	1.4	18.7	1.5	17.5	2.3
125	W.B.	21.2	2.0	16.3	1.4	17.3	2.9
R.T.	Dry	16.7	1.5	15.0	1.5	17.5	2.4
R.T.	Dry	12.1	1.3	15.7	1.4	18.7	2.5

TABLE 6. TENSILE DATA FOR 0/90° SPECIMENS

Temp. (°F)	Humidity (%)	V_f = 28		V_f = 43		V_f = 62	
		S_x^{ut}	E_x	S_x^{ut}	E_x	S_x^{ut}	E_x
175	95	24.5	5.3	51.2	7.5	83.7	9.4
175	70	0*	0*	72.7	7.1	75.7	10.4
175	40	41.3	6.6	73.3	8.3	83.6	11.6
125	95	33.7	6.1	63.5	8.3	88.3	10.1
125	70	42.1	5.8	82.2	8.3	91.9	11.7
125	40	36.8	5.4	61.4	8.2	46.7	10.2
75	95	37.8	4.6	58.5	7.2	89.0	9.3
75	70	37.7	9.4	66.8	8.1	58.5	8.1
260	W.B.	12.8*	2.8*	30.9	6.6	68.6	17.6
175	W.B.	46.0	5.9	58.3	7.4	85.5	9.6
125	W.B.	30.3	4.8	66.9	8.4	52.4	7.5
R.T.	Dry	46.5	6.7	56.1	6.9	63.1	10.9
R.T.	Dry	25.6	4.8	59.3	7.4	56.8	8.1

*Defective Specimen

TABLE 7. TENSILE DATA FOR NEAT RESIN SPECIMENS

Temp. (°F)	Humidity (%)	V_f = 0% S_x	E_x
175	95	4.3	.67
175	70	5.1	.56
175	40	4.5	.54
125	95	0	0
125	70	3.5	.56
125	40	3.9	.55
75	95	6.6	.49
75	70	0*	0*
260	W.B.	4.8	.86
175	W.B.	0*	0*
125	W.B.	4.8	.49
75	W.B.	0*	0*
R.T.	Dry	3.6	.50
R.T.	Dry	3.8	.50

Strengths - 10^3 psi

Moduli - 10^6 psi

W.B. - Water Bath

R.T. - Room Temperature

*Defective Specimen

based on single specimen tests, are more scattered than might normally be observed. Figure 25 shows the effect of environmental exposure temperature on the tensile strength of the unidirectional specimens of three volume fractions. As would be expected, the lowest fiber volume specimens show the lowest strength. However, the middle volume fraction showed higher strengths than did the higher 0.67 percent fraction. The results for the three exposure temperatures are consistent although the 0.37 specimen at 305°K failed prematurely in the grip and so the low temperature regime is shown dotted. Generally, this data agrees with other published data indicating that below 300°F, there is not much effect of humidity on the tensile strength. Rather, as the temperature is increased, there is a small decrease in tensile strength, indicating that temperature rather than humidity is the primary influence on tensile strength.

The two low fiber volume baseline strengths are considerably lower than the environmentally exposed specimens. This is not surprising as the low fiber volume specimens would be expected to show much more scatter. The 0.67 specimen showed a 20 percent higher baseline strength than the environmental specimens. However, this baseline strength is only half the manufacturer's specified value, even though the modulus agreed with the specified values. Since a number of long term exposure tests were already in progress when these results were obtained, and since the tensile results for the panel were self-consistent, it was decided to go ahead with the existing panels since the behavior trends for the given panel are the important features.

Figures 26 and 27 show similar results for the 0°/90° and the $\pm$45° specimens. The 0°/90° lay-up shows a large effect of fiber volume on the tensile strength. Also, the specimens generally showed a small decrease in tensile strength with environmental exposure temperature. On the other hand, the 45° layup showed little effect of volume fraction, while also showing a slight temperature effect.

As noted in the tables, there was generally little effect of moisture on either the tensile strength or the modulus. The exception to this is the unidirectional, 67 percent fiber volume specimens which showed dramatic strength increases after exposure to low humidities; the modulus, however, was unaffected and agreed with published values. Since it is difficult to obtain proper alignment when applying tabs to individual small specimens and a number of these specimens failed at the grips, this suggests that there may have been a problem with the tabs on these specimens. Possibly, this did not show up on the lower fiber volume specimens as the increased resin content allowed for some minor self-alignment and more uniform load transfer to the smaller number of fibers.

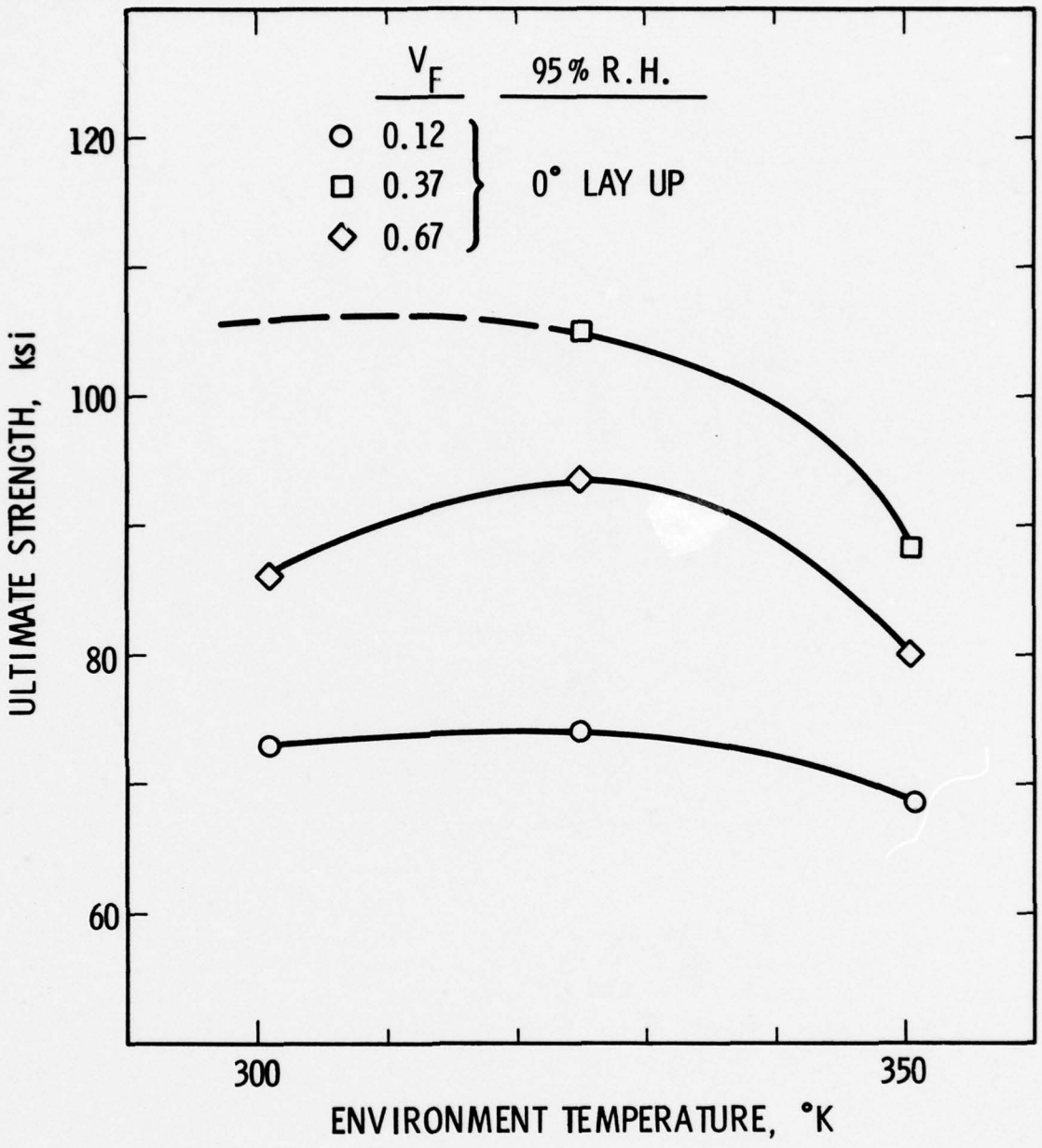

FIGURE 25. TENSILE TEST RESULTS, 0° LAMINATE.

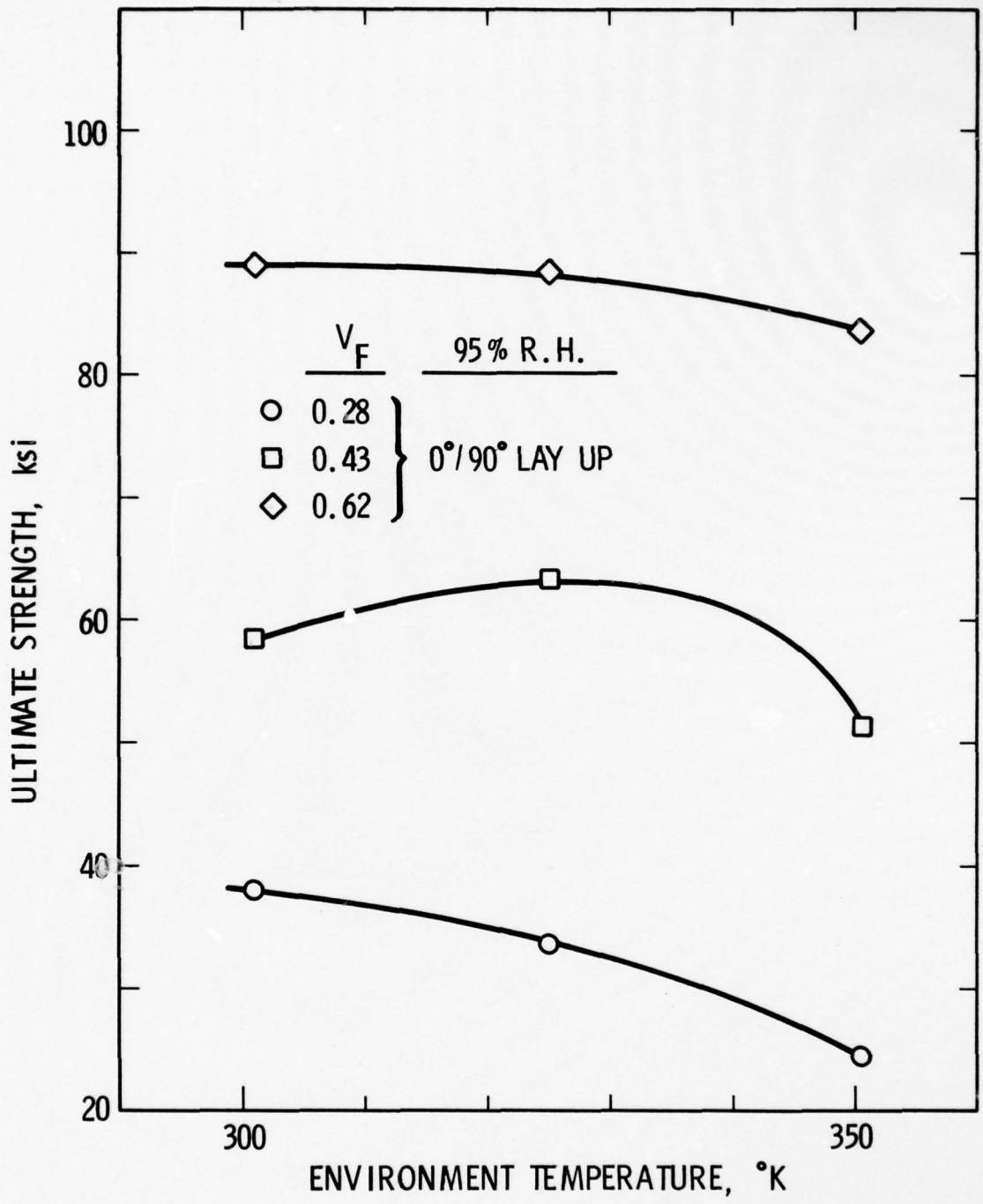

FIGURE 26. TENSILE TEST RESULTS, 0°/90° LAMINATE.

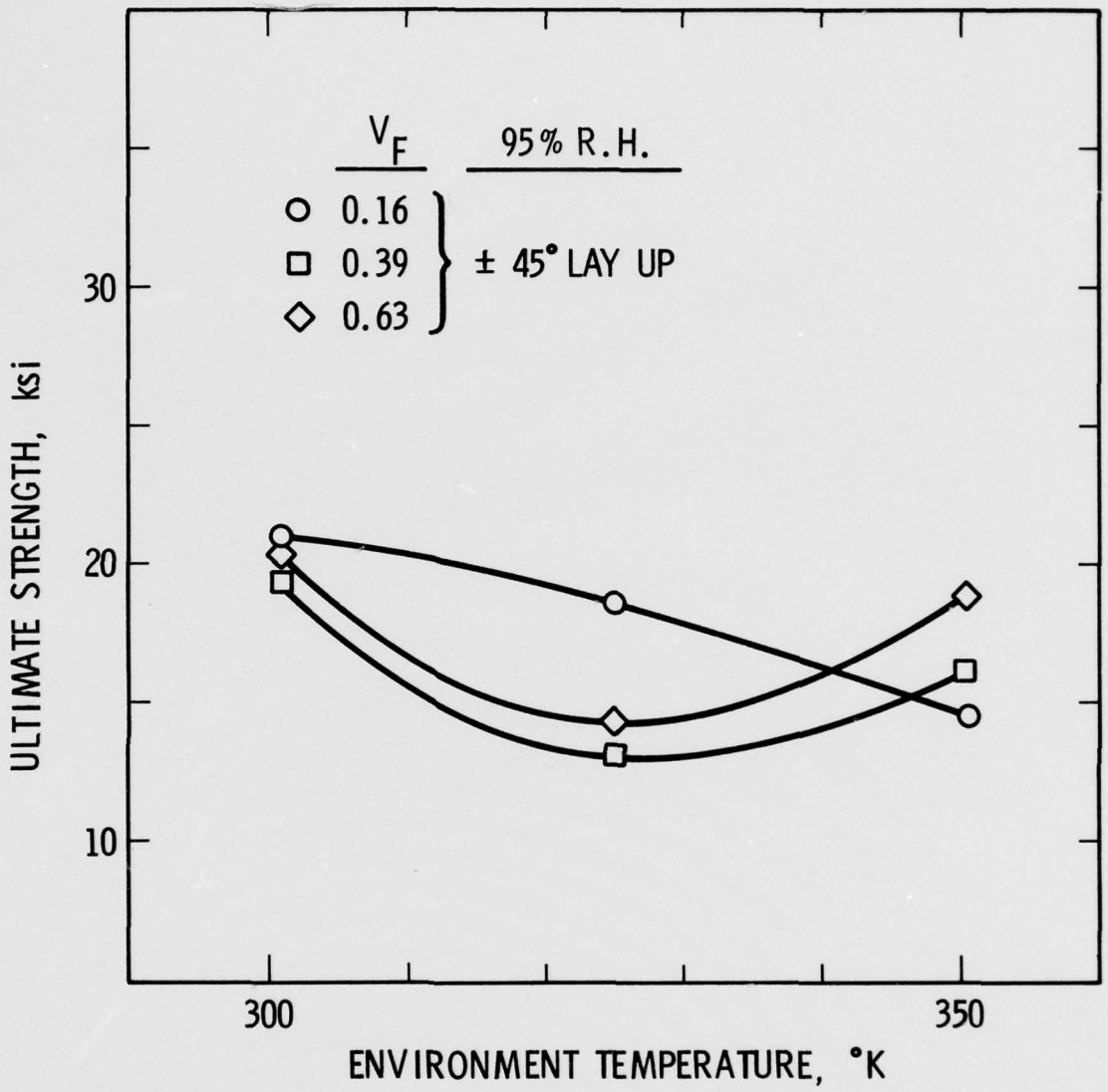

FIGURE 27. TENSILE TEST RESULTS, ±45° LAMINATE.

In addition to the normal tensile tests, a number of specimens were heated from ambient laboratory temperature to 300°F, cooled, and then tensile tested. The spiking was accomplished by filling an aluminum cylinder with water and the specimen, sealing the ends, and then immersing in an oil bath. The bath was heated at several rates to vary the spiking ramp; the temperature of the water in the cylinder was monitored with a thermocouple. The heating rates and tensile results are given in Table 8.

Comparing the spiking tensile results to the environmental tensile results showed that the rapid heating had no appreciable degradation on the tensile strength of the material. The possible exception to this was the 0°/90° layup where two of the three specimens showed lower strengths after spiking. There did not appear to be any effect of rate over the small range of rates utilized. Apparently, any surface cracking or damage introduced by the spike did not affect the strength. The modulus values obtained after spiking did not differ appreciably from the moduli obtained previously.

TABLE 8. SPIKING DATA

Time to 300°F, (sec)	Laminate	V_F	$S^{ut}_{x.}$ (ksi)	$E_x \times 10^3$ (ksi)
134	0/90°	26	18.4	1.4
156	±45°	41	21.5	2.5
186	∓45°	36	14.5	1.4
228	∓45°	16	13.0	1.1
231	$\bar{0}$/90°	40	46.7	6.6
162	0/90°	66	96.4	11.0
137	0°	37	90.9	12.8
132	0°	66	84.7	13.6
200	0°	12	81.8	10.9
199	Neat Resin	-	6.2	0.5

V. DIFFUSIVITY COEFFICIENTS

In addition to the complete set of specimens tested at the four levels, some preliminary tests were conducted at 150°F, 95% relative humidity. These tests involved a number of different size specimens, different fiber volumes and ply configurations, and different sealing techniques. The usual practice in performing small specimen tests is to have the samples unsealed. This is usually done because sealing is difficult and because most sealing techniques are of uncertain effectiveness. Moreover, because most small specimens are only a few layers thick, the edge effects are not thought to be large. To see if there is an effect of edge area, two unsealed undirectional specimens, 4.0" x 2.0" and 1.0" x 1.0", both 0.06" thick were placed in a 150°F, 95% relative humidity environment. The results are shown in Figure 28. As would be expected, the smaller piece shows more scatter in the weight gain data, but the overall behavior is the same. There is some slight difference in the maximum weight gain but the difference could well be normal scatter. Since there is a factor of 3 difference in the areas of the lateral edges, this suggests that there is not a large effect of edges in these small specimens.

Since the two specimens were of different sizes, two methods were used to compute the diffusion coefficients. First, the two point matching technique was used with the assumption that the edge effects could be ignored and the problem treated as one dimensional; this yielded

$$D_y = 1.68 * 10^{-6} \text{ in}^2/\text{hr}. \tag{36}$$

For the second computation, we assumed the two specimens to be transversely isotropic i.e., $D_y = D_z$. Using the short time solution of (3) in the form,

$$\frac{M}{M_m} = \frac{4}{\sqrt{\pi}} \left(\frac{\sqrt{D_x}}{\ell} + \frac{\sqrt{D_x}}{h} + \frac{\sqrt{D_z}}{b} \right) \sqrt{t} \tag{37}$$

substituting for the dimensions of the two specimens, and solving simultaneously, we obtain

$$\begin{aligned} D_x &= 2.43 * 10^{-5} \text{ in}^2/\text{hr} \\ D_y &= D_z = 1.72 * 10^{-6} \text{ in}^2/\text{hr} \end{aligned} \tag{38}$$

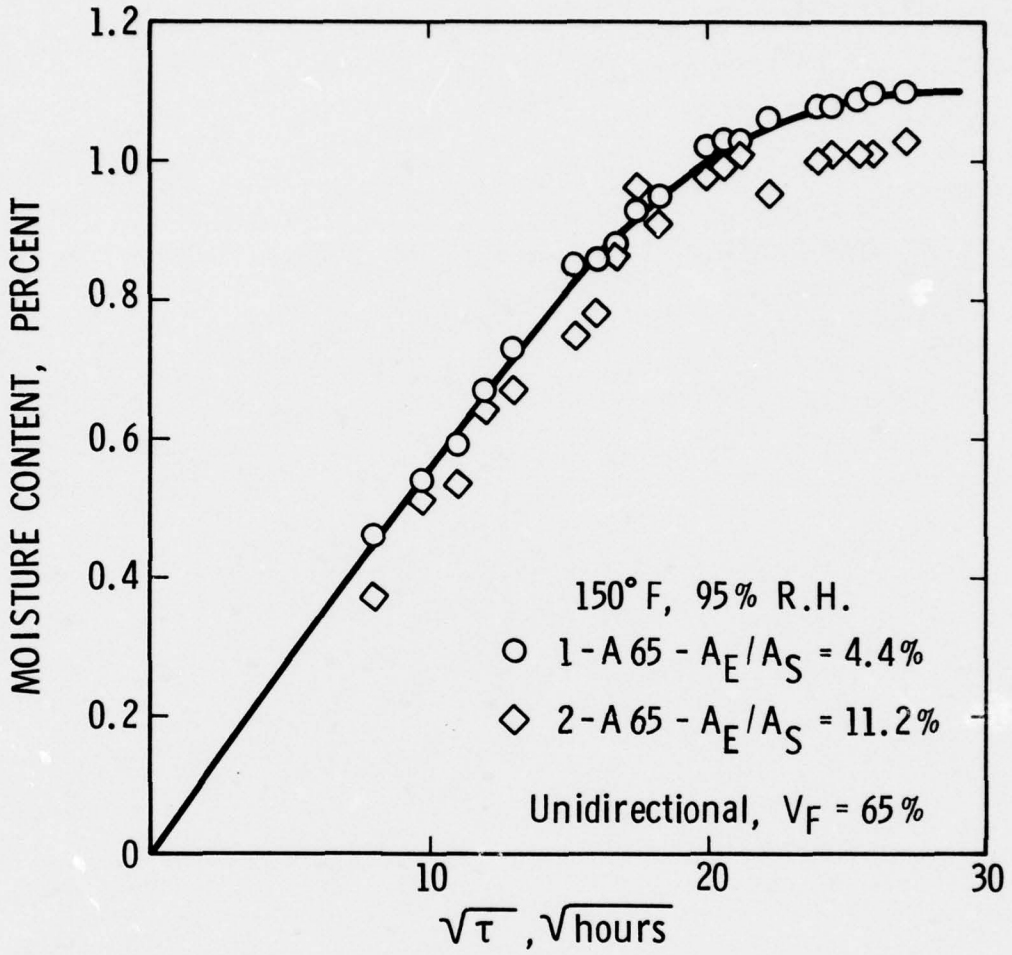

FIGURE 28. MOISTURE CONTENT IN TWO UNSEALED COMPOSITES.

During these preliminary tests, some attempts were made to determine the diffusion coefficients by sealing individual pairs of surfaces. The tests, shown in Figure 29, gave diffusivities which did not agree particularly well with the previous values. When the lateral edges were coated, the computed value was

$$D_y = 5.7 * 10^{-7} \text{ in}^2/\text{hr} \qquad (39)$$

which is a factor of three less than the earlier value, (38). On the other hand, when the lateral top and bottom surfaces were sealed, the constant in the fiber direction was

$$D_x = 3.4 * 10^{-4} \text{ in}^2/\text{hr} \qquad (40)$$

which is an order of magnitude larger than (38). The latter is not too surprising since the very small weight gain of this specimen means that the computation is sensitive to the particular values chosen to represent the data.

Figure 29 also compares the various models with data for the two specimens. The two one dimensional plots are data fits and so represent the data as expected. The solid curve is a three dimensional prediction obtained by using the diffusion coefficients (38). Since the D_y values for both the one and three dimensional curves are essentially the same, the difference between the upper two curves represents the effect of the edges. The difference in the two values is small enough that it would be covered by the scatter in the data in an experiment. It must be emphasized though that these are quite thin specimens.

The other pair of curves show a much wider divergence between the one and three dimensional models. In this case, the data is obtained from an edge sealed specimen, and hence is a one dimensional problem. The 3-D model assumes that moisture is entering from all edges and, from (40), the value of D_x is three orders of magnitude larger than D_y. This shows that, in spite of a very small area involving D_x, the diffusivity is large enough to have significant edge effects.

Figure 30 shows the predicted weight gain curves of Figures 6 and 7 replotted against the actual weight gain of specimens B-65 and B-52. In both cases, the one dimensional approximation better represents the data. For the higher volume fraction material, both predictions fall short by 10-15 percent; the one dimensional approximation does do a fairly good job representing the 52 percent fiber volume material.

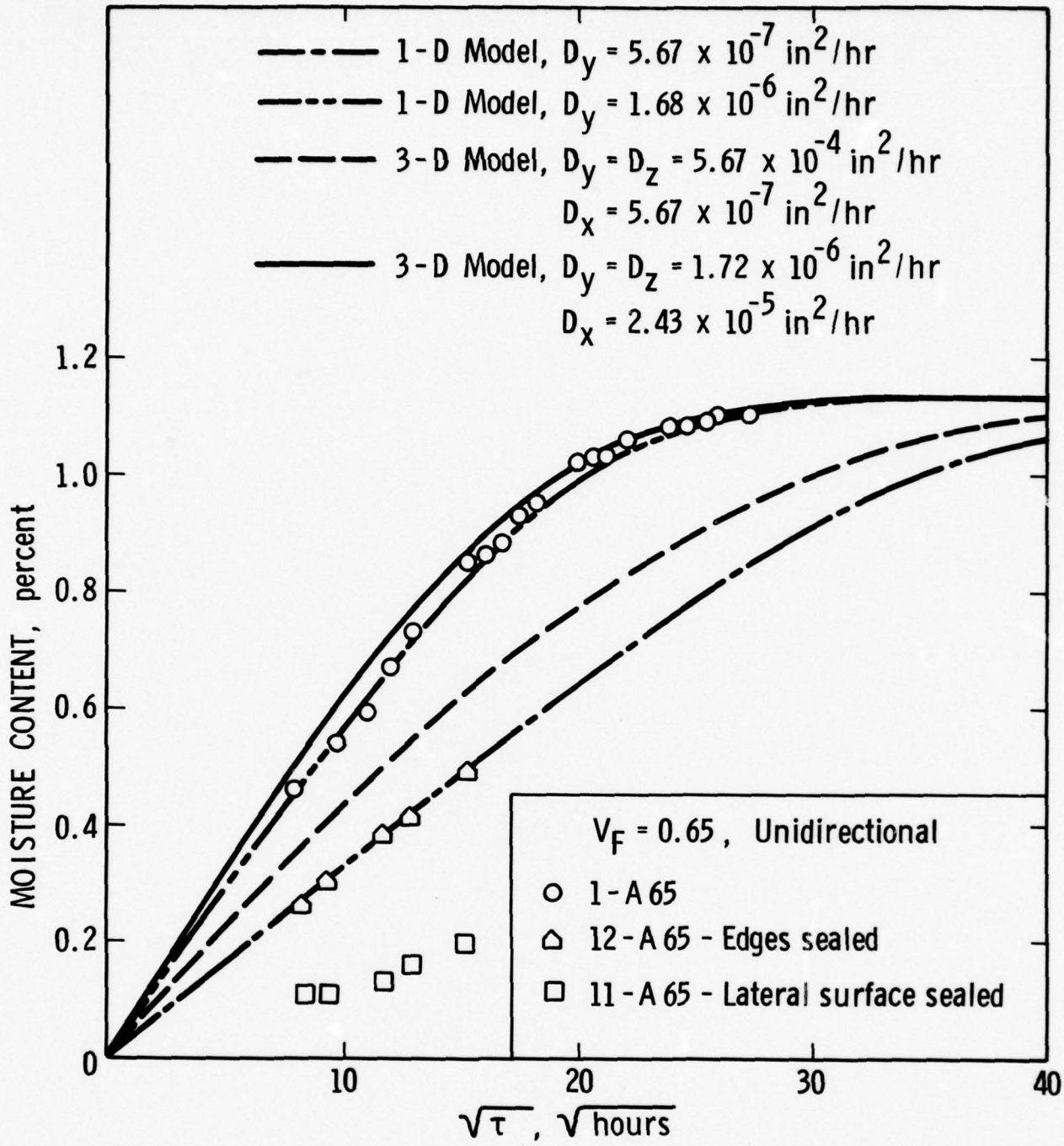

FIGURE 29. EXPERIMENTAL AND ANALYTICAL MOISTURE ABSORPTION DATA.

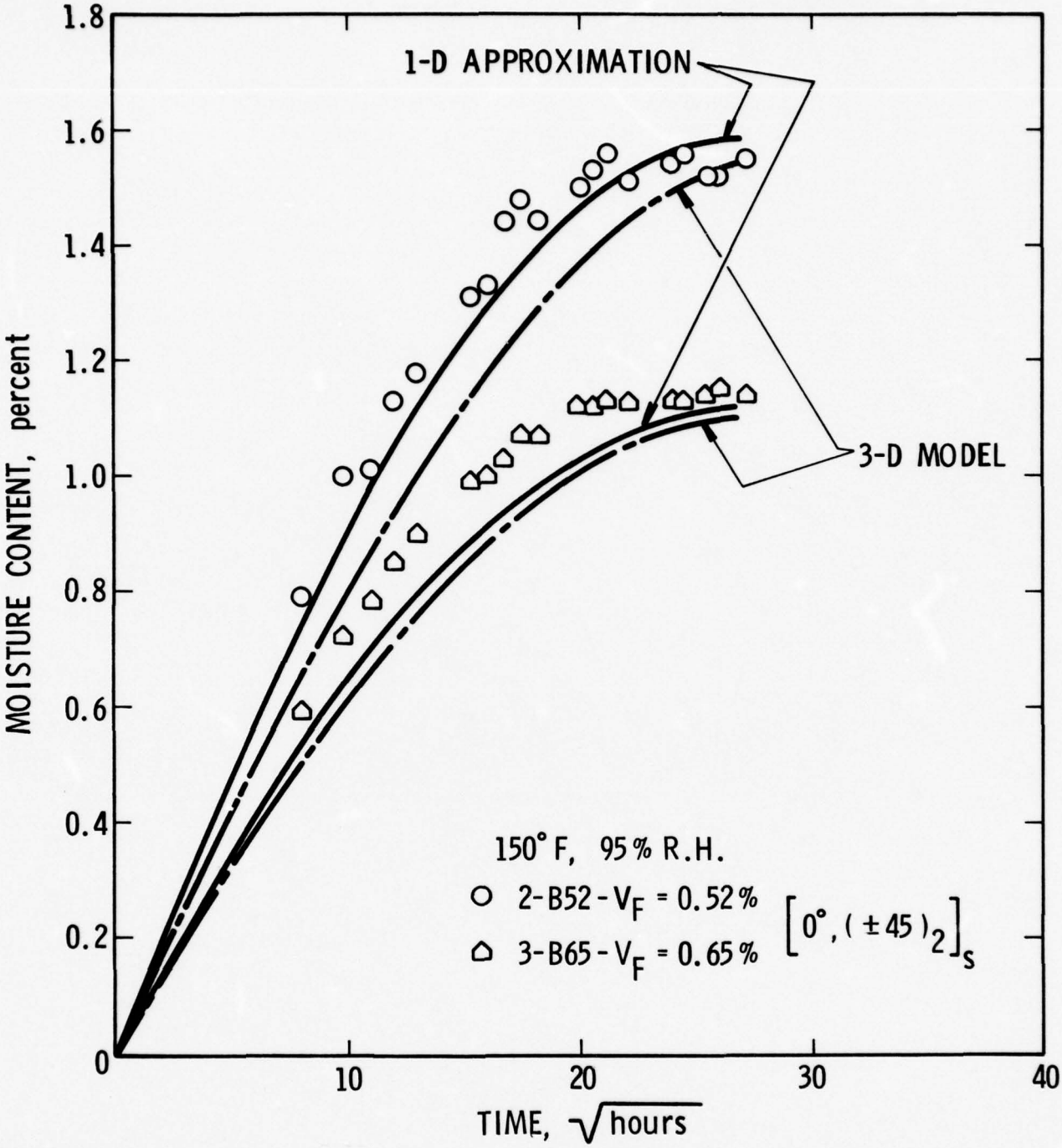

FIGURE 30 . PREDICTED AND EXPERIMENTALLY MEASURED WEIGHT GAINS.

It is, however, of interest to view the results of Figure 30 differently. Instead of elminating the matrix diffusivity D_m, we can use (16) to check the effective diffusivity of the laminate. For the 150°F test, we estimate the value of D_m as

$$D_m = 2.0 * 10^{-5} \text{ in}^2/\text{hr}$$

Using the values for the several volume fractions in this test, the data points are compared to the relation (16) in Figure 4. It is seen that, for the higher volume fractions, $V_F = 0.65$, (16) provides a reasonable estimate of the effective diffusivity of the laminate. Both the unidirectional and the crossply diffusivities fit the model leading to (8) which assumes no effect of stacking sequence; this fits the results of Shen and Springer [4] who also reported no difference between the two layups at $V_F = 0.68$. Figures 31 and 32 show the same comparison for all the specimens at two different environments. These results show that the unidirectional laminate tends to agree best with the model as would be expected. Overall, the model gives a fairly good lower bound, but the accuracy decreases as the volume fraction decreases. This lack of agreement is primarily due to the lower fiber volume material not being as homogeneous as the higher fiber content material. Moreover, the low V_F material will contain higher percentage of voids. An attempt was made to include void effects in the unit cell model of Figure 3, but the results indicated only a small effect at realistic void contents. It should be noted that when compared on the basis of diffusivity, any small perturbations in the diffusivity values are magnified. Comparisons on the basis of weight gain, Figure 20, do not show this effect as strongly as presenting the data in the form of Figures 31 and 32.

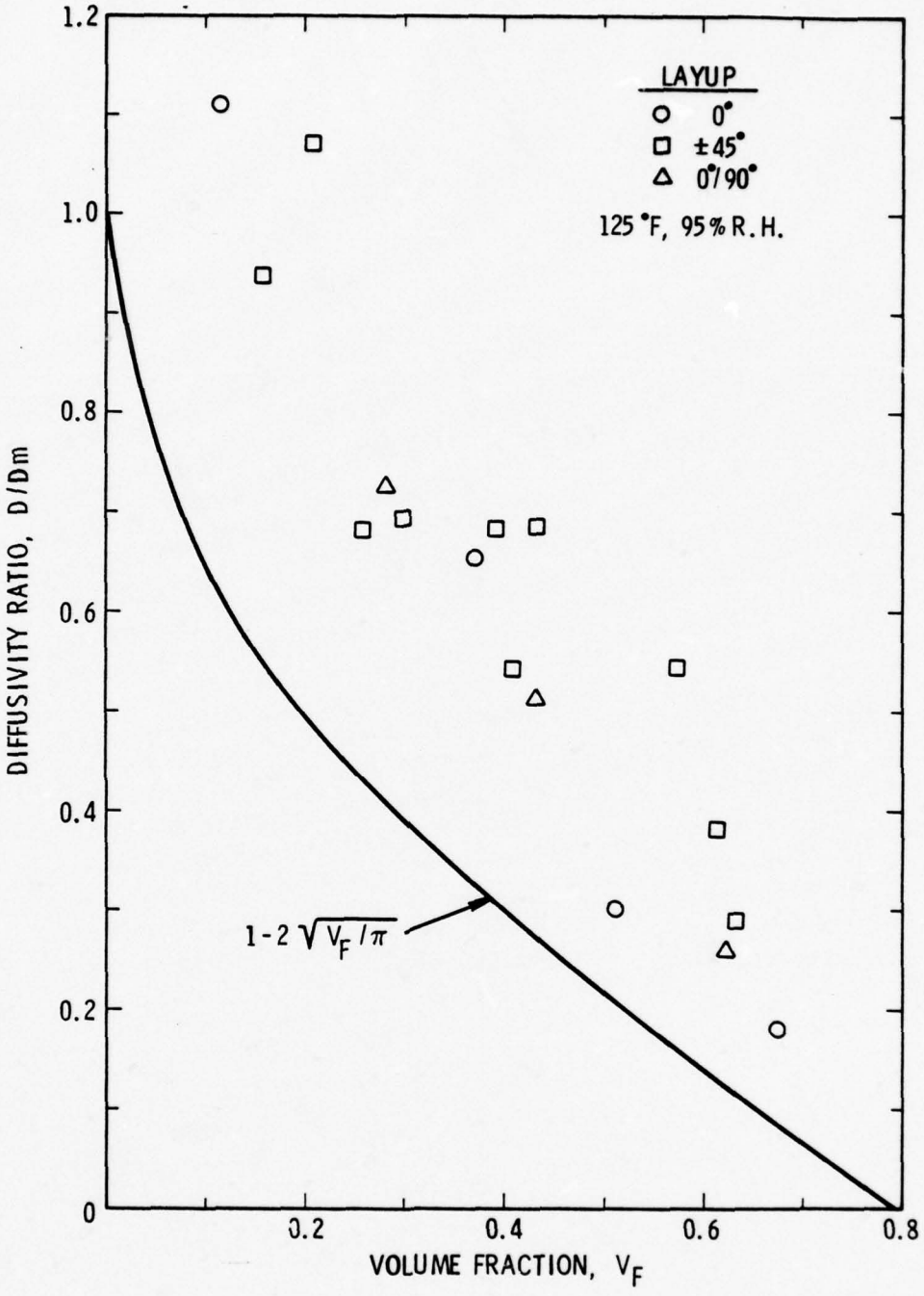

FIGURE 31. EFFECTIVE DIFFUSIVITY AT 125°F, 95 PERCENT RELATIVE HUMIDITY.

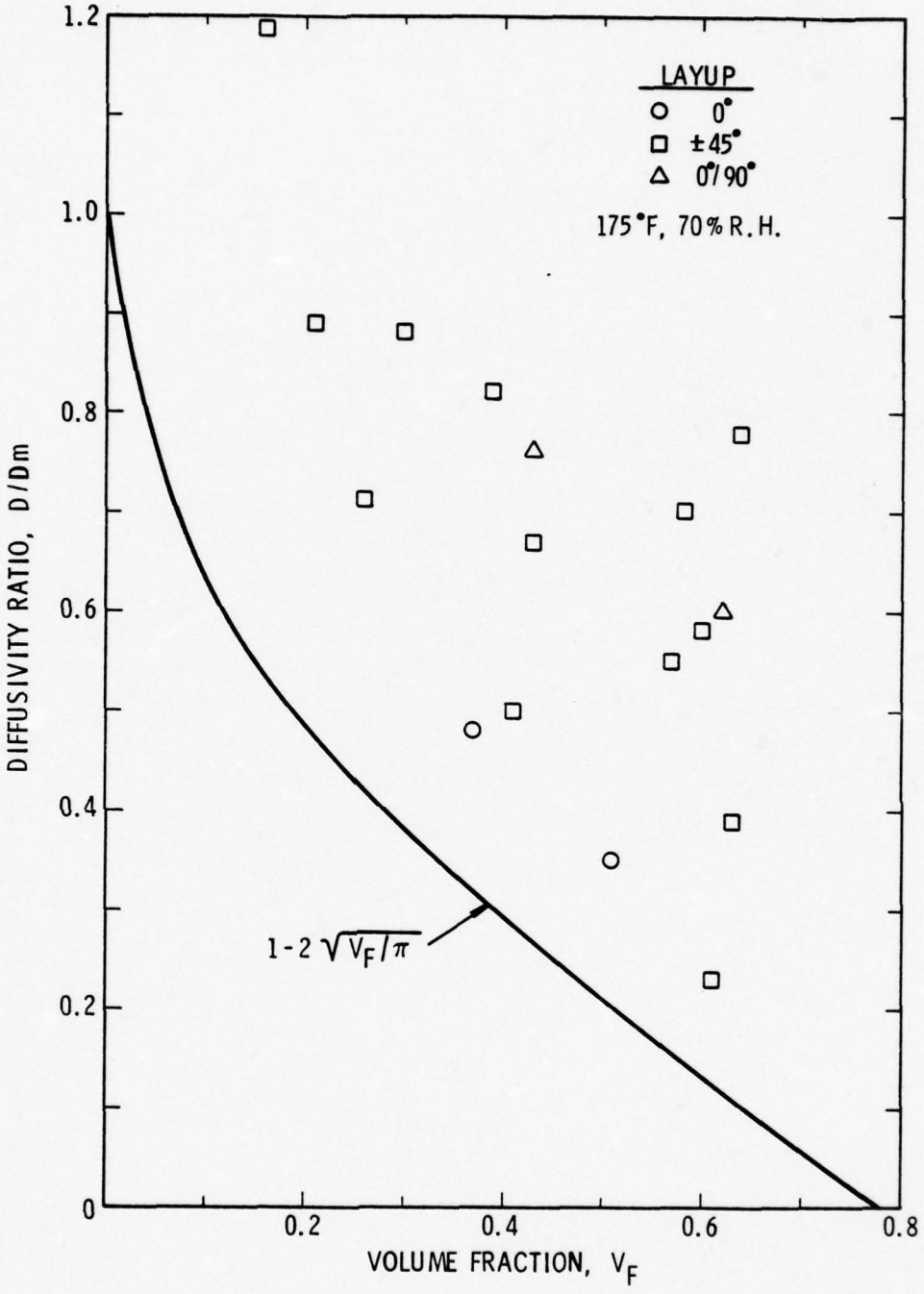

FIGURE 32. EFFECTIVE DIFFUSIVITY AT 175°F, 70 PERCENT RELATIVE HUMIDITY.

VI. CONCLUSIONS AND RECOMMENDATIONS

Based on the work discussed in this report, the following conclusions can be made.

1. Moisture absorption by graphite-epoxy is described to engineering accuracy by Fick's law. This analysis cannot account for effects such as secondary diffusion. Thus a careful study of the operating environment of the structure is necessary before maximum anticipated levels of moisture can be set. That is not only the temperature and humidity levels during operation, but any damage inducing conditions, e.g. fatigue, must be examined since these will affect the ultimate amount of moisture absorbed.

2. Normal graphite-epoxy composites, operating year round at 70 percent relative humidity, would absorb less than 0.7 percent water. As noted above however, if damage in the form of cracks and voids is introduced into the laminate, the structure may absorb considerably more moisture.

3. Lower fiber volume composite materials show more rapid weight gain and reach higher equilibrium moisture contents. This can be important in special use structures where either the low fiber material is used as a filler or as a separation in a sandwich laminate.

4. The maximum amount of moisture absorbed increases as a function of relative humidity. The increase is rapid above 70 percent, suggesting the beginning of concentration dependent diffusion.

5. In spite of theoretical expectations, there was an effect of layup, with the largest weight gain being for the 0°/90°, followed by the $\pm$45° and the 0° layups. However the differences generally were small.

6. A micromechanics model based on a unit cell and laminate theory can be used with the matrix diffusivity to obtain a lower bound for the effective diffusion coefficient of a composite laminate. This model becomes increasingly inaccurate at low fiber volumes however.

7. The tensile strength of the composites showed little effect of humidity but did show some decrease with increasing environment temperature. Spiking the specimens to 300°F at several rates showed no decrease,

and in fact in most cases, a small increase in tensile strength. This small change could be due to residual compressive surface stresses.

8. The sequencing tests demonstrated that the short time weight gain or loss is largely a surface phenomenon resulting from the large moisture gradients near the surface. The predictions of weight loss underestimated the loss following a change in environment; the overall behavior was predicted quite accurately however.

9. For specimens tested in four point bending, for low applied strains, there was no effect on weight gain of the applied load. No consistent pattern of weight gain as a function of applied strain was observed for the four levels of strain used in this program. This suggests that at higher strains, the material is damaged which accounts for the observed coupling of moisture and stress.

Recommendations for future work are as follows:

1. Develop a nondestructive method of determining the concentration distribution in the material. Most experimental work is based on weight gain measurements which yields only an average concentration value. Slicing techniques yield some distribution information but the material is destroyed. A nondestructive technique would not only aid moisture modelling but would also serve to aid maintenance of in-service aircraft.

2. The reasons for secondary diffusion and other anomalous behavior are needed. This report has suggested that void and crack entrapment of moisture is the cause. Other researchers cite stress-diffusion coupling while others suggest thermal diffusion as the cause. This must be clarified before the effects of moisture on long term aircraft exposure can be completely turned over to the designers.

3. This program explored the use of a micromechanics model to predict absorption behavior of a laminate. Since this model provides a lower bound, effort should be devoted to developing an upper bound solution. An attempt was made to broaden the current model by including voids in the unit cell, but this was not successful. Apparently, a more sophisticated analysis is needed.

4. In line with the introduction of damage into composite materials, a specific problem that has not been addressed is the effect of a bearing load on moisture

absorption. Since the problem encompasses fretting, applied loads, and moisture, it is a very complicated problem but one that should be addressed for safe aircraft operation.

5. More attention should be paid to dynamic problems. Some results have indicated that moisture absorption can produce serious modulus and damping effects. Since this has implications for structural application of composites, more attention should be paid to these areas.

VII. REFERENCES

1. W. Jost, Diffusion in Solids, Liquids, Gases, Academic Press, New York, 1952.

2. J. Crank, The Mathematics of Diffusion, Oxford University Press, London, 1956.

3. Y. Weitsman, Journal of Compoiste Materials, 10, 1975, p. 193-204.

4. Chi-Hung Shen and G. S. Springer, Journal of Composite Materials, 10, 1976, p. 36-54.

5. M. E. Gurtin, presented at "Mechanics of Composites Review," Dayton, Ohio, 26-28 October, 1976.

6. L. J. Broutman, presented at "Mechanics of Composites Review," Dayton, Ohio, 26-28 October, 1976.

7. E. L. McKague, Jr., J. D. Reynolds, J. E. Halkias, ASME Paper No. 76-Mat-G, 1976.

8. G. S. Springer and Chi-Hung Shen, AFML-TR-76-102, March 1976.

9. C. E. Browning, G. E. Husman, and J. M. Whitney "Moisture Effects in Epoxy Matrix Composites," Composite Materials: Testing and Design (Fourth Conference), ASTM STP 617, American Society for Testing and Materials, Philadelphia, 1977.

10. C. D. Shirrell, "Diffusion of Water Vapor in Graphite/Epoxy Composites," presented at ASTM Symposium on Environmental Effects on Advanced Composites, Dayton, Ohio, 29-30 September, 1977.

11. G. R. Caskey, Jr., and W. L. Pillinger, Met. Trans., 6A, March 1975, p. 467-476.

12. A. McNabb and P. K. Foster, Trans. AIME, 227, 1963, p. 618-627.

13. M. E. Gurtin, presented at "Mechanics of Composites Review," Dayton, Ohio, 25-27 October, 1977.

14. G. J. Van Amerongen, Rubber Chemistry and Technology, 37, 1964, p. 1965.

APPENDIX A

PUBLICATIONS

PUBLICATIONS

Results of work conducted during AFOSR Contract No. F44620-76-C-0093 were presented to the SAMPE meeting in San Diego in April 1977.

T. S. Cook, D. E. Walrath, and P. H. Francis, "Moisture Absorption in Graphite-Epoxy Composite Materials," Proceedings, 22nd National Symposium, 1977, p. 339.

Another article has been submitted to an ASTM Symposium.

T. S. Cook and D. E. Walrath, "Moisture Absorption Effects in Graphite-Epoxy Composites".

APPENDIX B

WEIGHT GAIN RESULTS FOR 125°F, 95% RELATIVE HUMIDITY

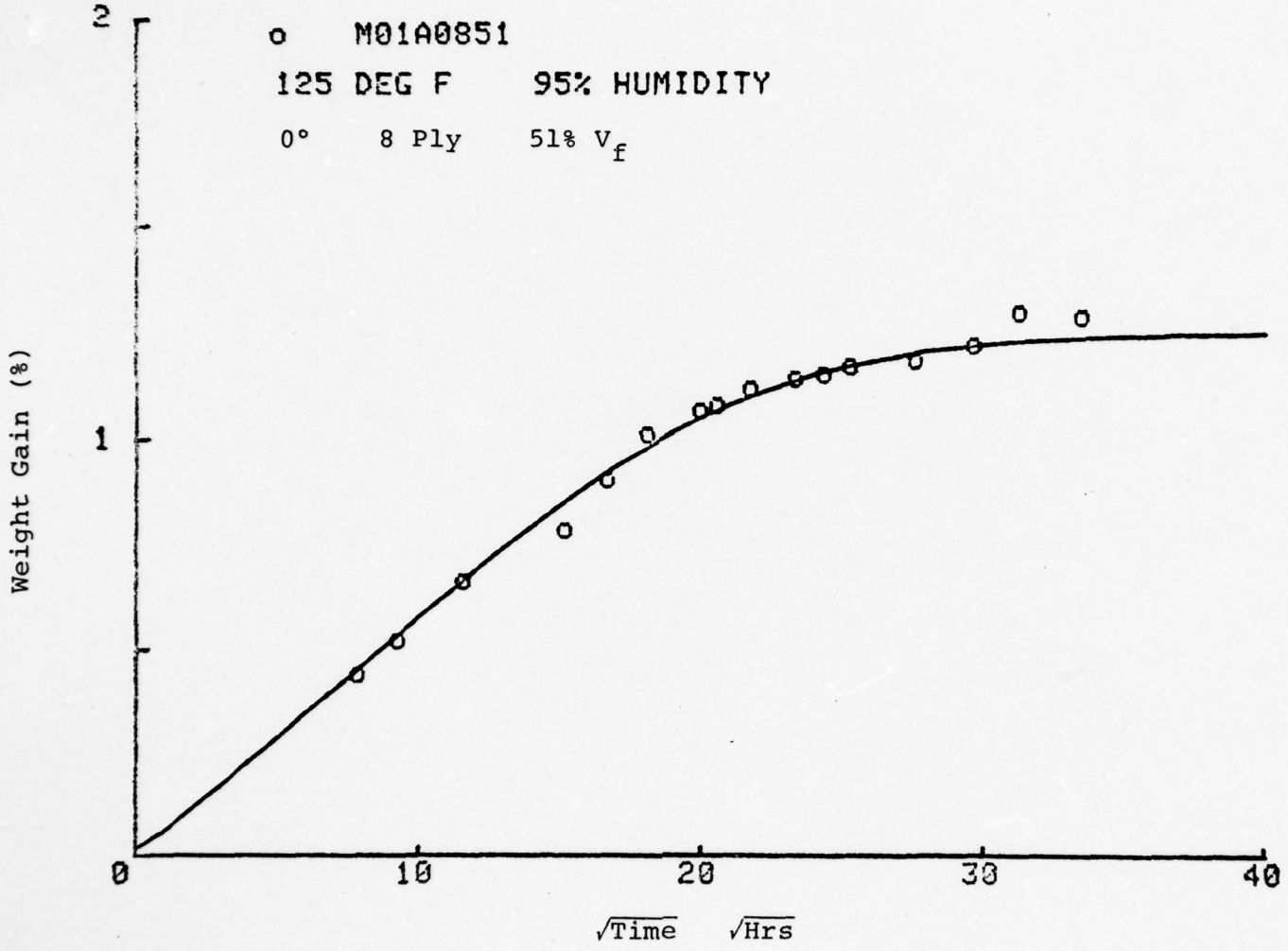
o M01A0851
125 DEG F 95% HUMIDITY
0° 8 Ply 51% V_f
Weight Gain (%)
2
1
0
10
20
30
40
√Time √Hrs

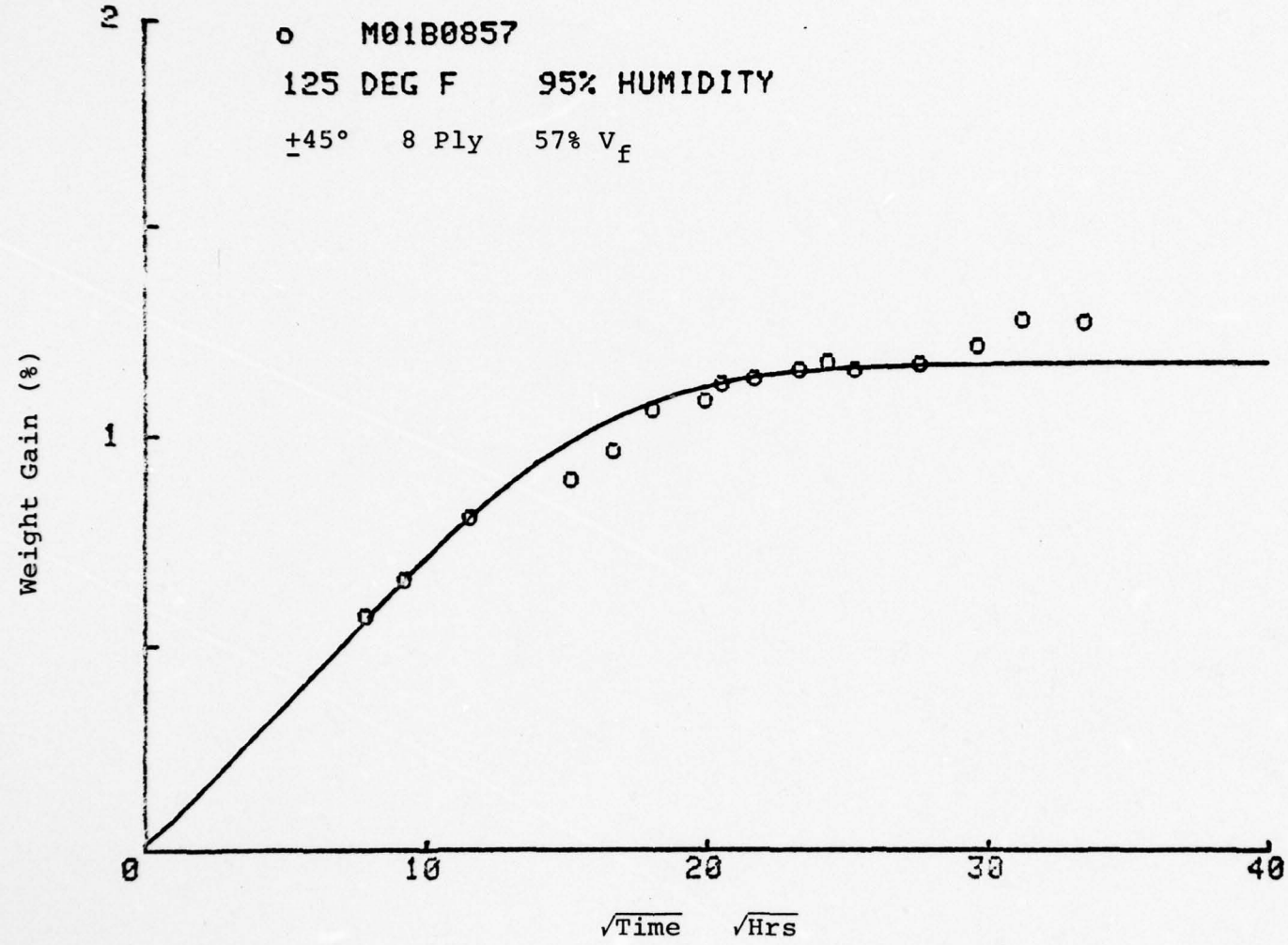
o M01B0857
125 DEG F 95% HUMIDITY
±45° 8 Ply 57% V_f
Weight Gain (%)
2
1
0
10
20
30
40
√Time √Hrs

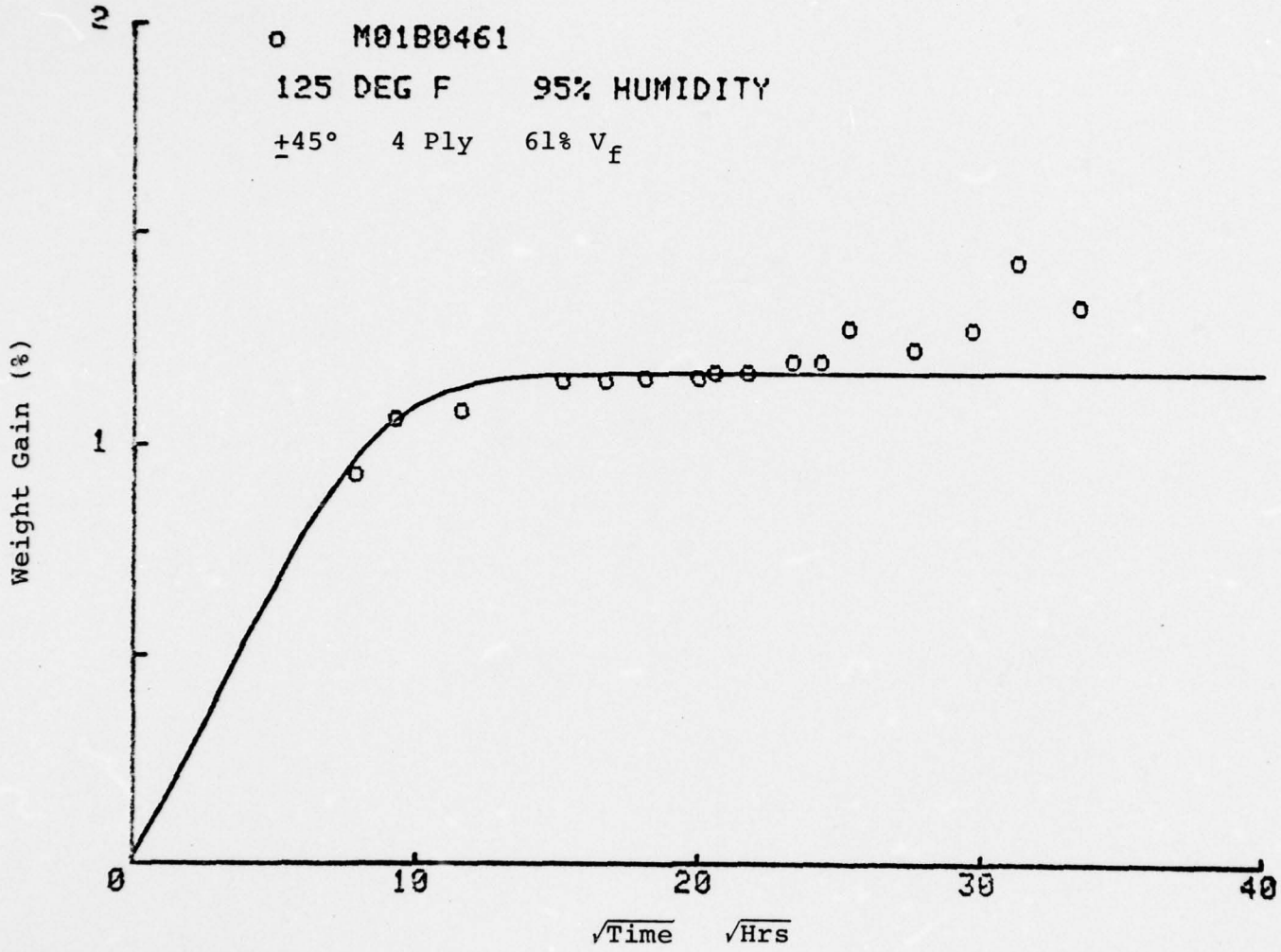
o M01B0461
125 DEG F 95% HUMIDITY
±45° 4 Ply 61% V_f
Weight Gain (%)
2
1
0
10
20
30
40
√Time √Hrs

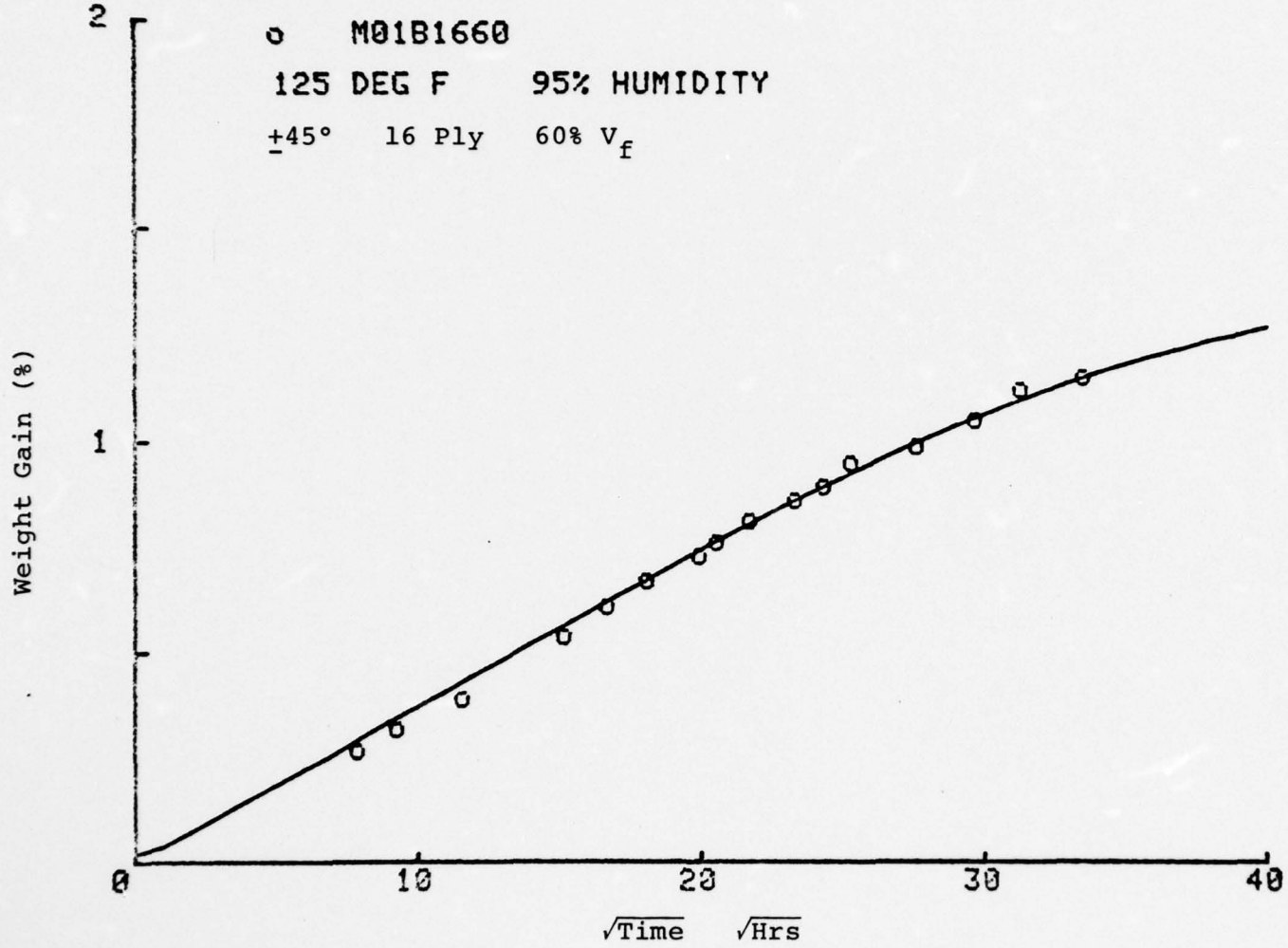
o M01B1660
125 DEG F 95% HUMIDITY
±45° 16 Ply 60% V_f
Weight Gain (%)
2
1
0
10
20
30
40
√Time √Hrs

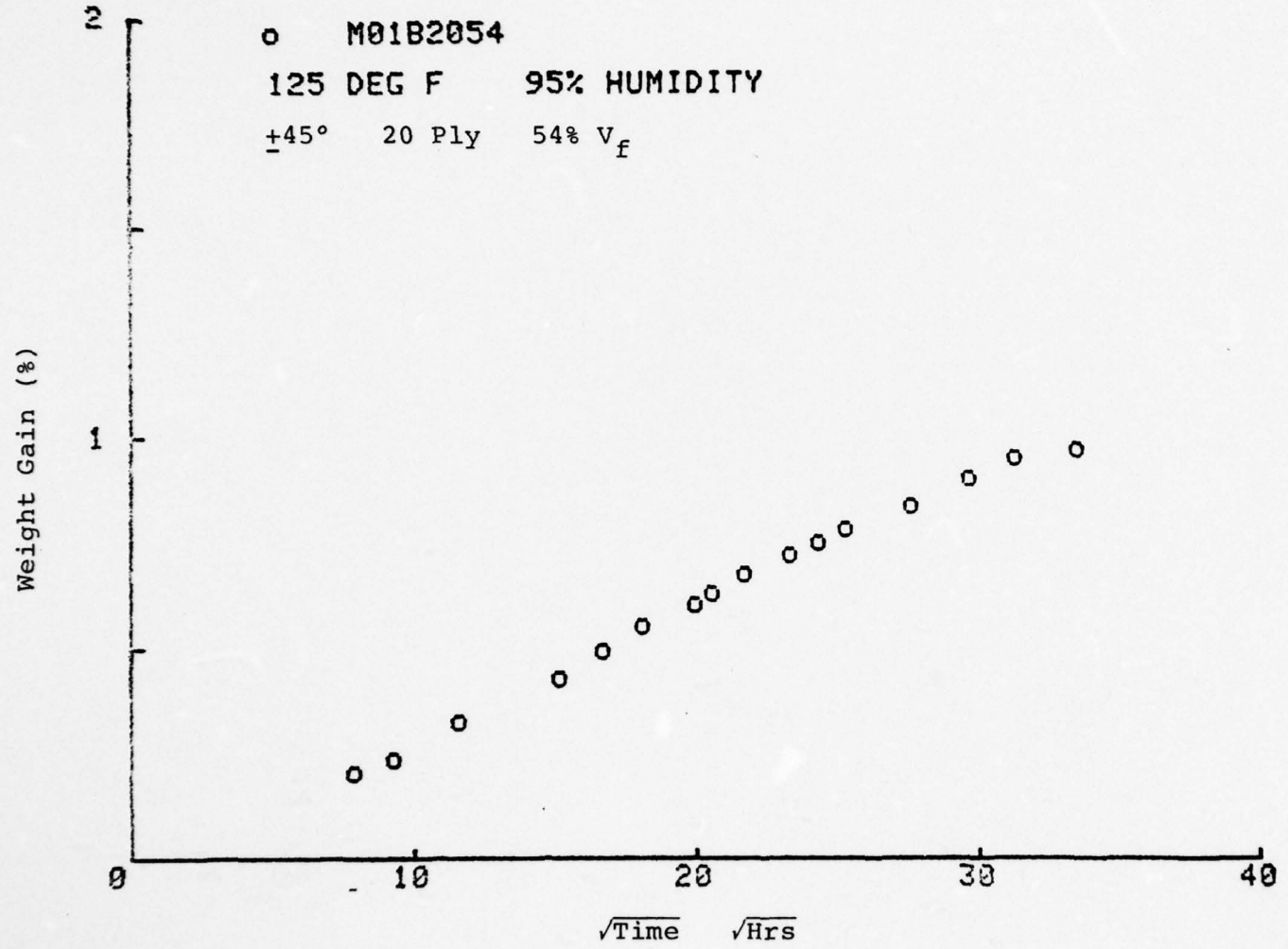
o M01B2054
125 DEG F 95% HUMIDITY
±45° 20 Ply 54% V_f
Weight Gain (%)
2
1
0
10
20
30
40
√Time √Hrs

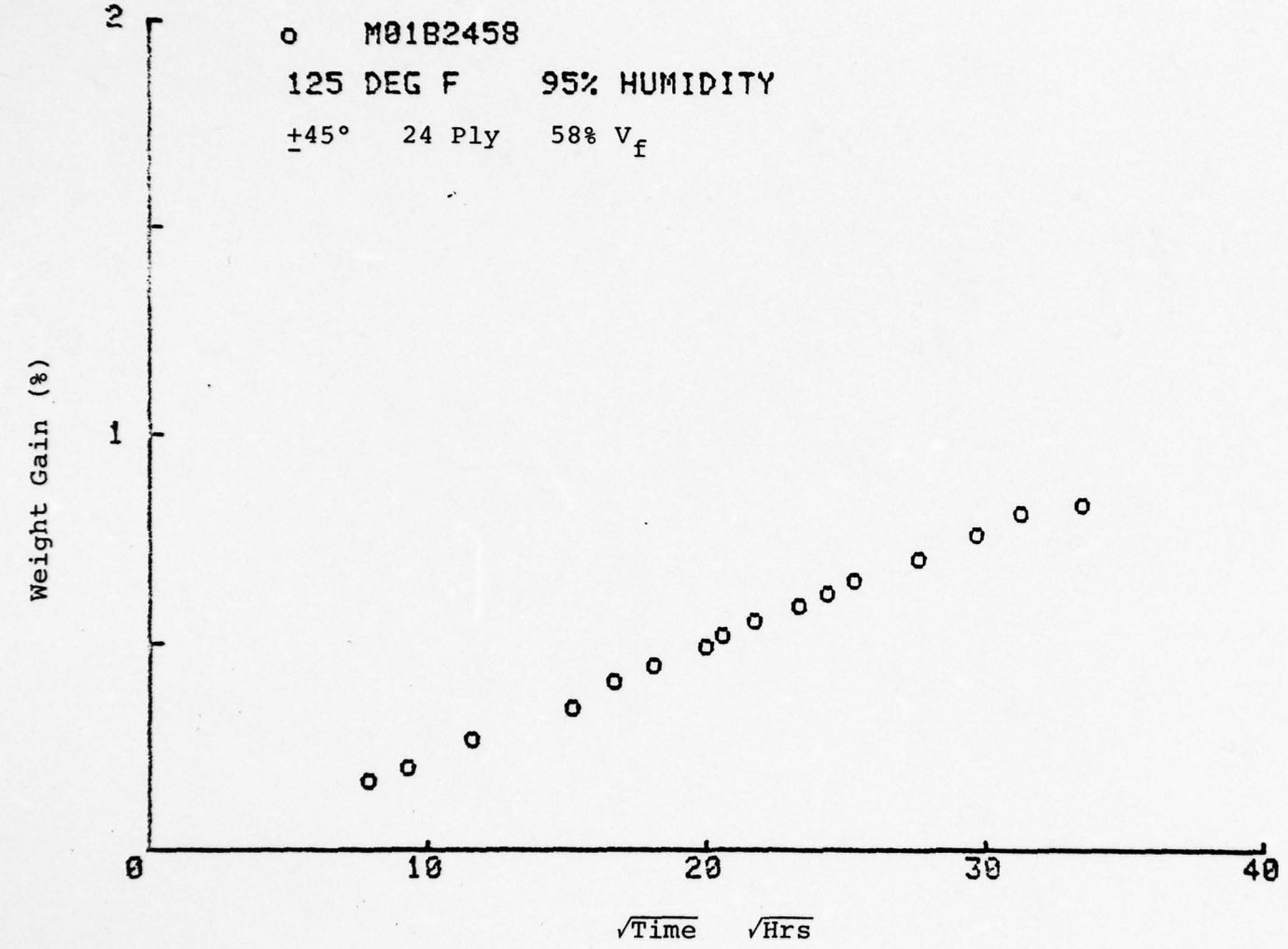
o M01B2458
125 DEG F 95% HUMIDITY
±45° 24 Ply 58% V_f
Weight Gain (%)
2
1
0
10
20
30
40
√Time √Hrs

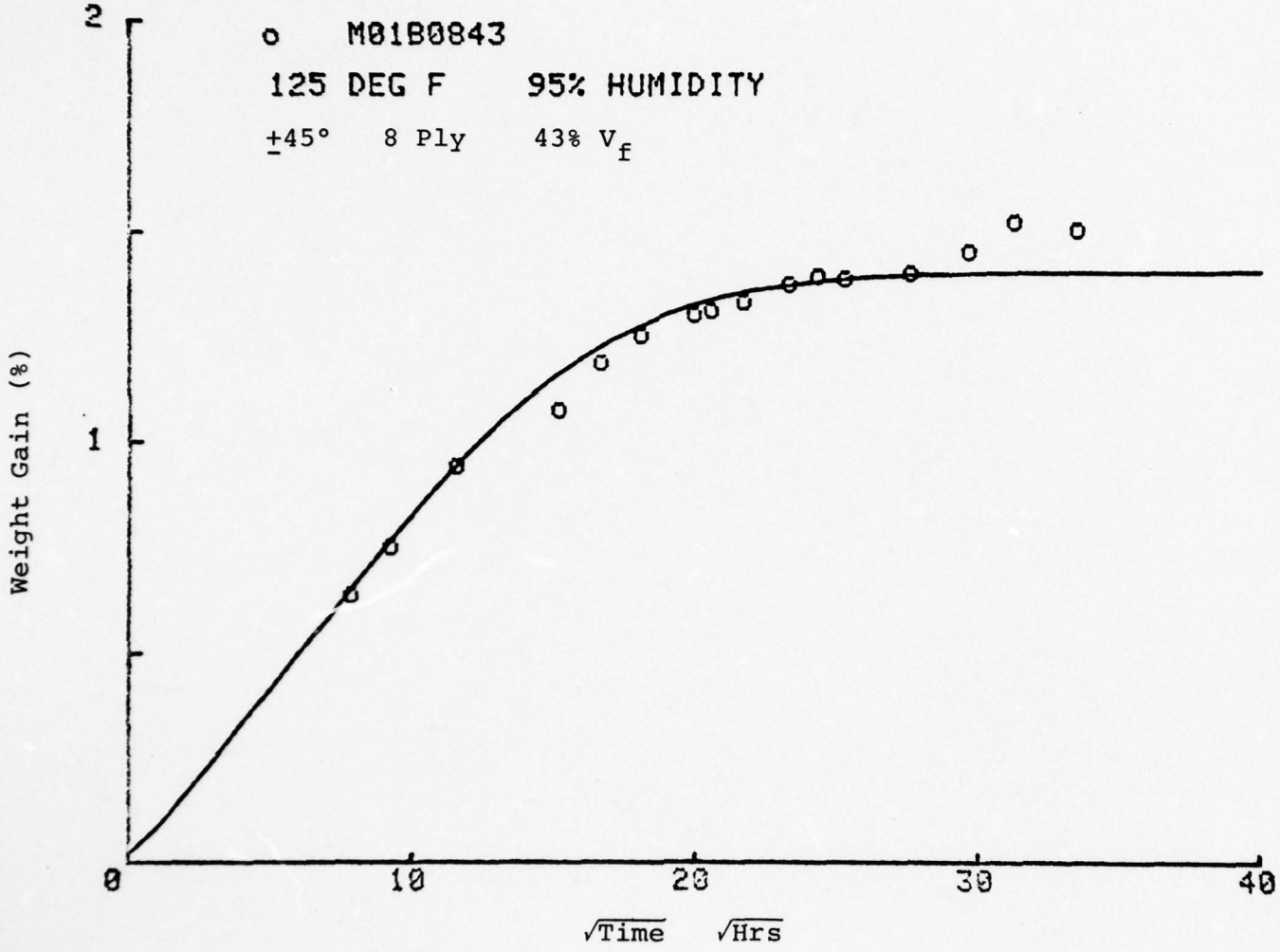
o M01B0843
125 DEG F 95% HUMIDITY
±45° 8 Ply 43% V_f
Weight Gain (%)
2
1
0
10
20
30
40
√Time √Hrs

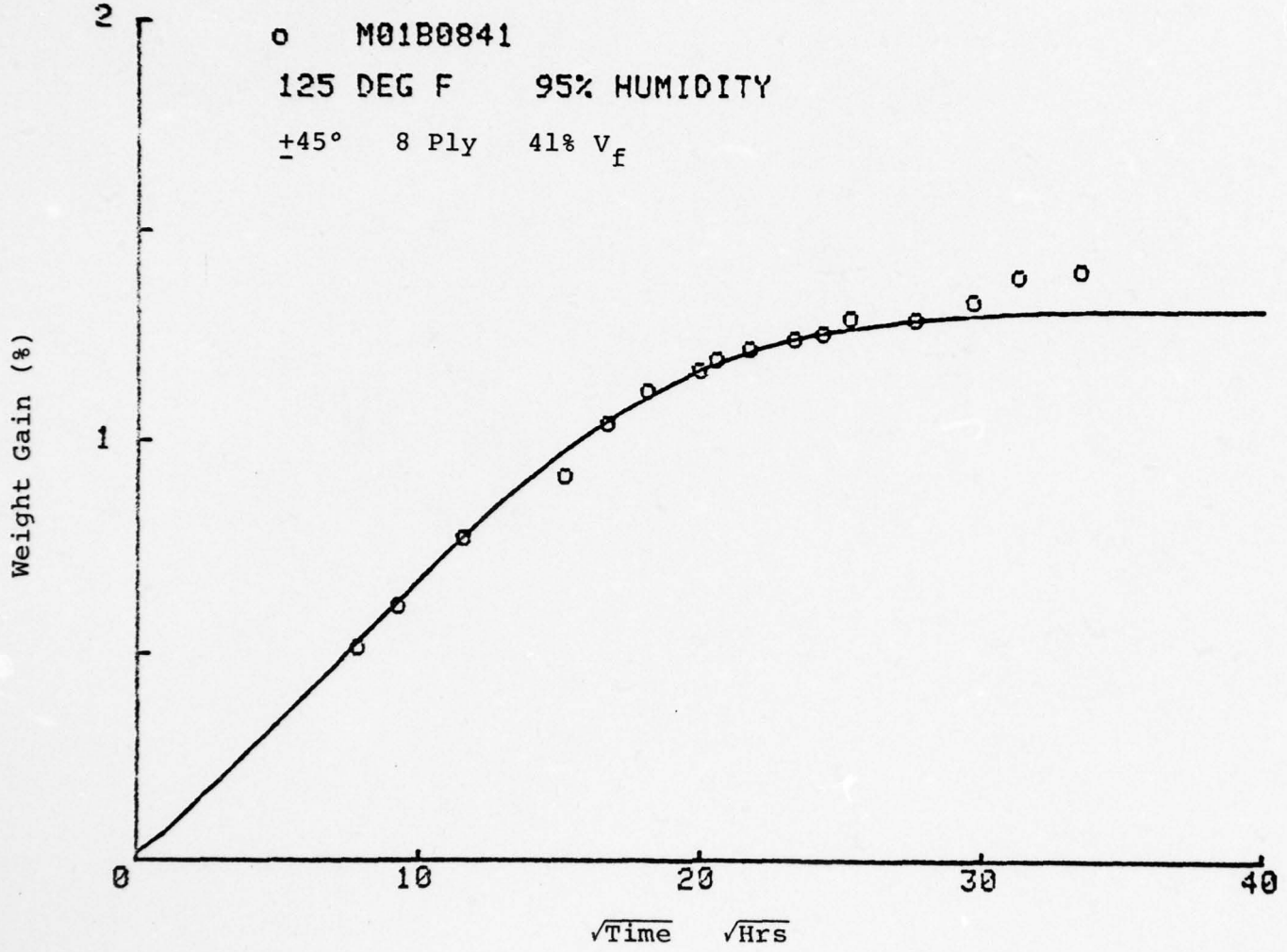
o M01B0841
125 DEG F 95% HUMIDITY
±45° 8 Ply 41% V_f
Weight Gain (%)
2
1
0
10
20
30
40
√Time √Hrs

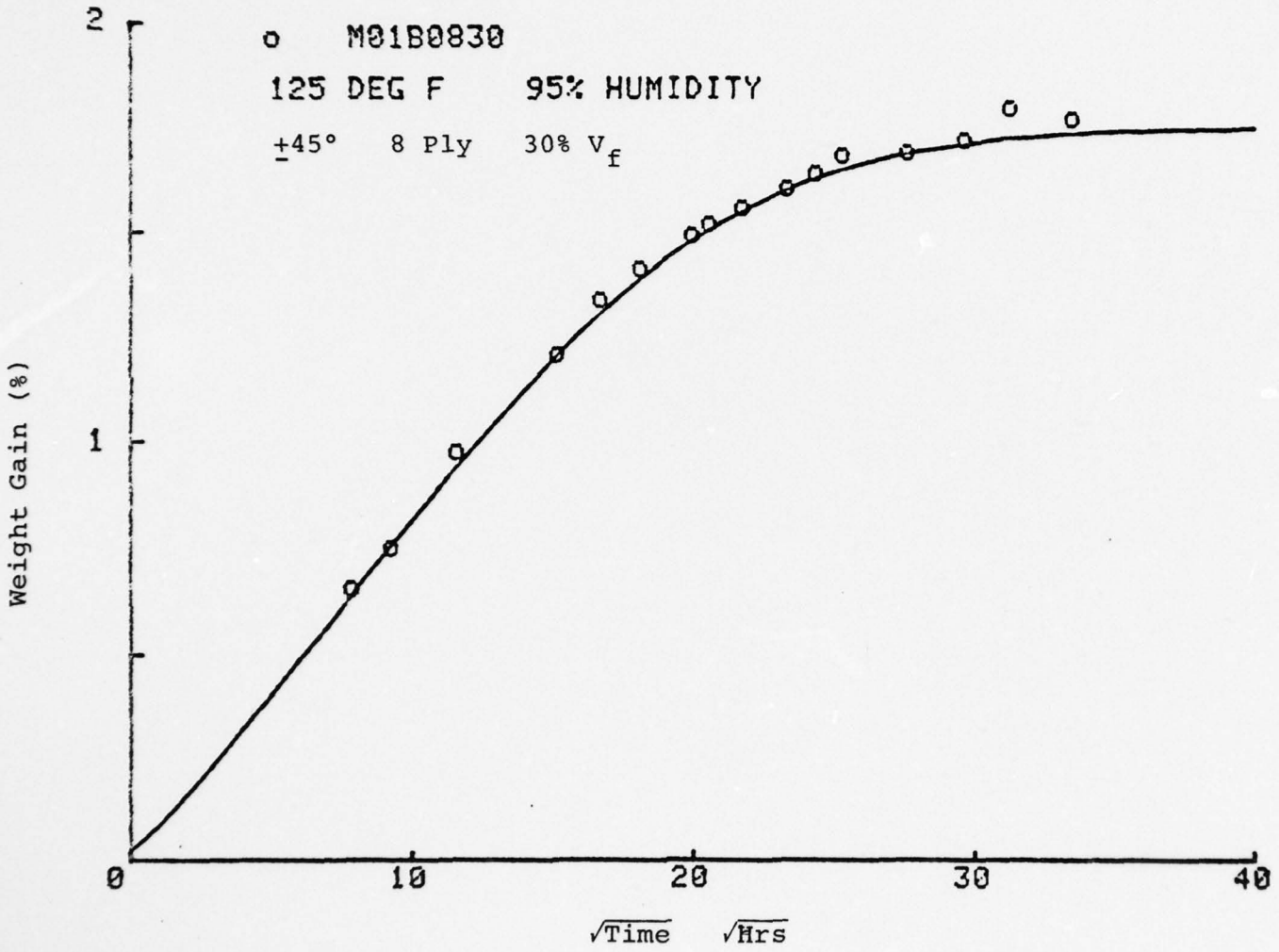
o M01B0830
125 DEG F 95% HUMIDITY
±45° 8 Ply 30% V_f
Weight Gain (%)
2
1
0
10
20
30
40
√Time √Hrs

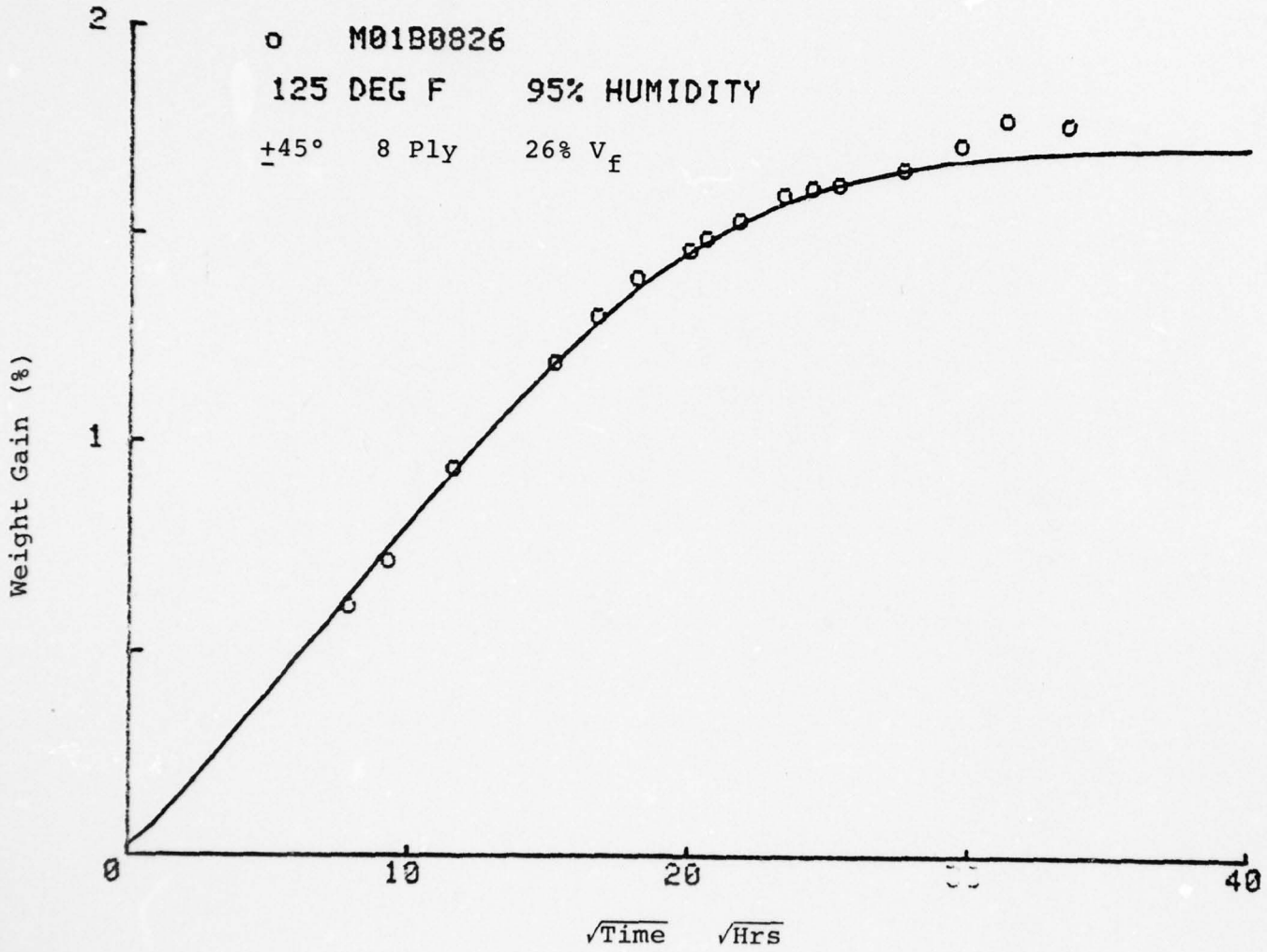
o M01B0826
125 DEG F 95% HUMIDITY
±45° 8 Ply 26% V_f
Weight Gain (%)
2
1
0
10
20
40
√Time √Hrs